

Influence of various Reductants on the Ilmenite Smelting technology

Pieter Andries Strydom

Research report submitted to the Faculty of Engineering and the Built Environment,
University of the Witwatersrand Johannesburg, in partial fulfillment of the degree of
Master of Science in Engineering

2013

TABLE OF CONTENTS

ABSTRACT	9
ACKNOWLEDGMENTS	11
1 INTRODUCTION	12
2 LITERATURE REVIEW	16
2.1 Reactions in ilmenite smelting	16
2.2 Mass and energy balancing	25
2.3 Suitability of reductants in ilmenite smelting.....	35
3 METHODOLOGY	41
3.1 Methodology of preparation.....	41
3.2 Data obtained after test campaigns	43
3.3 Methodology of evaluation	43
4 RESULTS	46
4.1 Petrographics results	46
4.2 Carbon efficiencies results	46
4.3 Slag products.....	49
4.4 Metal products.....	50
4.5 Reductant analyses.....	51
4.6 Summary of Results	53
5 DISCUSSION - ENERGY ALGORITHM CORRECTION.....	61
5.1 Energy algorithm correction for Reductant A.....	61
5.2 Energy algorithm correction for Reductant B.....	63
5.3 Energy algorithm correction for Reductant C.....	64
5.4 Energy algorithm correction for Reductant D.....	65
6 DISCUSSION - VALUE IN USE MODEL.....	66
6.1 Treatment cost value calculation	66
6.2 Reductant cost evaluation	68
6.3 Net smelter profit calculation.....	68
6.4 Value in Use results	69
7 CONCLUSION.....	74

8	RECOMMENDATION	76
9	LIST OF REFERENCES	77
10	APPENDICES	78
10.1	Reductant A size analysis.....	79
10.2	Reductant A XRF press powder and Proximate analysis.....	80
10.3	Reductant A petrographics.....	81
10.4	Reductant A associated metal analysis.....	82
10.5	Reductant A associated slag analysis	83
10.6	Reductant A associated furnace data.....	85
10.7	Reductant B size analysis.....	86
10.8	Reductant B XRF press powder and Proximate analysis.....	87
10.9	Reductant B petrographics.....	88
10.10	Reductant B associated metal analysis.....	89
10.11	Reductant B associated slag analysis	90
10.12	Reductant B associated furnace data.....	92
10.13	Reductant C size analysis.....	93
10.14	Reductant C XRF press powder and Proximate analysis.....	94
10.15	Reductant C petrographics.....	95
10.16	Reductant C associated metal analysis.....	96
10.17	Reductant C associated slag analysis	97
10.18	Reductant C associated furnace data.....	99
10.19	Reductant D size analysis.....	100
10.20	Reductant D XRF press powder and Proximate analysis.....	101
10.21	Reductant D petrographics.....	102
10.22	Reductant D associated metal analysis.....	103
10.23	Reductant D associated slag analysis	104
10.24	Reductant D associated furnace data.....	105
10.25	FactSage metal results.....	106
10.26	Value in Use model inputs and outputs.....	107

LIST OF FIGURES

Figure 1: Heavy minerals process flow to smelter processing.....	13
Figure 2: Calculated (Dotted line) vs. actual M_3O_5 stoichiometry between FeO and Ti_2O_3 for slags produced from South African and Canadian ilmenites. (Pistorius 2008).....	17
Figure 3: Constant FeO pseudobinary section through FeO- TiO_2 - Ti_2O_3 ternary phase diagram. (Pistorius 2008).....	18
Figure 4: Calculated liquidus temperatures as a function of mass fraction. (Pistorius 2008).....	20
Figure 5: Calculated liquidus solidus temperatures along the Ti_3O_5 and $FeTi_2O_5$ join (Pistorius 2008).....	21
Figure 6: Calculated relationship between theoretical energy required as a function of FeO content in the slag and carbon input (Pistorius 2008).....	22
Figure 8: Changes in FeO and Ti_2O_3 content of ilmenite smelter (Zietsman and Pistorius,2004).....	24
Figure 9: Simplistic mass and energy balance representation in ilmenite smelting.....	26
Figure 10: The relationship between macro - and micro- composition of coal Falcon and Falcon(1987).....	39
Figure 11: Reductant to furnace flow sheet.....	43
Figure 12: Vitrinite content against calculated carbon efficiency for Reductant A – Reductant D.....	54
Figure 13: Mean particle diameters (D50) of Reductant A to Reductant D.....	55
Figure 14: Mean particle diameters (d50) correlated against carbon efficiency.....	55
Figure 15: 1-mm size fraction of Reductant A to Reductant D correlated against carbon efficiency.....	56
Figure 16: Percentage carbon to metal for various reductant carbon efficiencies.....	57

Figure 17: Percentage carbon to metal compared to TiO₂ % slag for various reductants.....58

Figure 18: Percentage carbon to metal compared to metal temperatures for various reductants.....59

Figure 19: Equilibrium carbon in metal for given temperatures as calculated through FactSage.....59

Figure 20: Carbon % in metal to Ti % in metal (Open marker adapted from (Pistorius et al, 2012) against solid markers indicting the various reductant campaigns60

Figure 21: Reductant % A required per ton ilmenite to obtain a desired TiO₂ slag chemistry.....62

Figure 22: Cold theoretical energy requirement for various reductant A feed ratios62

Figure 23: Reductant %B required per ton ilmenite to obtain a desired TiO₂ slag chemistry.....63

Figure 24: Cold theoretical energy requirement for various reductant B feed ratios63

Figure 25: Reductant %C required per ton ilmenite to obtain a desired TiO₂ slag chemistry.....64

Figure 26: Cold theoretical energy requirement for various reductant C feed ratios64

Figure 27: Reductant %D required per ton ilmenite to obtain a desired TiO₂ slag chemistry65

Figure 28: Cold theoretical energy requirement for various reductant D feed ratios.....65

Figure 29: Illustrates the value chain flow and metal treatment costs in relation.....67

Figure 30: Treatment cost percentage deviation expressed against the best performer for various reductant ratios.....70

Figure 31: Carbon efficiency against Net Operating Profit percentage deviation from best performer.....71

Figure 32: Net operating profit deviation percentage from the best performer as a function of reductant ratio.....72

Figure 33: Fixed carbon percentage relative to the treatment costs.....72

Figure 34: Net operating profit deviation percentage from the best performer.....73

LIST OF TABLES

Table 1: Illustration of mass balance inputs for an ilmenite smelting process.....	27
Table 2: Illustration of mass balance outputs for an ilmenite smelting process.....	30
Table 3: Breakage and strength characteristics of lithotypes adapted from Falcon and Falcon 1987).....	40
Table 4: Summary of petrographic results.....	46
Table 5: Summary of reductant efficiency results and leading parameters.....	48
Table 6: Summary of slag products.....	50
Table 7: Summary of metal products.....	51
Table 8: Summary of reductant analysis.....	52

DEFINITIONS AND ABBREVIATIONS

LMPI – Low Manganese Pig Iron

VIU – Value In Use

MVA – Mega Volt Ampere

DC – Direct Current

MJ – Mega Joule

MWh – Mega Watt hour

Ilm – ilmenite

EE – Excess energy

PF – Peripheral feed

CTE – Cold Theoretical Energy

PFTE – Peripheral Feed Theoretical Energy

NOP – Net Operating Profit

ABSTRACT

Anthracites are the preferred reductant for utilization in the ilmenite smelting industry mainly due to the higher fixed carbon units, lower sulphur contents and relatively lower impurities found in the mineral matter content. The primary purpose of the reductant used in the process is to affect reduction of iron oxide forms and titanium oxide forms to yield a product of a low Mn pig iron (LMPI) and a slag containing titanium dioxide and iron oxide.

Industrial test work on various anthracites were undertaken to obtain a better understanding of reductant performance and their effect on process efficiency. The tests were designed to establish reductant efficiency per reductant type as a function of its petrographic characteristics, its influence on a mass and energy balance scale as applied to furnace energy algorithms and its contribution to the smelter Value In Use (VIU) total cost model.

Good correlations were found to exist between the vitrinite content and reductant efficiency. Lower reductant efficiencies are associated with higher vitrinite contents.

The mechanism of reductant loss, expressed as carbon efficiency, seems to be related to the shattering of anthracite when exposed to furnace freeboard conditions at approximately 1600°C in the presence of inherent and surface moisture associated with the reductant.

The d50 particle sizes between the reductants were found to be very similar due to a deliberate size processing step prior to the reductant utilization. Although no good correlation was found between d50 and reductant efficiency, a fair correlation exists between the -1mm particles and reductant efficiency. A finer size fraction has a higher propensity to escape from the offgas and report to losses.

A reduction in dissolved carbon in the metal for a decrease in TiO₂ percentage in the slag was found to occur in all likelihood as a result of a combination of carbon losses occurring due to decrepitation and reporting to dust losses or insufficient carbon units added initially.

A strong linear dependence exists between reductant ratio percentage and TiO₂ percentages in the slag. A strong linear dependence exists between theoretical energy requirements for varying reductant percentages. It was found that the reductant requirements are strongly dependent on reductant fixed carbon and reductant efficiency.

The carbon percentage in the metal is generally an order of magnitude higher than calculated equilibrium carbon percentage in the metal, indicating that non equilibrium conditions prevail in the metal bath.

Higher carbon content and lower vitrinite content anthracites performed better on overall Value In Use model due to the following reasons:

- ❖ **Higher carbon efficiencies** associated with lower vitrinite or rather higher inertinite contents lead to the use of **lower proportions of reductants** to obtain the desired chemistry in the product.
- ❖ **Higher carbon efficiencies** were also found to require **less energy** to obtain final product.
- ❖ **Lower energy inputs** lead to increasing the overall raw material feed input and ultimately increasing the final product output.
- ❖ **Lower treatment costs** of low manganese pig iron occurred due to **lower portions of reductant, less impurities** (sulphur) as a result of lower mineral matter in the reductant and **higher excess carbon** in the low manganese pig iron product.

ACKNOWLEDGMENTS

I would like to acknowledge the following individuals and institutions.

- Professor Rosemary Falcon for her guidance and supervision.
- Vincent Strangfeld and Willem Jordaan for their guidance and operational support.
- Tronox KZN Sands management providing me with the opportunity to lead the reductant test work.
- Dr. Johan Zietsman, Samantha Moodley and Jeremy de Souza on discussions around carbon equilibrium in iron as applicable to ilmenite smelters.
- Lara and Ethan Strydom for their moral support.

1. INTRODUCTION

Heavy minerals sands are mined from inland marine-derived dune deposits. The heavy minerals concentrate is separated from the sand and transported to a processing facility. Zircon, rutile and ilmenite are produced from the concentrate by means of magnetic and electrostatic processes. Crude ilmenite is refined and conveyed to the smelter to form the primary feed source to 36MVA DC arc furnaces.

The ilmenite smelting technology utilises a reductant as a direct carbon source for the reduction of ilmenite (FeTiO_3) to produce titanium slag and Low Manganese Pig Iron (LMPI). The reductant characteristics are primarily chosen to effect highly efficient reduction. This is determined in terms of high carbon content and good reactivity. Furthermore, the mineral matter content of the reductants play a role in the final specification of slag and metal products and directly affects the downstream yield and costs.

The simplified reaction for the production of slag and LMPI is as follows:



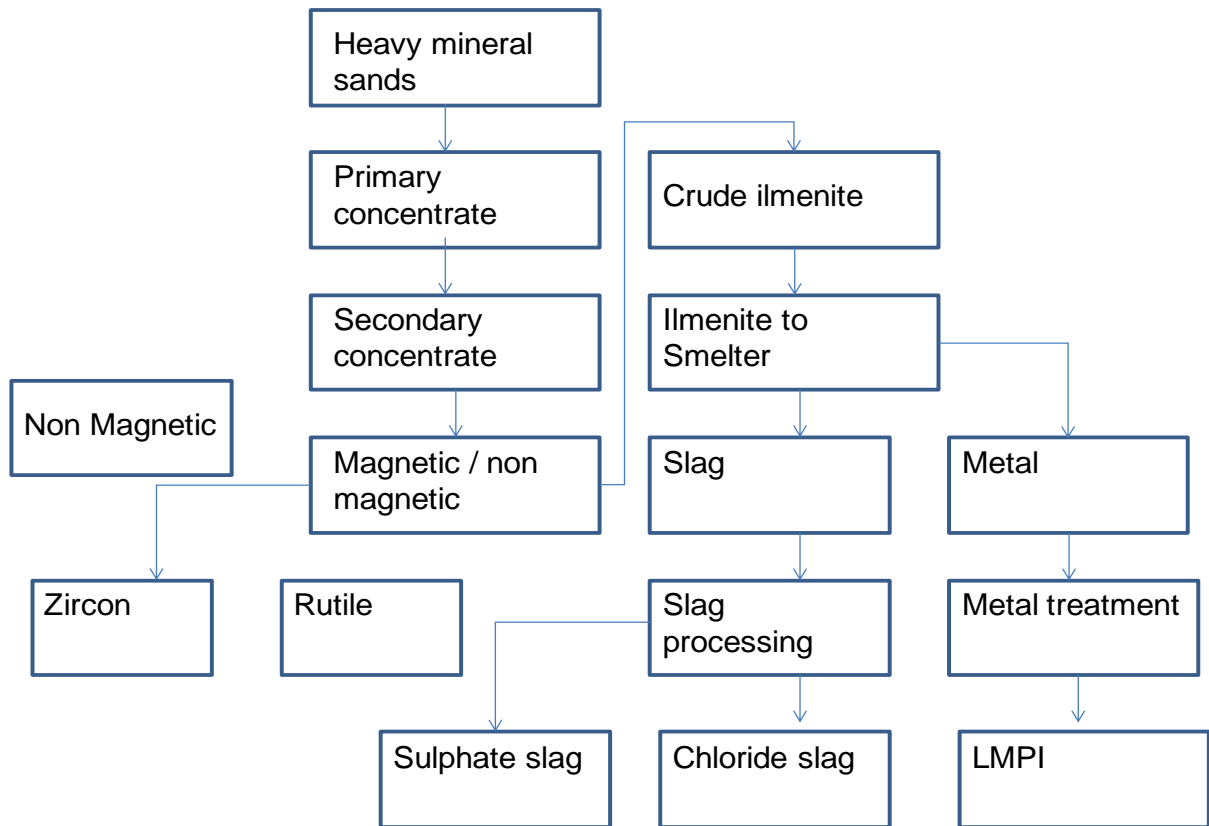


Figure 1: Heavy mineral process flow to smelter processing

The scarcity of reductants in South Africa requires the industry to look for alternative carbon sources of reductants. As reductants play a key role in furnace operation as the secondary feed source, it is paramount to understand the behavior of various reductants within the ilmenite smelting technology on an industrial scale.

The significance of this research is to determine, and then be able to predict, the behavior of various reductants in the DC ilmenite smelting environment. Such primary reduction raw materials have a direct and significant impact on the smelter value chain in as far as smelting energy, furnace chemistry control, freeze line behavior and final product quality are concerned. Choosing a suitable reductant for the ilmenite smelting process therefore entails a fundamental

understanding of the behavior of the reductant as applied in a large scale industrial operation.

Alternative carbon sources of reductants are sometimes only chosen and evaluated on a fixed carbon price basis, which only forms part of a fraction of the total value in use cost contribution, thereby overlooking the complete impact on a Value In Use (VIU) scale.

This study aims to quantify the Net Operating Profit (NOP) of specific reductants to the ilmenite smelter value chain based on various reductant characteristics as applied on an industrial scale. Broad based knowledge exists on reductant characteristics and behavior in ilmenite smelting using the test work that was completed on small scale pilot plant furnaces. However, these tests cannot accurately simulate the effect of a large scale industrial furnace operation. Very little if any knowledge exists on performance of various reductants on large scale operations.

The study will be used as a future guide for reductant selection for ilmenite smelters. In summary, this study aims to enhance the understanding of the performance of a specific reductant on the smelter value chain, the final product quality, furnace behavior and energy control.

In order to achieve these objectives, the following steps were undertaken:

- a. Analysis and evaluation of various reductants in terms of their reduction performance on specific ilmenites on a mass and energy balance scale to determine the theoretical energy requirement for smelting.
- b. Construction of an energy algorithm per reductant type based on the mass and energy balance outcome. Determination of the excess energy of the furnaces by using theoretical modelling, and empirical heat losses derived

from actual recorded furnace heat losses. Compilation of an integrated algorithm per reductant type for automatic feed control.

- c. Testing of the various reductants as secondary feed on an industrial scale to determine the actual reductant performance.
- d. Application of large scale test results into the mass and energy to recalculate reductant efficiency.
- e. Determination of the correlation between actual reductant efficiencies and a range of analyses including petrographic characteristics. Determine the correlation between reductant size and efficiency.
- f. Determination of the actual ilmenite feed rate (energy) per reductant type. properties suited for the ilmenite smelting process.

2. LITERATURE REVIEW

2.1 REACTIONS IN ILMENITE SMELTING

Ilmenite is one of the raw materials used in the production of TiO₂ slag and Low Manganese Pig Iron (LMPI). Ilmenite has a nominal composition of FeO.TiO₂ (Pistorius, 2008). This ilmenite composition is generally found in South African beach sands. This also contains approximately 3% impurities by mass. The associated impurities are mostly comprised of MnO, MgO, Al₂O₃ and SiO₂.

The ilmenite smelting process in South Africa utilizes electrical energy to smelt the ilmenite and anthracite is used as the carbon source for reduction.

The two (2) basic reactions in ilmenite smelting are as follows:



The first reaction proceeds further to the right than the second reaction, yielding a net composition that follows M₃O₅ stoichiometry. The slag composition can be viewed as a mixture of Ti₃O₅, FeTi₂O₅, MnTi₂O₅, Al₂O₅, MgTi₂O₅, V₂TiO₅ and Cr₂TiO₂. The mixture expressed as a single phase is better known as the M₃O₅ phase or karrooite. (Zietsman and Pistorius, 2004).

As a result of the FeO and Ti₂O₃ relationship in the slag following M₃O₅ stoichiometry, the slag chemistry can be represented as [(FeO.MgO.MnO).2(TiO₂)]_x . [(Ti₂O₃,Cr₂O₃, V₂O₃, Al₂O₃). (TiO₂)]_y. The expression entails that each divalent cation is associated with two tetravalent cations in the slag and each pair of trivalent cations is associated with one tetravalent cation in the slag.

The FeO and Ti₂O₃ relationship in the slag following the M₃O₅ stoichiometry can be tested by calculating the equivalent FeO in the slag (excluding CaO), expressed in moles FeO and the equivalent Ti₂O₃ content expressed as Ti₂O₃ moles.

$$(\%FeO)_{eq} = (FeO\%) + (M_{FeO} / M_{MgO})(MgO\%)+(M_{FeO} / M_{MnO})(MnO\%) \dots\dots\dots(3)$$

$$(\%Ti_2O_3)_{eq} = (\%Ti_2O_3) + (M_{Ti_2O_3} / M_{V_2O_5})(\%V_2O_5)+(M_{Ti_2O_3} / M_{Cr_2O_3})(\%Cr_2O_3)+ (M_{Ti_2O_3} / M_{Al_2O_3})[\%Al_2O_3 - (\%SiO_2)/3] \dots\dots\dots(4)$$

Figure 1 illustrates the actual trend of FeO to Ti₂O₃ relationship of slags produced from South African and Canadian (open circles) ilmenites to the calculated (broken line) M₃O₅ stoichiometry.

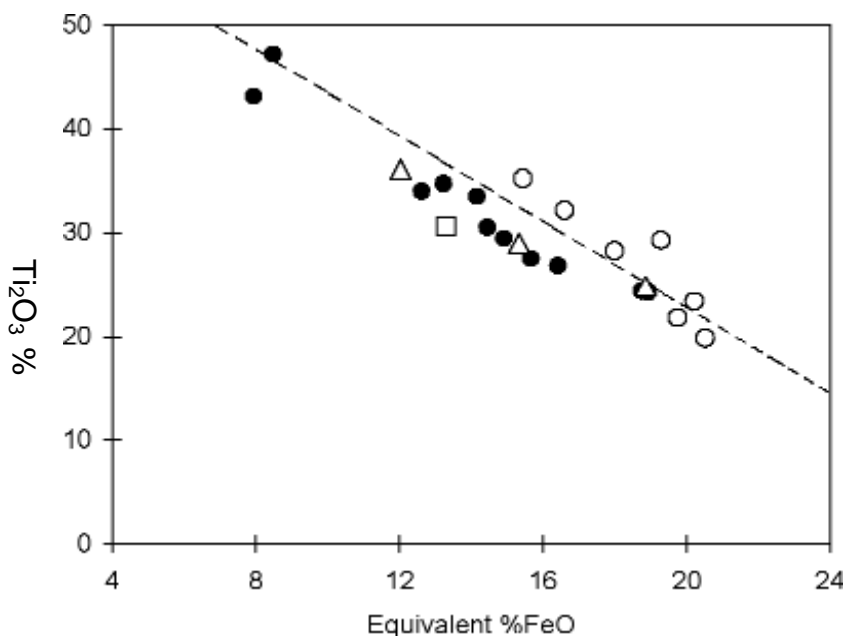


Figure 2: Calculated (Dotted line) vs. actual M₃O₅ stoichiometry between FeO and Ti₂O₃ for slags produced from South African and Canadian ilmenites. (Pistorius 2008)

The origins of the compositional relationship between FeO and Ti₂O₃ were previously broadly identified as reaction equilibria, kinetic effects and phase chemistry (Zietsman and Pistorius, 2004).

Equilibria between the iron and slag baths are reached at higher FeO and Ti_2O_3 levels than required by the M_3O_5 stoichiometry, as suggested in Figure 3, ruling out that reaction equilibrium is the controlling factor in the compositional correlation.

Zietsman and Pistorius (2004) suggested that the kinetic effects through reduction of FeO to Fe and TiO_2 to Ti_2O_3 governing the effect of slag composition to deviate from equilibrium to be unlikely due to the following reasons:

- The FeO and Ti_2O_3 are too consistent for furnaces that vary significantly in size and would have different stirring patterns.
- The TiO_2 concentration in the slag is much higher when compared with the FeO in the slag, decreasing the likelihood of mass transfer to cause lower reduction rates of TiO_2 to Ti_2O_3 .
- Canadian ilmenites show lower Ti_2O_3 concentrations for various FeO contents as compared to South African ilmenites.

The influence of phase chemistry through the effect of freeze lining in the furnace on the compositional formation FeO and Ti_2O_3 relationship was investigated to rule out that phase chemistry is a likely mechanism for the formation of the FeO and Ti_2O_3 relationship.

A new mechanism was proposed by Zietsman and Pistorius (2004) on the basis of the following criteria: (i) That the mechanism must have a sustained influence on the composition of the slag bath while ilmenite, reductant and energy is fed into the furnace and (ii) that the mechanism must be able to adjust the slag composition towards M_3O_5 stoichiometry.

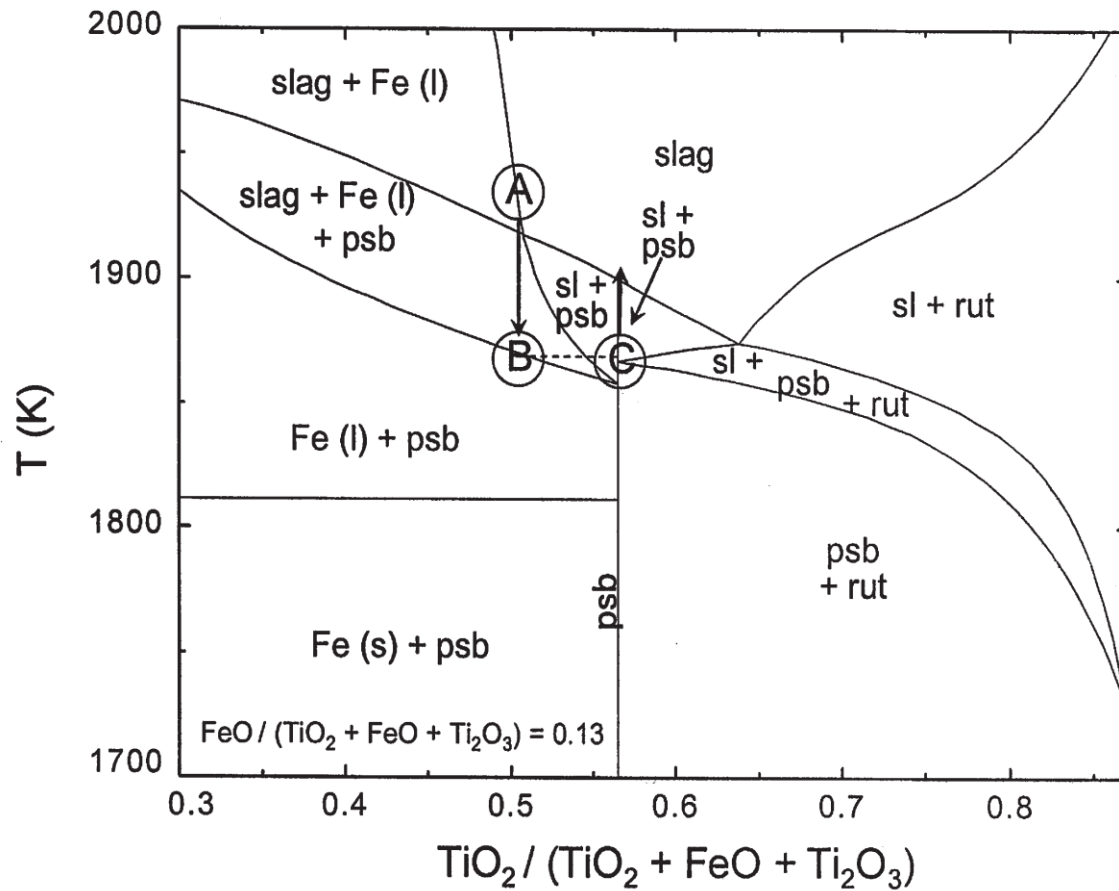


Figure 3: Constant FeO pseudo-binary section through FeO- TiO₂- Ti₂O₃ ternary phase diagram. 'rut' = rutile solid solution phase. 'psb' = pseudo-brookite solid solution phase (M₃O₅). Mass percentage of FeO = 15.0% (Pistorius 2008).

Pistorius (2008) proposes the following mechanism in order to adjust the slag composition towards M₃O₅ stoichiometry.

Ilmenite and reductant react to achieve equilibrium with iron in the hotter zones close to the electrode. This region corresponds with point A in figure 3. The slag in point A circulates towards point B in figure 3 causing precipitation of pseudo-brookite and iron. The denser iron is then drained to the metal bath. The formation of the metallic iron occurs as a result of the disproportionation reaction as expressed in equation 5. The loss of iron shifts the remainder of the oxides to M₃O₅ stoichiometry (pseudo-brookite).

The pseudo-brookite circulates to the hotter areas of the bath where it is remelted. The heat of solidification of the M_3O_5 phase releases energy that would have an expected increase in heat extraction on the hearth as production rates increases.



Reductant particles have the tendency to float on top of the bath due to their lower density. It is proposed that the mechanism of reduction of FeO and TiO_2 takes place by means of mass transfer of the CO gas through the gas halo of the reductant particle and regeneration of CO gas through the Boudouard reaction (reaction 8)



Reductant size might play a role in the reduction reactions if the area of the gas halo is dependent on the reductant size. It could then be expected that smaller reductant fractions will increase the area for reduction to take place.

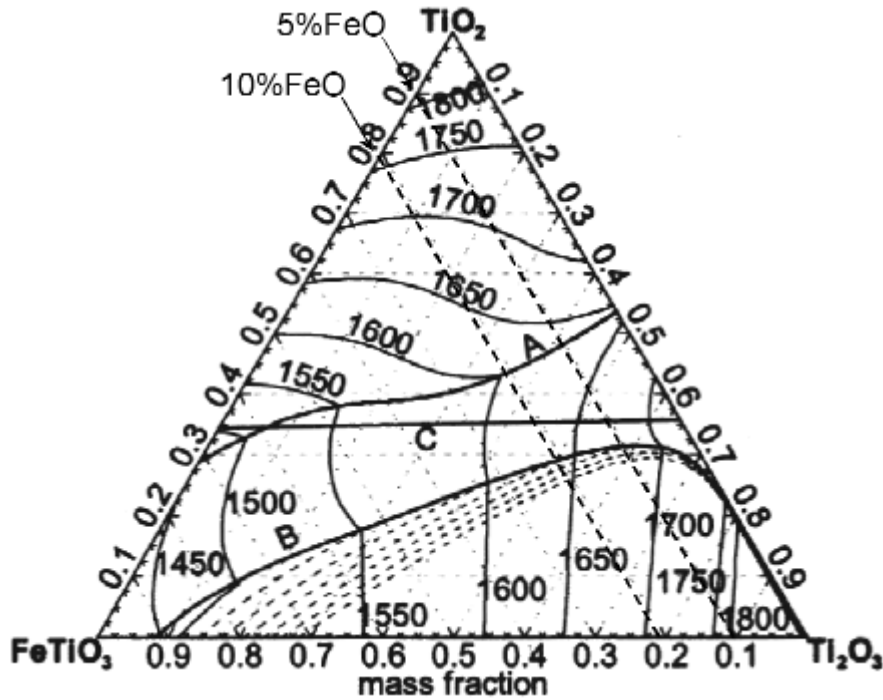


Figure 4: Calculated liquidus temperatures as a function of mass fraction. (Pistorius 2008).

Figure 4 illustrates the effect of varying FeO and $\text{TiO}_{1.5}$ on the liquidus temperature of the slag. The FeO and $\text{TiO}_{1.5}$ serves as a flux and tends to lower the slag liquidus temperature. Figure 5 illustrates the narrow gap between liquidus and solidus temperatures for varying FeTi_2O_5 fractions

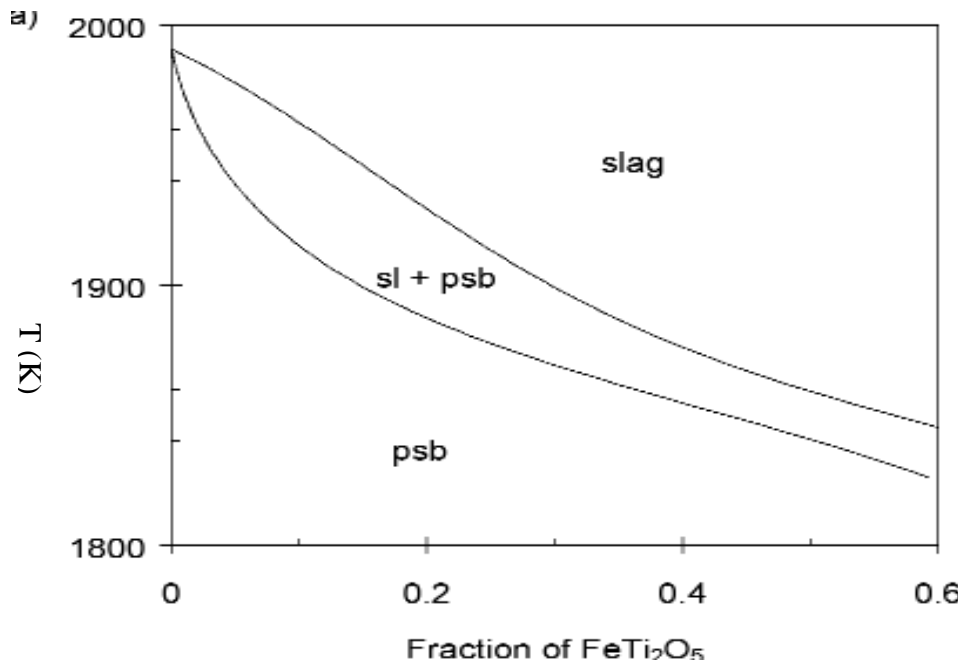


Figure 5: Calculated liquidus solidus temperatures along the Ti₃O₅ and FeTi₂O₅ join (Pistorius 2008).

Energy balancing with the ilmenite smelting process is a challenge since the final product composition and final product temperature cannot be controlled independently. A balance between raw material inputs and electrical energy must be achieved to obtain a desired chemistry and to maintain freeze line control.

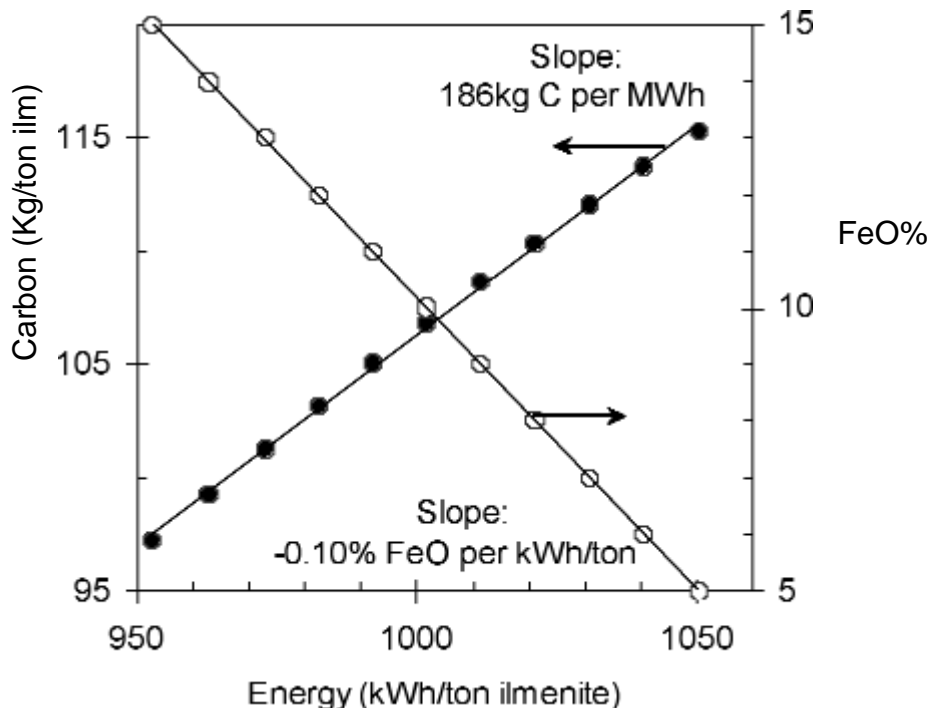


Figure 6: Calculated relationship between theoretical energy required as a function of FeO content in the slag and carbon input (Pistorius 2008)

The aim final product chemistry is directly influenced by the amount of carbon used and the amount of energy added to obtain that specific chemistry for a given ilmenite composition. Figure 6 indicates that to aim for a low FeO chemistry in the slag will require more energy input and will thus require more carbon input.

Figure 8 shows the empirical correlations between FeO, TiO₂ and Ti₂O₃. The correlation is typically used for mass and energy balance estimations and conforms to South-African ilmenites.

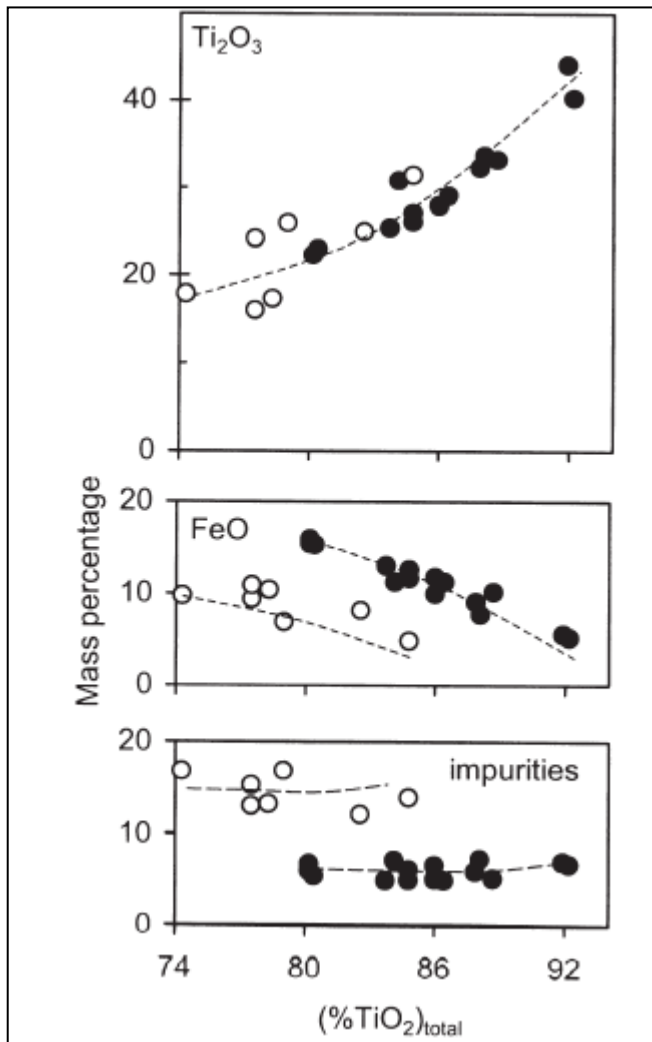


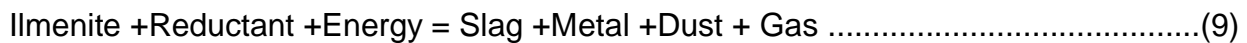
Figure 8: Changes in FeO and Ti₂O₃ content of ilmenite smelter (Zietsman and Pistorius, 2004). The filled circles indicate South-African ilmenites and the open circles indicate Canadian ilmenites.

2.2 MASS AND ENERGY BALANCING

Theoretical mass and energy balancing is crucial in the industrial furnace operations as it provides a tool for controlling mass and energy inputs for maintaining product quality and protecting furnace integrity. The first mass and energy balances for industry are normally developed under pilot plant conditions.

The basic principle of a mass and energy balance is that the law of conservation is applied on both mass and energy inputs and outputs.

In the case of ilmenite smelting the following simplistic mass flow is applied:



Equation 9 can be represented in the following simplistic equation chemical equation:

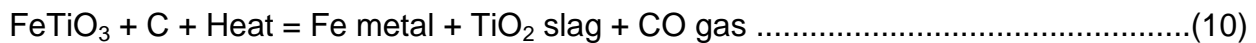


Figure 8 shows a basic layout of a DC arc furnace depicting the elements used in mass and energy balancing. The feed materials and heat losses mostly absorbs the heat while electrical energy is added to overcome the energy deficit.

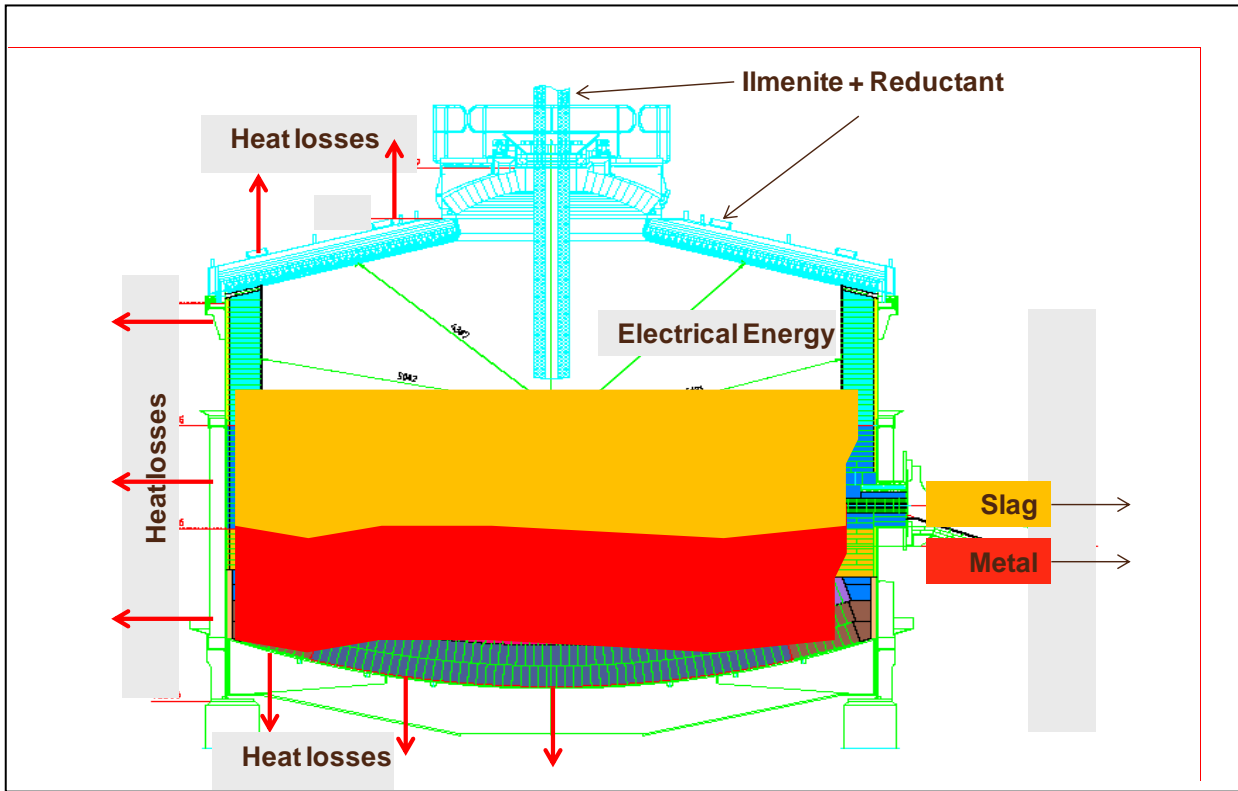


Figure 9: Simplistic mass and energy balance representation in ilmenite smelting.

2.2.1 MASS AND ENERGY BALANCE INPUTS

The mass balance inputs are comprised of ilmenite and reductant. The chemical analyses (XRF Press powder) of the ilmenite must be converted to elemental cations and then normalized to 100% to improve the accuracy of calculation. The reductant analysis method comprises of a proximate, ultimate and XRF press powder analysis for mass and energy balance purposes. The reductant analyses are also normalized for more accurate calculations.

Table 1 illustrates the conversion from ilmenite and reductant oxides to elemental cations.

Ilmenite chemical components %	Ilmenite elemental %	Reductant	Reductant typical %	Reductant oxides %	Reductant elemental %
TiO ₂ = 48	Ti = 28	Surface moisture	1	TiO ₂ = 1.45	Ti= 0.86
FeO = 35	Fe ²⁺ = 27	Inherent moisture	2	FeO= 0	Fe ²⁺ = 0
Fe ₂ O ₃ = 15	Fe ³⁺ = 10	Ash	10	Fe ₂ O ₃ = 12	Fe ³⁺ = 9
SiO ₂ = 1	Si= 0.46			SiO ₂ = 45	Si= 21
Al ₂ O ₃ = 0.3	Al= 0.16			Al ₂ O ₃ = 24	Al= 12.7
MgO= 0.5	Mg= 0.32			MgO= 0.9	Mg= 0.5
CaO= 0.11	Ca= 0.07	Ultimate analysis		CaO= 1.5	Ca= 1.1
MnO= 1.1	Mn= 0.86			MnO=0.1	Mn= 0.07
V ₂ O ₅ = 0.2	V= 0.13	C	85	V ₂ O ₅ = 0.04	V= 0.02
Cr ₂ O ₃ = 0.1	Cr= 0.07	H	2.4	Cr ₂ O ₃ = 0.03	Cr= 0.01
ZrO ₂ = 0.17	Zr= 0.12	O	0.99	ZrO ₂ = 0	Zr= 0
P ₂ O ₅ = 0.01	P= 0.004	N	1.8	P ₂ O ₅ = 0.1	P= 0.04
K ₂ O	K	S	0.9	K ₂ O= 2.5	K= 2.3
Na ₂ O	Na			Na ₂ O= 0.6	Na= 0.4
SO ₃	S			SO ₃ = 0	S = 0

Table 1: Illustration of mass balance inputs for an ilmenite smelting process.

2.2.2 MASS AND ENERGY BALANCE OUTPUTS

The mass balance outputs are divided into slag, metal, dust and gas components. A starting point of mass calculation is to assign a tap mass to the main product (slag) together with a projected TiO₂ percentage to the slag. The assignment in conjunction with the elemental distribution coefficients between slag, metal, dust and gas will enable the calculation towards ilmenite mass determination.

The distribution coefficients are empirically determined and will vary as a function of furnace design, ilmenite composition, reductant composition and furnace operating philosophy. The distribution coefficients will vary as a function of the required chemistry that is associated with varying degrees of reduction. It is to this end that the elements that are affected by the degree of reduction are correlated to required aim chemistries.

The ilmenite mass can be calculated as follows:

$$\text{Ilmenite mass} = [\text{TiO}_2 \text{ aim}\% / (\text{molar mass TiO}_2)(\text{molar mass Ti})(\text{slag mass})] / \text{Ti}\% \text{ dist. to slag} / \text{Ti}\% \text{ in ilmenite} \dots\dots\dots(11)$$

The equivalent FeO percentage in the slag is empirically assigned as a function of the TiO₂ and FeO relationship as illustrated in figure 8 .This correlation is very specific to the input materials and is calibrated on actual plant data. The Ti⁴⁺ and Ti³⁺ relationship is empirically derived from the FeO percentage in the slag and is illustrated in figure 8.

An initial reductant ratio is assumed to calculate the first order material mass outputs as a function of the partition coefficients. Since the slag mass, ilmenite mass and initial reductant mass are known, the masses can be distributed to the output components.

2.2.3 CARBON REQUIREMENT

The carbon requirement is calculated stoichiometrically from the following reaction based on the known mass of the components:





Reactions 12 to 26 all occur to the extent that is determined with partition coefficients of elements between slag metal and dust.

The excess carbon requirement to the metal must be included in the total carbon requirement. The iron mass is calculated in order to obtain the excess carbon mass. The excess carbon percentage requirement is assigned and is a known value.

The iron mass will typically be calculated with the formula in equation 27:

$$\text{Total Fe in metal} = \text{Total Fe in feed} - (\text{Fe in slag} + \text{Fe in dust}) \dots\dots\dots(27)$$

The total Fe units in the feed, slag and dust are stoichiometrically converted to obtain an iron mass. Once the iron mass in metal is obtained the assigned percentage of excess carbon can be converted to mass in equation 28.

$$\text{Tons excess carbon} = [\% \text{ Excess carbon} \times (\text{Fe in metal} - \sum \text{ elemental components in metal mass})] / (100\% - \% \text{ Excess carbon}) \dots\dots\dots(28)$$

The total reductant requirement is calculated to include the electrode consumption, the fixed carbon percentage in the reductant and an assigned carbon efficiency percentage and is expressed in equation 29.

$$\text{Total carbon mass} = (\text{Stoichiometric requirement} + \text{Tons excess carbon} - \text{Electrode consumption tons}) / \text{Fixed carbon \% in reductant} / \text{carbon efficiency \%} \dots\dots\dots(29)$$

2.2.4 GAS VOLUME DETERMINATION

The CO gas volume is determined by stoichiometric conversion of equations 12 to equation 26. The total CO gas tons is then converted to STP conditions. CO₂ is primarily determined from assigned air ingress value into the furnace and CO₂ produced from surface and inherent moisture obtained from the reductant feed. H₂ mass is obtained from the total moisture in the reductant and the moisture associated with the air ingress into the furnace. Sulphur in the reductant is stoichiometrically converted to sulphur in the gas. All the gas masses are converted to standard temperature and pressure conditions. Table 2 illustrates the typical species and elements in the slag, metal, dust and gas phases

Slag chemical components %	Metal chemical components %	Dust chemical components %	Gas chemical components %
TiO ₂ = 52.8	Fe = 97	TiO ₂ = 62	CO = 81
Ti ₂ O ₃ = 30.7	C = 2.3	FeO = 12.8	H ₂ = 16
TiO ₂ Eq = 85	Ti = 0.05	SiO ₂ = 15.46	N ₂ = 1.8
FeO = 9	Si = 0.015	Al ₂ O ₃ = 0.81	S ₂ = 0.04
SiO ₂ = 2.1	Al = 0.004	MgO = 0.5	O ₂ = 0
Al ₂ O ₃ = 0.9	Mg = 0	CaO = 0.04	CO ₂ = 0.8
MgO = 0.9	Ca = 0	MnO = 2	
CaO = 0.1	Mn = 0.035	V ₂ O ₅ = 1.4	
MnO = 1.9	V = 0.02	Cr ₂ O ₃ = 0.6	
V ₂ O ₅ = 0.4	Cr = 0.06	ZrO ₂ = 0.06	
Cr ₂ O ₃ = 0.3	Zr = 0	P ₂ O ₅ = 0.01	
ZrO ₂ = 0.2	P = 0.023	K ₂ O = 0.7	
P ₂ O ₅ = 0	K = 0	Na ₂ O = 0.2	
K ₂ O = 0.01	Na = 0	S = 3.1	
Na ₂ O	S = 0.11	C = 0.9	
SO ₃			

Table 2: Illustration of mass balance outputs for an ilmenite smelting process.

2.2.5 ENERGY DETERMINATION

The energy associated with the input and output masses are determined by using the Factsage model and by calculating the enthalpy for input and output temperatures. Total energy of the species is determined by converting the moles of the species into energy expressed in MJ.

Enthalpy is defined by equation 30.

$$H = U + PV \dots\dots\dots(30)$$

P and V represent pressure and volume whereas U represents internal energy. Internal energy can be interpreted as energy that is required to create a system in the absence of changes in temperature and pressure.

The generic energy equation can be expressed as follows:

$$\text{Energy (MJ)} = (\text{Moles of specie} \times H^0_{Tx}) / 10^6 \dots\dots\dots(31)$$

Since the specie masses are known, the mole values for the individual species can be calculated. The slag temperature is empirically calculated based on industry data and linked to an output variable such as FeO percentage in the slag. The metal temperature is an assigned value and is related to typical metal temperatures in industry. The dust and gas temperatures are equated to the slag temperature.

Theoretical energy is determined on the basis of smelting 1 ton of ilmenite to obtain a specific chemistry. The theoretical energy required is essentially governed by input materials and the extent of reduction required.

The total theoretical energy requirement per ton of ilmenite can be expressed in equation 32.

$$\text{Theoretical energy (MWh/ton ilm.)} = [(\sum \text{ outputs} - \sum \text{ inputs}) / 3.6] / (\text{Kg ilm.}) \dots\dots\dots(32)$$

2.2.6 EXCESS ENERGY (EE)

Excess energy is defined as furnace heat losses. The furnace heat losses are continuously measured online as a function of water flow and differential temperature measurement. The heat losses are correlated against power input and an algorithm is created to determine the total ilmenite to be fed for a setpoint MWh power input. The excess energy is expressed in MW. See Figure 8 for a diagrammatic representation of this.

2.2.7 TOTAL ILMENITE FEED ALGORITHM

The furnaces are operated on the principle of constant power and therefore the total amount of ilmenite is calculated as a function of power setting, excess energy and theoretical energy. The ilmenite feed is determined as follows:

$$\text{Ilm. feed} = [(EE + \text{PF tons} \times (\text{CTE} - \text{PFTE})) / \text{CTE}] \dots\dots\dots(33)$$

EE = Excess energy

PF tons = peripheral feed tons

CTE = Cold theoretical energy

PFTE = Peripheral feed theoretical energy

CTE is expressed in an algorithm linked to reductant requirement.

2.2.8 CARBON EQUILIBRIUM

Pistorius et al (2011) noted that the typical carbon contents of iron in ilmenite smelting is around 2%, whereas the carbon content for equilibrium with molten slag will be one order of magnitude smaller than this, around 0.2%. This means that carbon in the metal can reduce TiO_2 and FeO in the slag, at the slag metal interface.

Pistorius et al (2011) explored the possibility of oxycarbide formation at the slag metal interface and used the following reactions in the assessment:



The principle of the test according to Pistorius et al (2011) was that if the sum of the oxygen activities equates to 1, then an ideal solid solution of TiO and TiC can form by reactions 34 and 35 as a separate phase. If the sum of the activities is smaller than 1 then oxycarbide cannot form.

Pistorius et al (2011) reported that the results show that the formation of oxycarbide to cannot take place under the prevailing conditions at the slag - metal interface. If the slag had to come into contact with pure graphite or carbon saturated iron, the higher carbon activity and lower oxygen activity would allow for the formation of oxycarbide. In reality (Pistorius et al, 2011), the carbon activity of iron with 2% carbon is much lower which will lead to no oxycarbide formation.

Pistorius et al (2011) constructed a correlation between carbon percentages in the metal to titanium percentage in the metal as follows:

$$[\% \text{Ti}] = 0.008 [\% \text{C}]^{2.54} \dots\dots\dots(36)$$

Carbon equilibrium in the metal was calculated by the use of the following equations:



$$K = (p_{\text{CO}} \times a_{\text{Fe}}) / (a_{\text{C}} \times a_{\text{FeO}}) \dots\dots\dots(38)$$

K = equilibrium constant

p = Partial pressure (atmosphere)

a = Raoultian activity

$$a_{\text{FeO}} = 0.061$$

$$\Delta G = -R \times T \times \ln K \dots\dots\dots(39)$$

$$\Delta G = G^{\circ} \text{ products} - G^{\circ} \text{ reagents} \dots\dots\dots(40)$$

At 1500°C with a FeO of 9%, the equilibrium carbon % equates to 0.261%. This value corresponds with Factsage results in Appendix 10.25.

2.3 SUITABILITY OF REDUCTANTS FOR ILMENITE SMELTING

2.3.1 TESTING OF REDUCTANT SUITABILITY IN ILMENITE SMELTING

Jordan (2009) characterized various reductants with existing and newly developed techniques and tested CO₂ reactivity as a behavioural analysis. A range of reductants were selected for characterization.

On reaction rates, an equation developed by Grigo (2008) was used to evaluate the apparent reaction rates of anthracites. Equation 41 expresses the reaction rate of the reductants as gram per gram per second. C_r is grams of carbon reacted and C_i is the grams of carbon remaining.

$$R_R = (C_r / C_i) / \text{Time}_{\text{seconds}} \dots\dots\dots(41)$$

Jordan concluded that the reaction rates are a useful tool as part of the reductant characterization for furnace utilization for anthracites with a diverse maceral and mineral composition.

Jordan (2008) referred to decrepitation as a measure of breakdown of material during heating. Walsh, Jr. and Dutcher (1959) performed test work on various lithotypes of anthracite to determine the decrepitation under controlled heating rates and under thermal shock exposure conditions.

Walsh, Jr. and Dutcher (1959) tested the affect of decrepitation on vitrain, durain, clarain and fusain lithotypes. The test work indicated that that at controlled heating rates varying from 25°C/min. to 68°C/min, no visible decrepitation of any lithotypes occurred up to a maximum temperature of 980°C, although it was observed that the fusain particles after treatment was much weaker than before and was easily crushed.

The thermal shock treatment test involved rapid heating of the lithotypes to temperatures ranging from 500°C to 950°C. The clarain particles almost immediately fractured at 800°C and 950°C. The fusain particles underwent no cracking from 500°C to 800°C although the treated product easily crushed when handled. Visible cracks and splitting could be observed on the fusain particles at 950°C. The durain particles only showed visible cracks at 950°C, while the vitrain particles showed cracking and splitting at 950°C.

Walsh, Jr. and Dutcher (1959) decrepitation test results indicated an increasing order of resistance to thermal shock of (1) fusain, (2) clarain, (3) vitrain and (4) durain. The test observations seem to be supported by the breakage and strength characteristics of lithotypes that is presented in table 3 page 38 adapted by Falcon and Falcon (1987)

2.3.1 CONSTITUTION AND THE PHYSICAL AND TECHNICAL PROPERTIES OF COAL

The organic composition of coal refers to the maceral composition of coal. The macerals are divided into three groups known as vitrinite, liptinite and inertinite. Discernable differences between these macerals can be expressed by means of reflectance, morphology, hardness, shape, size, colour and fluorescence.

According to Falcon and Falcon (1987), various proportions of macerals and minerals constitute microlithotypes and these are said to be a useful indicators of the environment in which coal was formed. Four (4) types of microlithotypes exist in the category of humic coals. These coals were basically formed by plant tissues that accumulated in different environments in the original peat swamp. The microlithotypes can be defined as follows: (See Figure 10)

Vitrain micro-lithotypes are the brittle bright bands that have a shiny lustre in coal. Clarain micro-lithotypes are intermediate bright banded coal that has less of a shiny lustre than the vitrain micro-lithotypes. Durain micro-lithotypes are associated with a dull

banded hard coal that is grey to black in colour. It represents the agglomeration of oxidized and carbonized plant remains (Falcon and Falcon, 1987). Fusain micro-lithotypes are composed of flat narrow bands that look like charcoal rectangular patches. Fusain micro-lithotypes are very friable.

Sapropelic coals are bands of organic matter that accumulated in open pools such as lakes and marshes. They are composed of windblown or water-carried plant material, algae and plankton that formed fine black slimy vegetable layers. These layers can be associated with mineral matter.

Coal has certain mechanical properties as a result of the petrographic structure thereof Falcon and Falcon (1987). See table 3 page 38. Coal strength refers to the coal's compressive strength and is governed by some basic factors as follows:

- Compressive strength is inversely proportional to the size of the coal. A larger coal size decreases the compressive strength required for breakage. Heterogeneous layer in a seam alternatively requires more compressive strength for breakage. Falcon and Falcon (1987)
- Compressive strength is also inversely proportional to the orientation of a particle in terms of its layering or bedding plane and to the amount of cracking in a coal. Breakage will increase when a particle is orientated parallel to bedding plane, and a higher propensity to cracking and an accompanying decrease in compressive strength with more cleats.
- Coal tends to break along the planes of maximum shear stress at elevated temperatures (100°C), and will preferentially break along parallel planes in the direction of compression at room temperature.
- Coal band composition correlates well with the strength of the bands since each lithotype has a specific breakage characteristic.

In terms of hardness, Jeremic (1980) suggested the following classification for coal:

Hard (durian, shaley coal and coaley shale).

Semi hard (clarian or combination of clarian, durian, vitrian).

Soft coal (vitrian).

Very soft coal (fusian).

The hardness of a coal is essentially related the maceral composition. The presence of mineral matter that is well dispersed in syngenetic forms in the matrix instead of epigenetic minerals filling the coal cleats, will increase the coal strength. Coal with the lowest hardness contain vitrite due to the highest frequency of fissures in vitrinitic coal bands and fusites as a result of their characteristic friability.

Weathered anthracite has the ability to store water in the cracked fissures and upon high temperature exposure the water can turn to steam causing thermal shattering resulting in deflagration and the shattering of particles (Falcon, 2005).

In terms of reaction (i.e. consumption of carbon in coal during heat-up), vitrinitic macerals are more reactive than inertinite in gaseous environments at temperatures below 1400°C. Falcon (2005) reports that between 1400°C and 1800°C, vitrinite and inertinite macerals are known to react at approximately the same rates in gaseous environments. Above 1800°C, vitrinite macerals begin to graphitise and bond more tightly, therefore becoming less reactive than inertinite in gaseous environments at those temperatures. However, once graphitised, vitrinite macerals become highly reactive in liquid bath environments. Falcon (2005) reports that vitrinite molecules at temperatures above 1800°C typically form large two-dimensional mono-layers of carbon-rich lamellae bonded together by very weak interconnecting bonds. These bonds break in high temperature liquid environments, thereby releasing the carbon molecules into the liquid bath permitting high carbon reactivity and metal reduction in this environment. In high temperature gaseous environments, the graphitic structure renders the vitrinite unreactive.

Inertinite macerals, on the other hand, remain in multidimensional disorientated aromatic structures with little or no change with increasing temperatures (Falcon, 2005). They do not break up in liquid environments but are more reactive than graphitised vitrinite in high temperature gaseous conditions.

In summary, liquid phase reactions will favour the preferential reaction with vitrinite due to the breakdown of the weak vertical bonds in the graphite structures as opposed to the stronger multidirectional bonds of inertinite. For these reasons the petrographic composition of coal has now become of considerable interest to those seeking more efficient carbon reductants in the metallurgical industry.

Relationship between macro- and micro- composition of coal

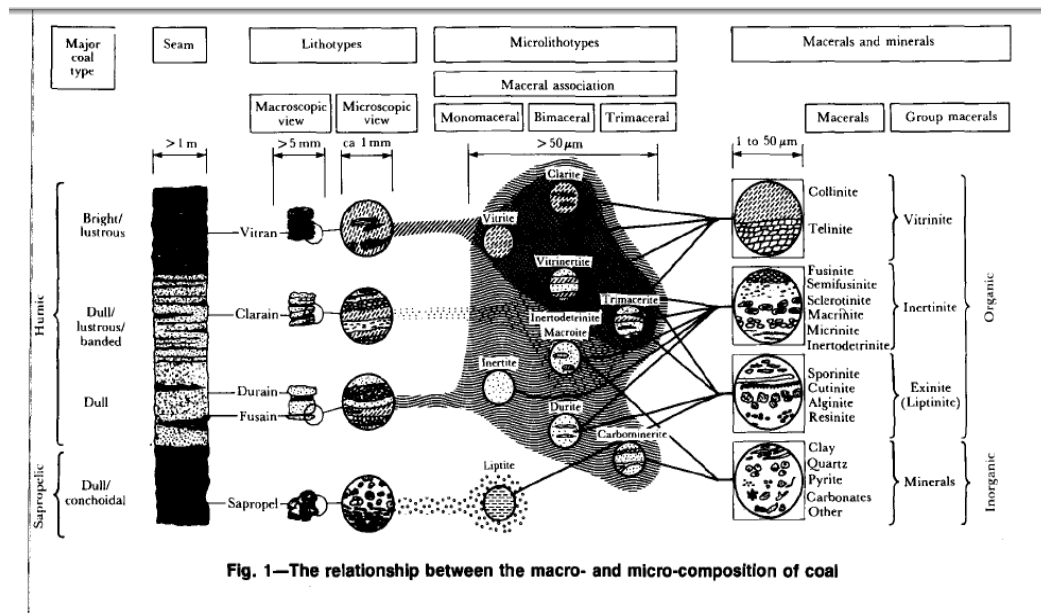


Fig. 1—The relationship between the macro- and micro-composition of coal

Figure 10: The relationship between macro - and micro- composition of coal. Falcon and Falcon (1987).

Breakage strength characteristics of lithotypes

Item	Vitrain	Clarain	Durain	Fusain
Description	Bright, shining vitreous	Bright to semi-bright laminated bands	Dull, dark grey to black; massive compact to granular; lustreless structures	Flat, fibrous, bright rectangular lenses.
Breakage characteristics	Brittle, cubic blocks, angular fractions	Semi-brittle to shattering and shearing	Inelastic, dense, solid, hard, tough, resistant to breakage	Friable, soft, easily pulverised to dust
Major microlithotypes	Vitrite, Clarite	Clarite, Vitrinertite, Trimacerite, Durite	Durite, Inertite, Semifusite, Inertodetrinite, Carboninerite	Fusite, Semifusite
Major macerals	Vitrinite	Mixed	Inertinite (no fusinite)	Inertinite (only fusinite)
Crushability (de-ashed ratio)	3.8	5.1	13.6	1.8
Density	1.3 – 1.4	1.3 – 1.5	1.5 – 1.7	1 – 1.25
Strength categories of Geremic	Soft, Vitrain	Semi hard clarain + composite of vitrain, clarain and durain	Hard, durain shaley coal, coaly shale	Very soft, fusain
Cleavage	Intensive regular	Irregular erratic	Traces or none, un-cleated	Open fractures
Uniaxial compressive strength, mega neutrons/m ²	1-7	7-18	20-40	0-1
Bore-hole core breakage	Often fragmented	Discs and half cylinders	Cylindrical core, height greater than diameter	Fines down to 320
Breakage on uniaxial compression	Cracking, compaction, yielding	Elasto-plastic failure	Elasto-brittle failure	Flow deformation and pulverization
Sizing after compression	Fine to nut size	Small lumps	Large lumps	Very fine sizes

Table 3: Illustrating the breakage and strength characteristics of lithotypes adapted from Falcon and Falcon (1987)

3. METHODOLOGY

Various Northern Hemisphere anthracites were tested on a large scale in a 36MVA DC arc furnace for various continuous periods of time. The methodology applied to each anthracite under investigation involved the following steps:

3.1 METHODOLOGY OF PREPARATION

3.1.1 Anthracite samples were analysed using XRF press powder tests, proximate analysis, ultimate analysis and petrographic analysis. The proximate analysis involved the determination of inherent moisture, volatile matter, ash content (mineral matter) and fixed carbon content by difference. The ultimate analysis provided the elements present in coal (i.e. C,H,O,N,S). The XRF press powder analysis measured the chemical oxides in the coal as mineral matter or ash after combustion. The petrographic analysis involved the examination of crushed coal particles using oil immersion under reflecting light using an ore microscope to determine the rank and maceral composition of coal.

3.1.2 The properties and technical performance of anthracite and ilmenite were analysed on a mass and energy balance scale.

3.1.3 Energy algorithms were compiled for each reductant based on the mass and energy balance outcome applied during testing. Theoretical energy was correlated with reductant percentage to enable a more efficient use of the energy algorithm.

3.1.4 Initial reductant requirement for full scale test was calculated based on the mass and energy balance. Initial carbon efficiency values were assigned.

- 3.1.5 The mass and energy balance was calibrated to reflect actual correlations between slag temperature, chemistry, TiO_2 and FeO . The calibration also involved the verification of the partition coefficients between slag, metal, dust and gas.
- 3.1.6 The test anthracites were phased into the furnace bins by ensuring that the preparation plant contained the test material and monitored the levels of the smelter bins. The duration of purging the system was estimated at 24 hours.
- 3.1.7 The test procedure stipulated that the anthracite samples be taken and composited per day. These samples were analysed daily to obtain the proximate and chemical analysis. Similarly, the ilmenite processed were analysed on a daily basis.

The reductant to furnace flow sheet is illustrated in Figure 11 below.

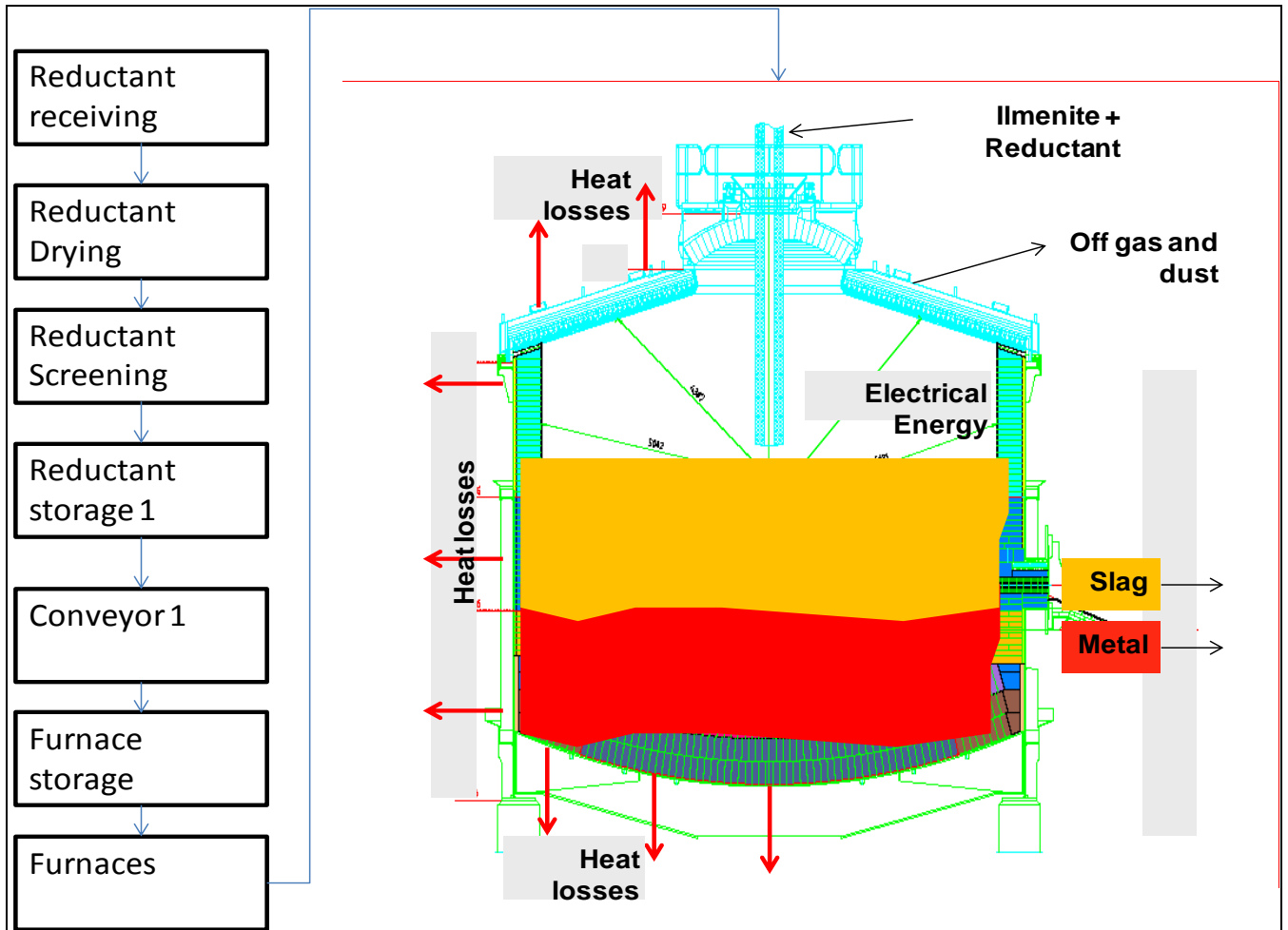


Figure 11: Reductant to furnace flow sheet

3.2. DATA OBTAINED AFTER TEST CAMPAIGNS

The following data was obtained after the various test campaigns.

3.2.1 XRF press powder chemical analysis of slag produced. Chemical and proximate analyses of the reductants. Reductant size analysis. Metal chemical analysis.

3.2.2 Slag and metal temperatures of each tap related to the campaign.

3.2.3 Furnace power settings.

3.2.4 The tonnages of ilmenite and reductant fed. The tonnages were recorded at 5 second intervals from the Schenk feeding systems and were cumulated over time.

3.2.5 Gas volume evolution recorded on gas flow meters past the gas scrubbing system.

3.3 METHODOLOGY OF EVALUATION

The approach undertaken to evaluate the data is summarised as follows:

3.3.1 Weighted average chemical analyses, weights and temperatures were determined for the data recorded per campaign.

3.3.2 Weighted average reductant size distributions were calculated per campaign.

3.3.3 Reductant efficiencies per campaign were determined by utilizing the weighted average data and applying it to the mass and energy balance. The efficiency determination is discussed in section 2.2.3.

3.3.4 Reductant efficiencies were correlated against petrographic data for the tested reductants.

3.3.5 Energy algorithms were corrected based on the determined carbon efficiency.

3.3.6 A smelter value in use model was created that describes the influence of various reductants on the value chain.

3.3.7 An algorithm was created to rate reductants on a VIU scale for suitability of use in ilmenite smelting. A matrix is derived from the VIU model that incorporates the influence of reductants on final products.

4. RESULTS

4.1 PETROGRAPHIC RESULTS

The petrographic analyses presented in Table 4 indicate that the reductants tested had vitrinite mean random reflectance values of between 3% and 4%, placing all four reductants in the category High Rank B or Anthracite, according to ISO11760 and SANS ISO 11760 International Classification of Coals. This analysis indicates there is little if any difference in rank between the coals.

In terms of maceral composition, all reductants have mid-ranging vitrinite contents (i.e. 48 to 62% with included mineral matter). Reductant D possesses the highest vitrinite value (62%,2) and Reductant C the lowest (48,0%). Reductants A and B possess 56% and 51% respectively.

	Reductant A	Reductant B	Reductant C	Reductant D
Rank (Degree of maturity)	Anthracite	Anthracite	Anthracite	Anthracite
ISO 11760-2005 classification of coals	High rank B	High rank B	High rank B	High rank B
Mean random reflectance%	3.85	3.22	3.35	3.23
Vitrinite content %	56	51	48	62.2
Total Inertinite %	35	37	45	36.9
Visible minerals %	6	6	4	1

Table 4: Summary of petrographic results

4.2 CARBON EFFICIENCY RESULTS

The total amount of ilmenite added into the furnace per reductant type and campaign was that of Reductant A at 7104 tons, Reductant B at 16893 tons, Reductant C at 15855 tons and Reductant D at 3263 tons. The campaign ilmenite tons varied as a result of the reductant availability and type of reductant.

The total reductant added per campaign was Reductant A at 1022 tons, Reductant B at 2167 tons, Reductant C at 2036 tons and Reductant D at 450 tons. The respective reductant ratios expressed as reductant divided by ilmenite per campaign was at 14.4 percent for Reductant A, 12.83 percent for Reductant B, 12.83 percent for Reductant C and 13.84 percent for Reductant D. The reductant percentage varied as a function of the fixed carbon units and reductant efficiency.

The power consumption expressed in megawatt hour was 10027MWh for Reductant A campaign, 21888MWh for Reductant B campaign, 20592MWh for Reductant C campaign and 4159MWh for Reductant D campaign. The furnaces are operated on a constant power principle and power follows the duration of the campaign.

The slag tons produced from the ilmenite and reductants added per campaign was 4257 tons for Reductant A, 9556 tons for Reductant B, 8867 tons for Reductant C and 1760 tons for Reductant D. The equivalent average slag temperature per campaign was 1688°C for Reductant A, 1679°C for Reductant B, 1679°C Reductant C and 1689°C for Reductant D. Slag tons were determined as a function of the yield which was determined from the ilmenite quality and the duration of the campaign.

The metal tons produced from the ilmenite and reductants added per campaign was 2767 tons for Reductant A, 5996 tons for Reductant B, 5547 tons for Reductant C and 1104 tons for Reductant D. The equivalent average metal temperature per campaign was 1543°C for Reductant A, 1473°C for Reductant B, 1512°C Reductant C and 1572°C for Reductant D. Metal tons were determined as a function of the yield which was determined from the ilmenite quality and the duration of the campaign.

The carbon percentage in the metal per campaign was 2.27 percent for Reductant A, 2.58 percent for Reductant B, 2.44 percent for Reductant C and 1.97 percent for Reductant D.

Side feed is the feed introduced through side ports situated on the periphery of the furnace and is expressed as a percentage of the total ilmenite feed. The respective side feed introduced per campaign was 7.2 percent for Reductant A, 28.9 percent for Reductant B, 13.25 percent for Reductant C and 28.8 percent for Reductant D.

The calculated carbon efficiencies, based on campaign data was calculated by using equation 12 to equation 29. The carbon efficiencies were calculated based on actual reductant ratio's and carbon percentage in metal from table 5. The carbon efficiency calculation also included the use of actual chemical analyses obtained (table 6).The calculated carbon efficiency per campaign was 91 percent for Reductant A, 96 percent for Reductant B, 96.35 percent for Reductant C and 87.9 percent for Reductant D.

Summary of campaign results illustrated in table 5 below:

	Reductant A	Reductant B	Reductant C	Reductant D
Total ilmenite (tons)	7104	16893	15855	3263
Total reductant (tons)	1022	2167	2036	450
Reductant ratio (%)	14.4	12.83	12.83	13.84
Power consumption(MWh)	10027	21888	20592	4159
Slag (tons)	4257	9556	8867	1760
Slag temperature (°C)	1688	1679	1679	1689
Metal (tons)	2767	5996	5547	1104
Metal temperature (°C)	1543	1473	1512	1572
Carbon in metal (%)	2.27	2.58	2.44	1.97
Side feed (%)	7.2	28.9	13.25	28.8
Calculated carbon efficiency (%)	91	96	96.35	87.9

Table 5: Summary of reductant efficiency results and leading parameters

4.3 SLAG PRODUCTS

The average slag analyses for the various reductant campaigns are summarized in table 6. The major oxides in the slag product are TiO_2 and FeO . The TiO_2 percentage for Reductant A to Reductant C varied from 85.22 percent to 85.3 percent, while Reductant C had an average analysis of 85.67 percent. Reductant D had a lower TiO_2 content of 83.06%.

The aim furnace TiO_2 was 85 percent for quality control purposes. The lower TiO_2 percentage of Reductant D campaign can be ascribed to insufficient reductant added during the initial stages of the campaign due to an over estimation of reductant efficiency.

FeO percentage in the slag is the second indicator for furnace quality control purposes and is correlated to TiO_2 in the approximate correlation indicated in figure 8. The FeO percentages for the various reductant campaigns was 8.73 percent for Reductant A, 9.75 percent for Reductant B, 10.43 percent for Reductant C and 10.76 percent for Reductant D.

The minor oxides of SiO_2 , Al_2O_3 , MgO , CaO , MnO , V_2O_5 , Cr_2O_3 and ZrO_2 was included in table 6 for the sake of completeness of the average campaign slag analyses. The minor oxides were used as inputs in the mass and energy balance in carbon efficiency determination. The oxides generally conformed to final product quality specification with the exception of SiO_2 in Reductant A campaign. Reductant A SiO_2 percentage was significantly higher than the others. The main reason for the increased SiO_2 content was that the fixed carbon units for Reductant A was significantly lower and the mineral matter content significantly higher than the other reductants, which led to increased amounts of reductant added to satisfy chemical reduction. The increased amounts of reductant added meant that an increased amount of mineral matter was added. Reductant A also contained a higher percentage of SiO_2 in the mineral matter (table 8). The increased mineral matter percentage that contained elevated SiO_2 percentages, directly contributed to a disproportionate increase of SiO_2 percentage in the final product, when compared to the other campaigns.

	Reductant A	Reductant B	Reductant C	Reductant D
TiO ₂	84.38	85.67	85.3	83.06
FeO	9.86	9.75	10.43	10.76
SiO ₂	2.97	2.33	2.4	2.38
Al ₂ O ₃	1.36	1.34	1.25	1.49
MgO	0.99	1.01	0.99	1.042
CaO	0.21	0.15	0.133	0.21
MnO	1.87	1.83	1.84	1.85
V ₂ O ₅	0.40	0.40	0.405	0.422
Cr ₂ O ₃	0.156	0.15	0.15	0.27
ZrO ₂	0.184	0.18	0.17	0.2
P ₂ O ₅	0.001	0.001	0.001	0.001
K ₂ O	0.023	0.02	0.02	0.018

Table 6: Summary of slag products

4.4 METAL PRODUCTS

The metal products contained more than 97 percent Fe. The carbon content of the metal product varied from 1.97 percent to 2.59 percent between the reductant campaigns. The carbon percentage is an important indicator to determine carbon partition between reduction reactions and excess carbon to metal, for the use of carbon efficiency determination. The carbon percentage in the metal after tap should typically be in excess of 2 percent, since carbon percentage in the metal has a direct impact on the liquidus temperature. Lower carbon percentages in the metal will increase the metal liquidus, causing a decrease in superheat (temperature above liquidus) and an increase in the propensity to freeze before treatment.

The metal elements of Ti, Si, Al, Mn, V, Cr, P and S were included in table 7 and were used in the mass and energy balance to complete the actual partition coefficients between metal, slag and dust. The Mn and Ti are good indicators of the level of reduction achieved in the process and will tend to increase with increased reduction. The comparison on the level of reduction becomes valid for specific feed materials and cannot be applied for comparison for this study due to different reductants used.

Mn contains a final product specification and impacts on the VIU costing when out of specification due to reclassification of the LMPI to a lower value. The Mn percentage in the metal is very dependent on the ilmenite feed, reductant feed and level of reduction achieved. Limited scope exists on influencing the level of reduction since decreasing the TiO₂ percentage will also lead to out of specification slag. The biggest contributor to Mn in the metal product can be assigned to the ilmenite.

P and S also directly impacts on VIU costing due to associated treatment costs involved. P was within specification for the various campaigns. P like Mn is largely dependent on the feed material and cannot be removed with the current processes. Dephosphorization can be performed at additional treatment costs when the need arise for P removal. S is removed by CaC₂ addition during treatment.

	Reductant A	Reductant B	Reductant C	Reductant D
Fe				
C	2.27	2.59	2.44	1.97
Ti	0.059	0.09	0.066	0.055
Si	0.099	0.041	0.029	0.053
Al	0.252	0.33	0.21	0.46
Mg				
Ca				
Mn	0.050	0.042	0.037	0.043
V	0.045	0.035	0.03	0.038
Cr	0.06	0.049	0.045	0.074
Zr				
P	0.024	0.023	0.023	0.033
K				
Na				
S	0.14	0.138	0.15	0.209

Table 7: Summary of metal products

4.5 REDUCTANT ANALYSIS

The average reductant analyses for the various campaigns are listed in table 8 and were used in performing mass and energy balancing calibrations. The proximate analyses shows that the inert moisture, surface moisture and volatiles are quite similar for the various campaigns, with the exception of the ash and fixed carbon of

Reductant A that contained much lower fixed carbons and higher ash contents when compared to the other campaigns.

The ash analyses for the various campaigns are fairly similar with the exception of Reductant A containing a significantly higher SiO₂ percentage when compared to the other campaigns.

	Reductant A	Reductant B	Reductant C	Reductant D
Inherent moisture	1.48	1.89	1.88	1.87
Surface moisture	1.4	1.88	1.85	1.49
Volatiles	6.63	4.69	5.27	5.14
Ash	15.09	9.67	9.27	12.48
Fixed Carbon	78.26	85.63	85.97	82.38
Ash analysis				
TiO ₂	1.13	1.74	1.76	1.85
FeO				
Fe ₂ O ₃	5.98	7.57	10.41	6.48
SiO ₂	60.77	45.94	45.54	40.8
Al ₂ O ₃	15.14	24.28	23.47	23.9
MgO	0.85	1.15	0.89	0.94
CaO	3.86	2.15	1.40	4.14
MnO	0.07	0.07	0.111	0.14
V ₂ O ₅	0.055	0.064	0.035	0.084
Cr ₂ O ₃	0.009	0.033	0.022	0.027
ZrO ₂				
P ₂ O ₅	0.094	0.106	0.12	0.107
K ₂ O	1.60	3.01	3.23	1.75
Na ₂ O	1.37	0.6	0.59	0.59
SO ₃				
Ultimate analysis (Dry ash free)				
C	78.26	85.63	85.97	82.38
H	2.48	2.48	2.48	2.48
O	1.4	1.4	1.4	1.4
N	1.73	1.73	1.73	1.73
S	0.83	0.83	0.83	0.83

Table 8: Summary of reductant analysis

4.6 SUMMARY OF RESULTS

Based upon the results obtained above, this section provides the interpretations and discussions as outlined below.

4.6.1 Carbon efficiency to vitrinite content correlation

Figure 12 indicates the correlation obtained between the vitrinite content of the various reductants and the calculated carbon efficiency. The results indicate that calculated carbon efficiency decreases with increasing vitrinite content. The carbon efficiency is associated with the carbon distribution for reduction and excess carbon to metal for specific initial carbon contents of the reductants. Any carbon lost due to shattering as a result of exposure to freeboard temperatures could influence the carbon efficiency. Similarly size in terms of d50 or -1mm could influence carbon losses.

The correlation holds for furnace operation where side feed was utilized. The side feed material is more exposed to furnace freeboard temperature conditions and is also closer to the off gas extraction system, increasing the probability of particle losses at a critical size dimension. Carbon efficiency is expected to decrease with an increase in vitrinite content in full scale operation due to the frail nature of the vitrinite maceral. The propensity for anthracites with higher bearing vitrinite maceral contents to shatter as a result of heat exposure and associated moisture with reference to furnace side feed configuration is higher than anthracites with lower bearing vitrinite contents. Full scale tests show a good correlation between vitrinite content and calculated carbon efficiency for fairly similar d50 particle size (Figure 13) between the campaigns.

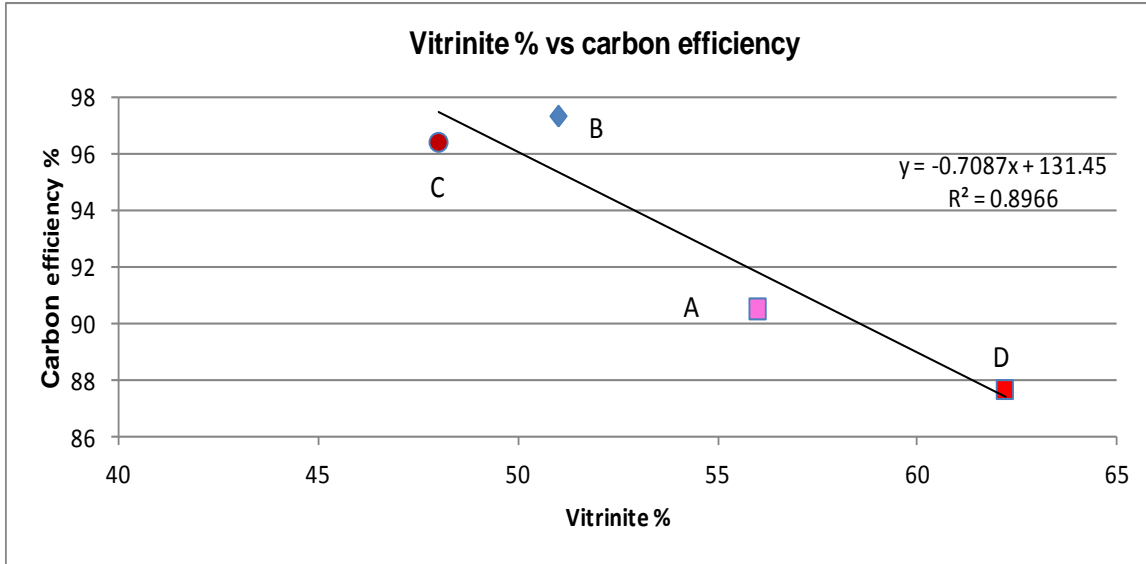


Figure 12: Vitrinite content against calculated carbon efficiency for Reductant A – Reductant D

4.6.2 Average reductant size

Figure 13 show that all the reductants had a similar mean particle diameter (D50). A poor correlation exists between d50 sizing and carbon efficiency as indicated by Figure 14. The main reason for the similar d50 can be ascribed to a deliberate size processing step prior to utilization of the reductants. Figure 15 indicates the correlation between carbon efficiency and -1mm size fractions of the reductants tested. A fair correlation exist between carbon efficiency and -1mm size due to the fact that an increase in fines (-1mm) would lead to the propensity toward increased dust losses.

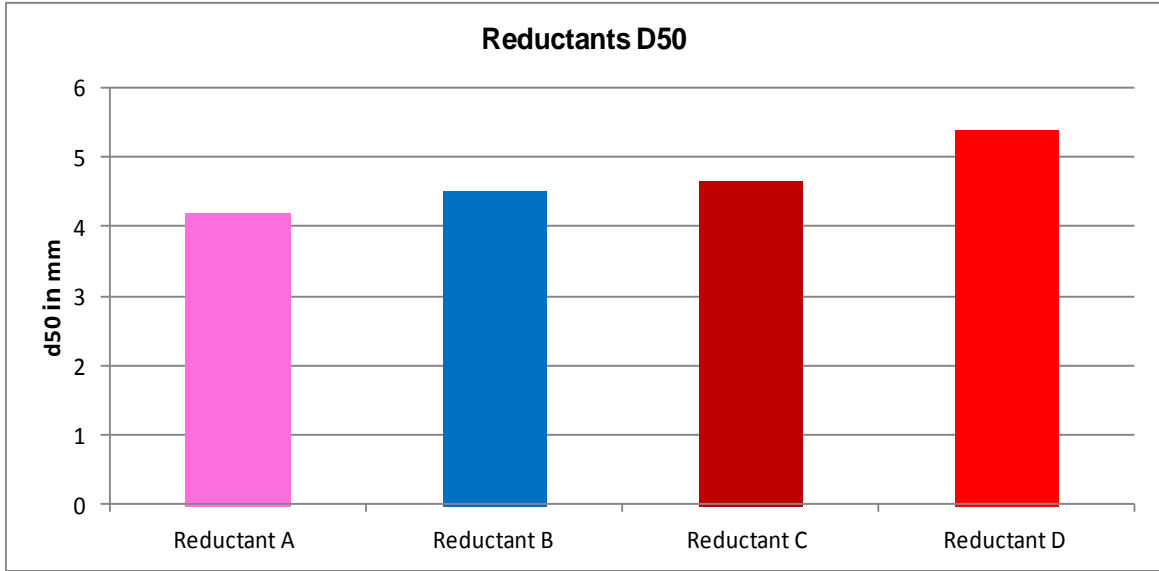


Figure 13: Mean particle diameters (D50) of Reductant A to Reductant D

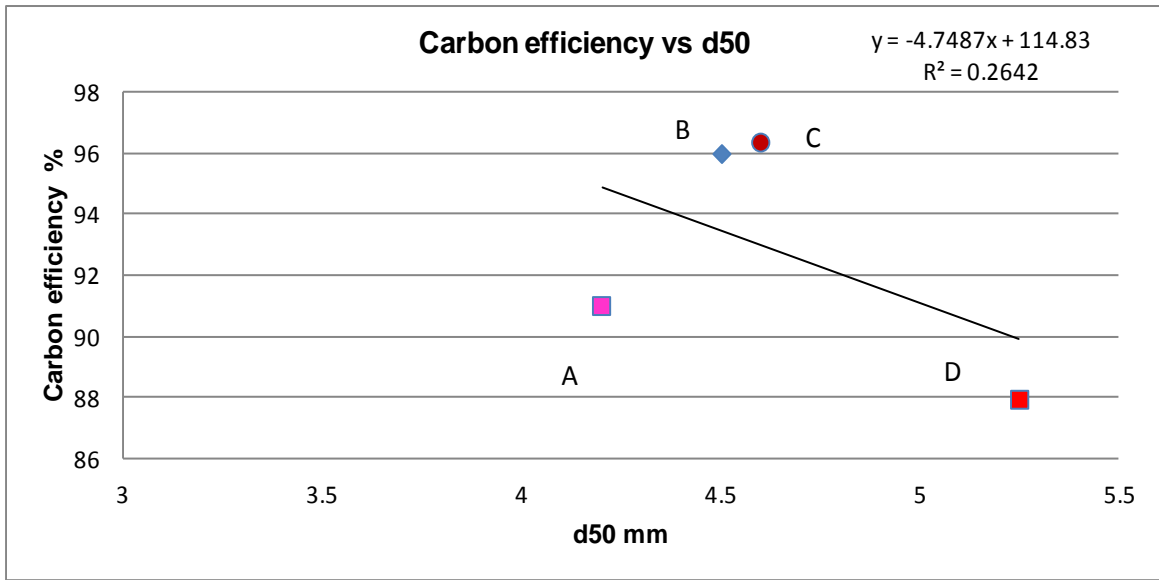


Figure 14: Mean particle diameters (d50) correlated against carbon efficiency

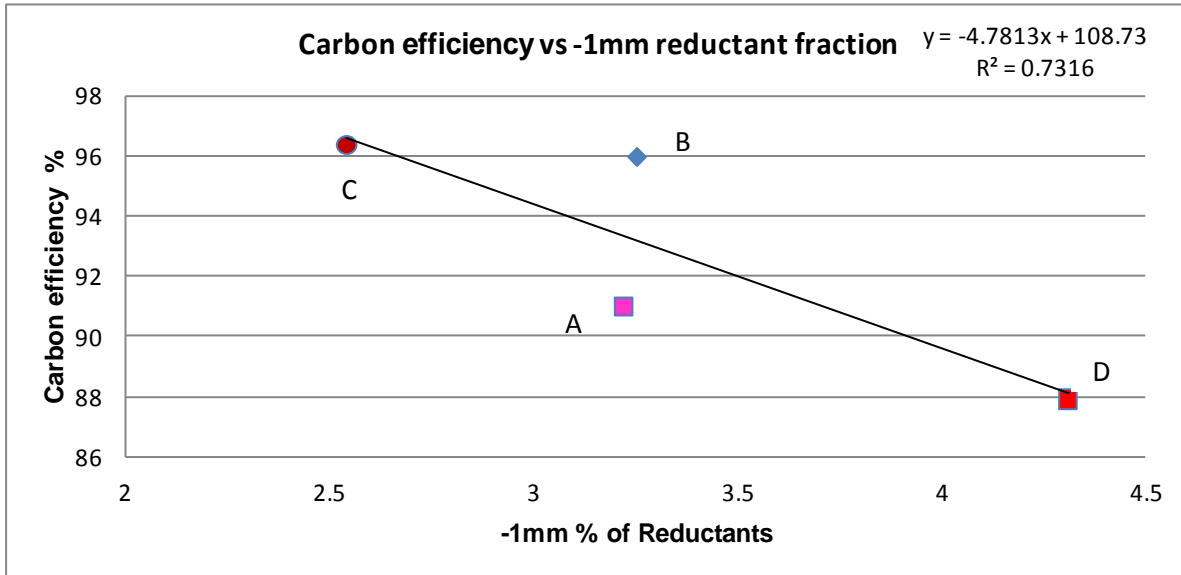


Figure 15: 1-mm size fraction of Reductant A to Reductant D correlated against carbon efficiency

4.6.3 Carbon percentage reporting to metal to carbon efficiency correlation

An increase in carbon to metal correlated well with an increase in carbon efficiencies, as illustrated in Figure 16. Although Figure 16 clearly indicates that a good correlation exists between carbon distribution to the metal and carbon efficiency, it must be stated, however, that the mechanism of carbon distribution to metal is not clearly understood.

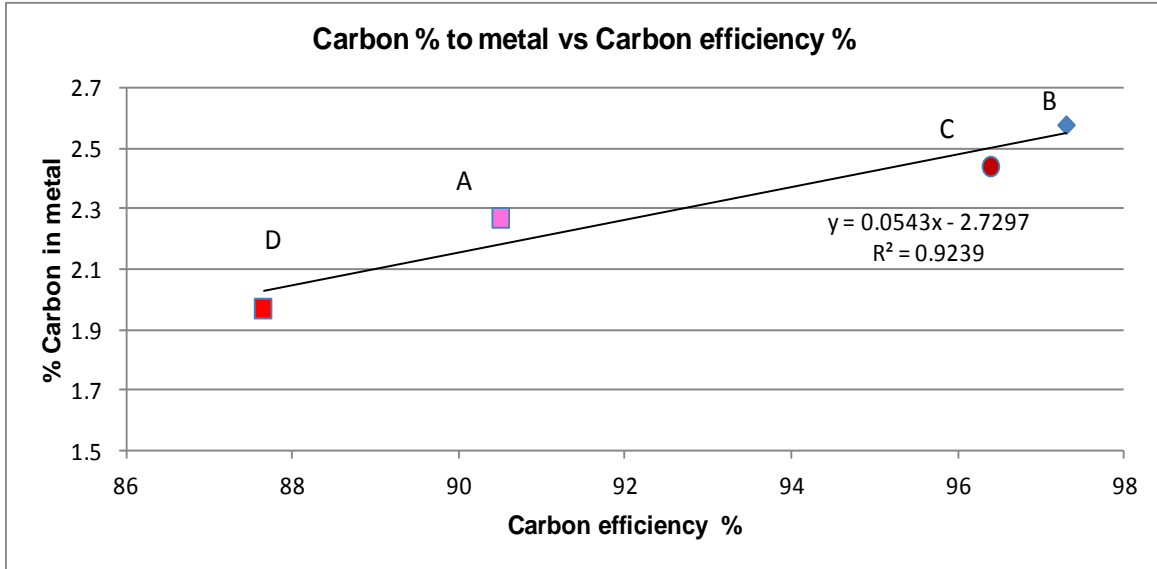


Figure 16: Percentage carbon to metal for various reductant carbon efficiencies

4.6.4 Carbon percentage in metal correlated to TiO₂ in the slag

A decrease in carbon percentage in the metal led to a general decrease in TiO₂ in the slag product as illustrated in Figure 17. The decrease in carbon in the metal for a decrease in TiO₂ percentage in the slag could suggest, (a) insufficient carbon units added initially, (b) carbon losses occurring due to decrepitation and reporting to dust losses, or (c) carbon losses to higher -1mm size fraction

Figure 17 shows a good correlation between TiO₂ percentages in the slag against carbon percentages in the metal, indicating that the mechanism for reduction is very much interlinked between slag chemistry and carbon in metal formation.

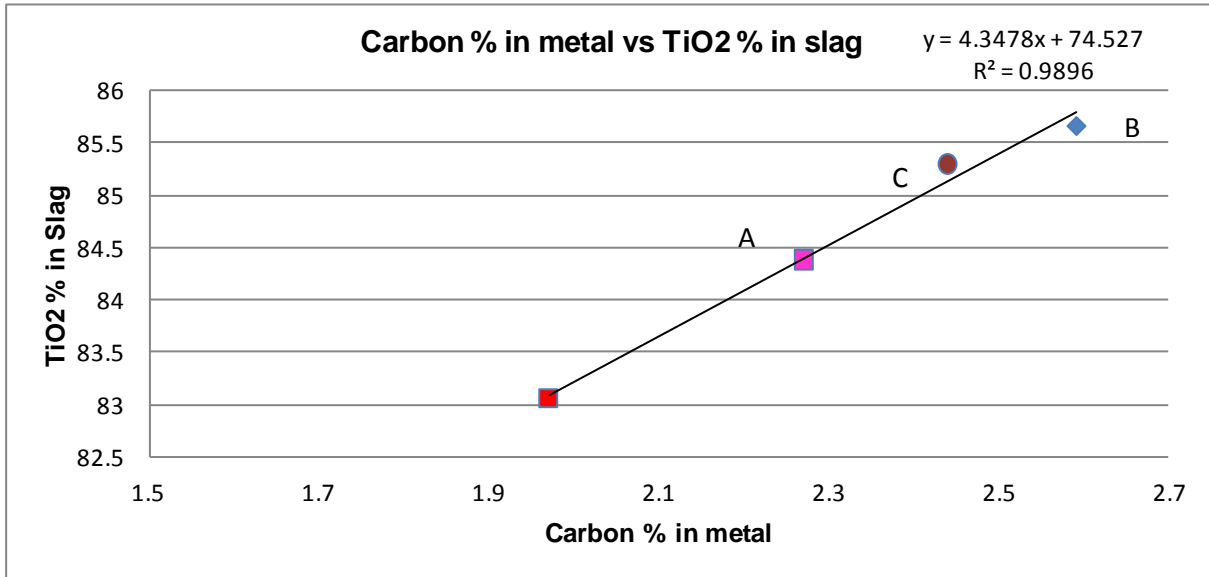


Figure 17: Percentage carbon to metal compared to TiO₂ % slag for various reductants

4.6.5 Carbon percentage in metal correlated to metal temperature

Carbon depletion in the metal leading to a general increase in metal temperatures is presented in Figure 18. Carbon depletion through loss or due to fixed carbon variation could lead to an increase in metal temperatures as excess energy is transferred as a result of a deviation from the normal energy algorithm. This is due to the fact that the algorithm is constructed for a specific raw material feed. Figure 18 indicates that for an increase in temperature a decrease in carbon can be expected.

The calculated carbon equilibrium percentage in metal is much lower as indicated by Figure 19, than the actual carbon percentages observed in reality. The higher (one order of magnitude) carbon percentages in the metal would suggest non equilibrium conditions in the metal bath when related to ilmenite smelting. Figure 19 indicates that for an increase in temperature a decrease of equilibrium carbon can be expected.

Figure 20 illustrates the carbon percentages in the metal correlated against the Ti percentages in the metal adapted from Pistorius et al (2011), against the actual Ti percentages for carbon percentages in the metal.

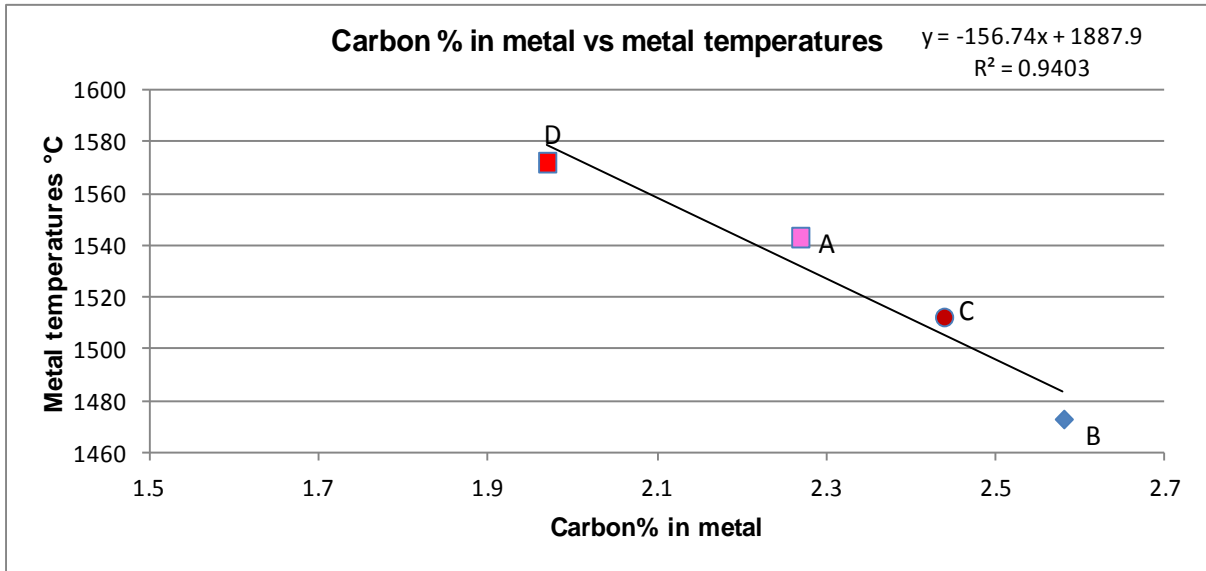


Figure 18: Percentage carbon to metal compared to metal temperatures for various reductants

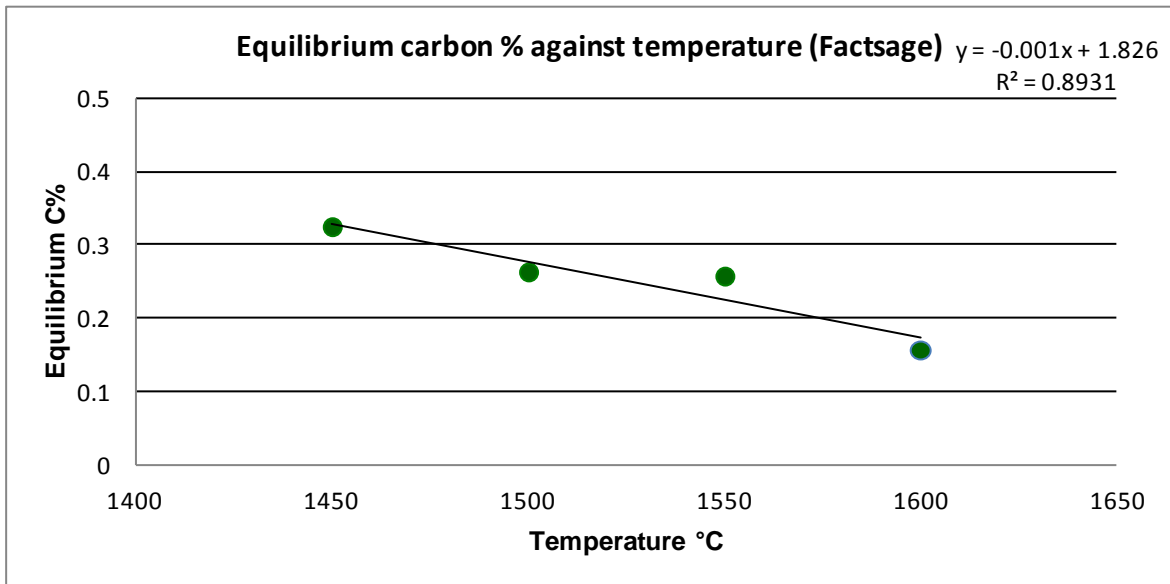


Figure 19: Equilibrium carbon in metal for given temperatures as calculated through Factsage

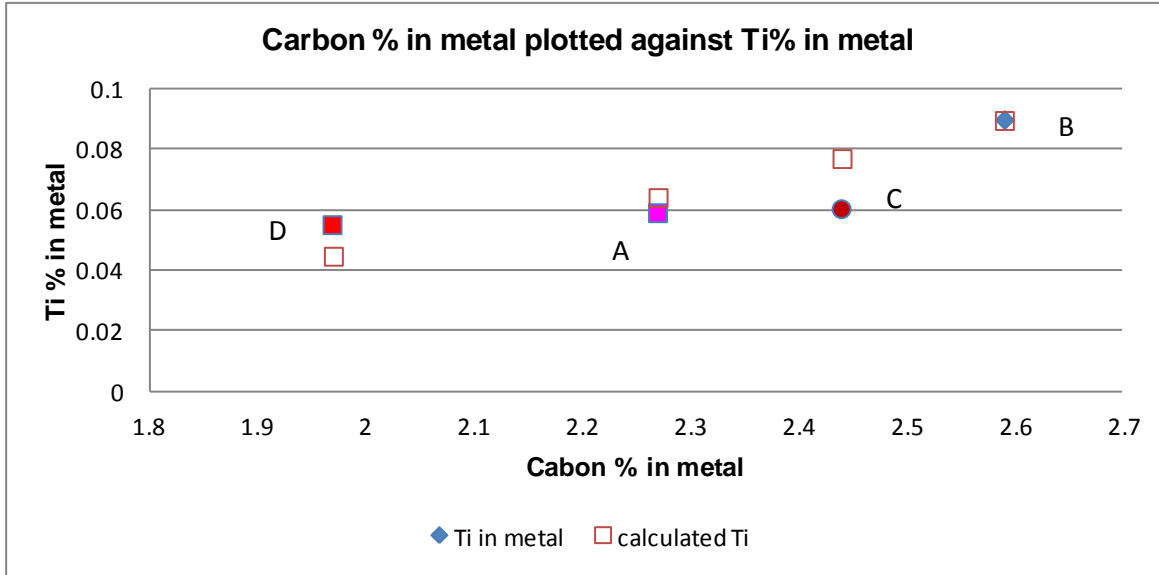


Figure 20: Carbon % in metal to Ti % in metal (Open marker adapted from (Pistorius et al, 2012) against solid markers indicting the various reductant campaigns

A fair correlation exists between the carbon percentages in the metal to the Ti percentages in the metal with the exception of Reductant C. The correlation can perhaps be used as an indication of carbon percentage to the metal related to Ti percentages in the metal.

5 DISCUSSION - ENERGY ALGORITHM CORRECTION

5.1 Energy algorithm correction for Reductant A

Algorithms were created for reductant ratios at various slag chemistries and linked to the theoretical energy component for ilmenite feed determination as one of the leading indicators in the VIU model. The algorithms were derived from the mass and energy balance.

The theoretical energy correction in this research was calculated based on the reductant efficiencies obtained in Table 5, the reductant ratio's in Table 5, slag and metal chemistries in Table 6 and Table 7, ilmenite analyses and reductant analyses in Table 8.

Figure 21 to Figure 28 shows the linear dependence of reductant ratio percentage required for various TiO_2 percentages in the slag for the different campaigns and the theoretical energy requirement for varying reductant percentages. The reductant requirement is strongly dependent on reductant fixed carbon and reductant efficiency. The theoretical energies for all the reductants are very similar due to the relative small effect of the reductants on the mass and energy balance when compared with the ilmenite input. All the equations in Figure 21 to Figure 28 were used in the VIU model.

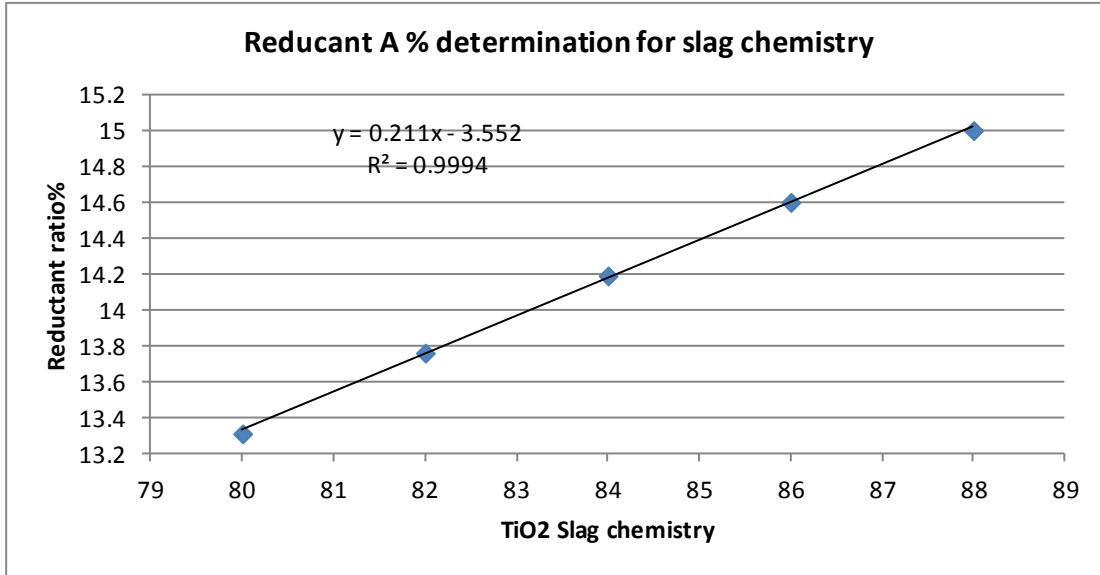


Figure 21: Reductant % A required per ton ilmenite to obtain a desired TiO₂ slag chemistry

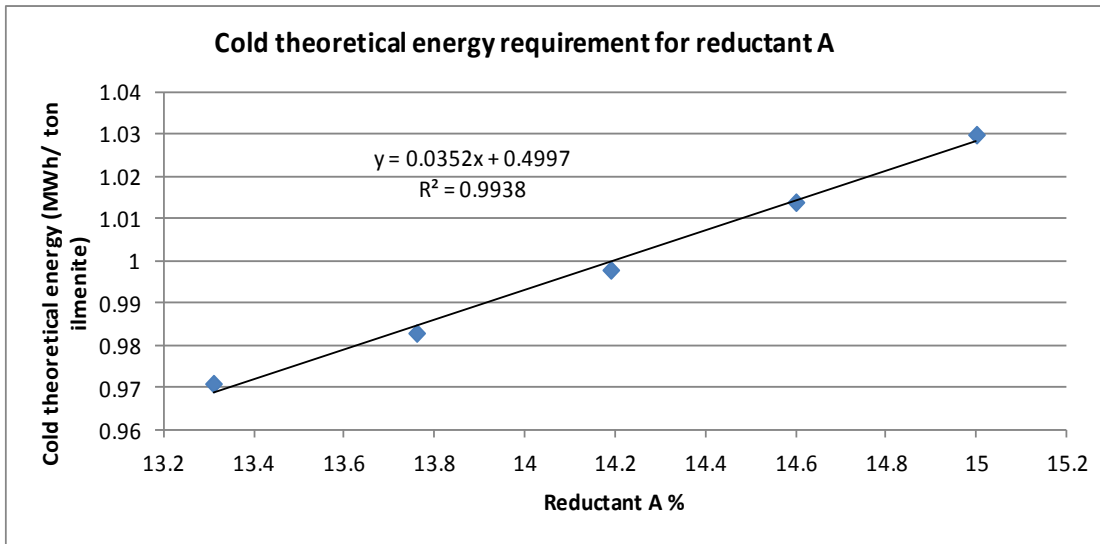


Figure 22: Cold theoretical energy requirement (MWh/Ton ilmenite) for various reductant A feed ratios

5.2 Energy algorithm correction for reductant B

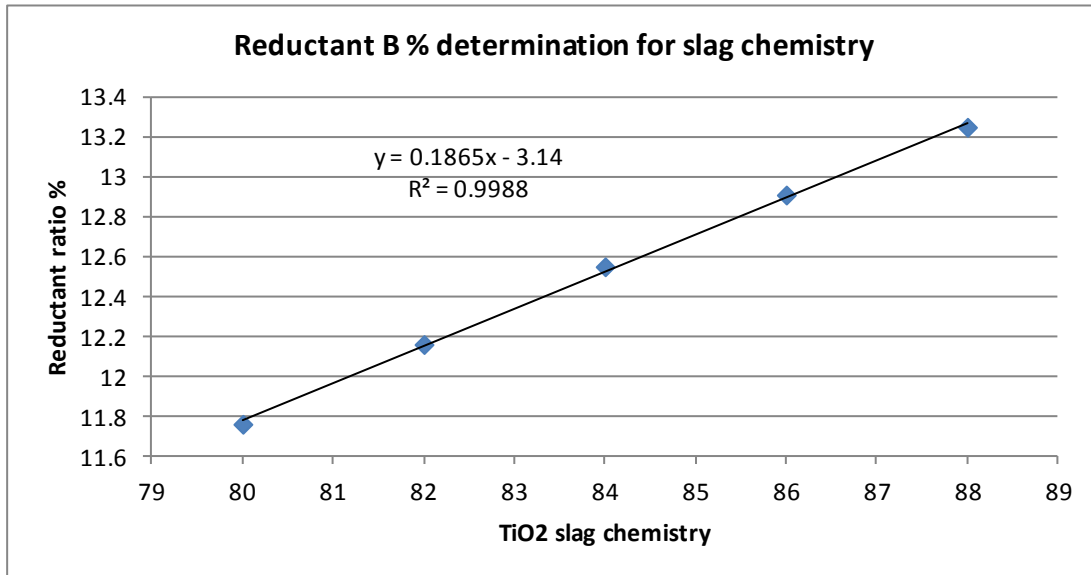


Figure 23: Reductant %B required per ton ilmenite to obtain a desired TiO₂ slag chemistry

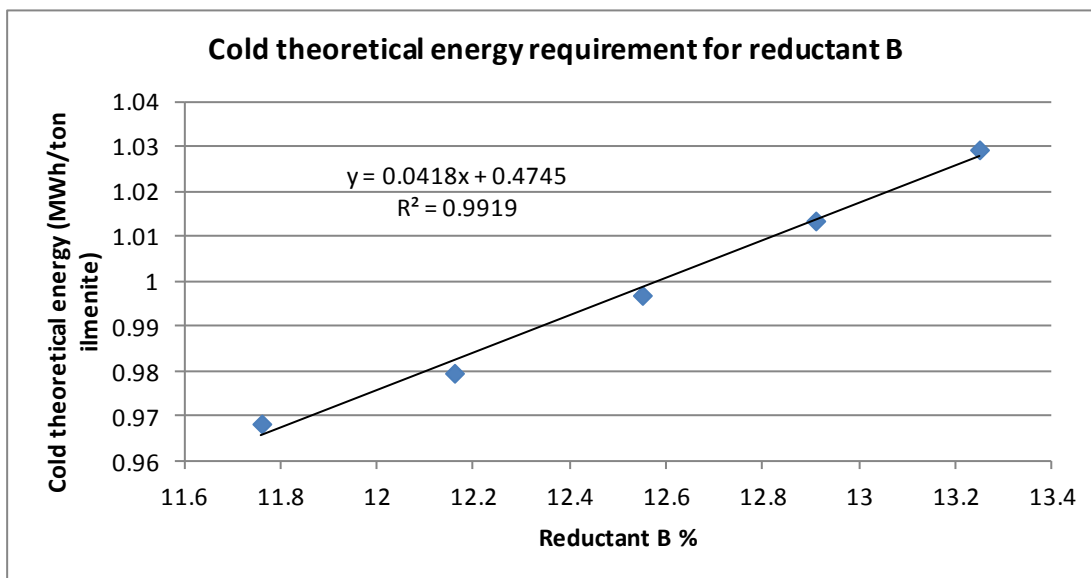


Figure 24: Cold theoretical energy requirement (MWh/Ton ilmenite) for various reductant B feed ratios

5.3 Energy algorithm correction for reductant C

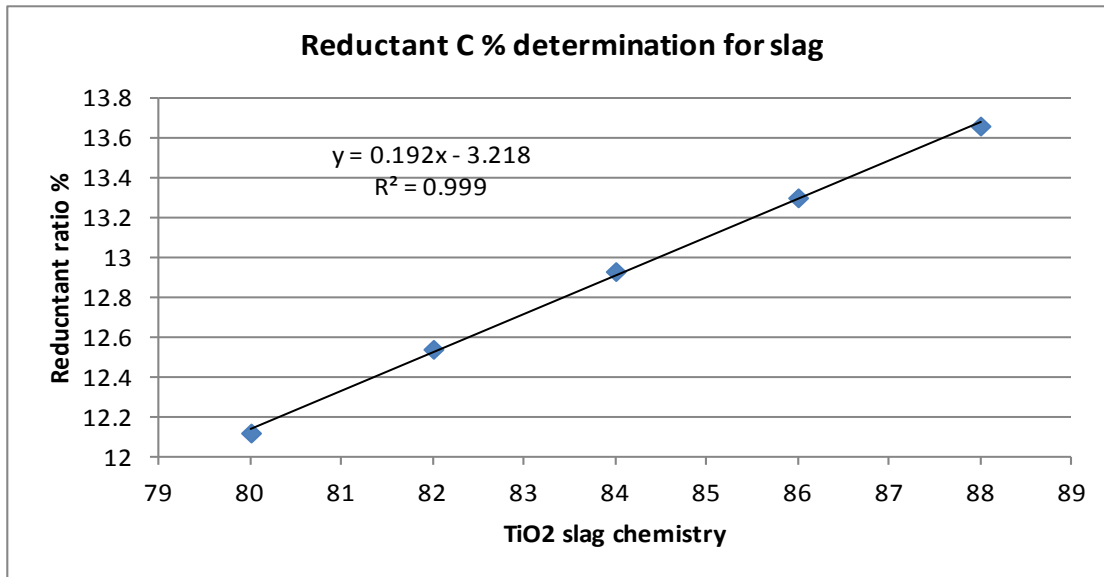


Figure 25: Reductant %C required per ton ilmenite to obtain a desired TiO₂ slag chemistry

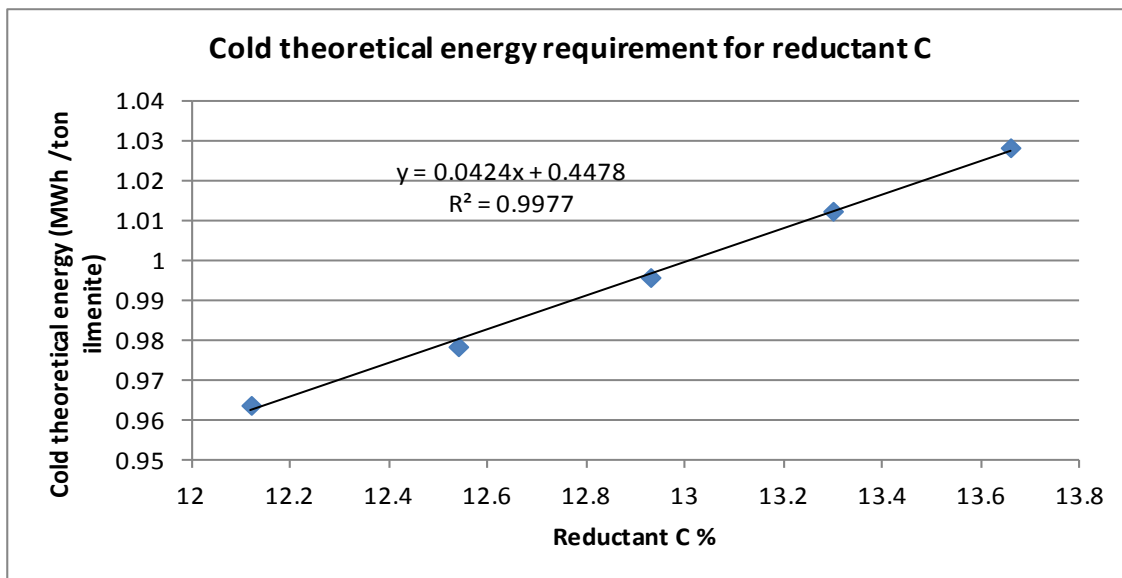


Figure 26: Cold theoretical energy requirement (MWh/Ton ilmenite) for various reductant C feed ratios

5.4 Energy algorithm correction for reductant D

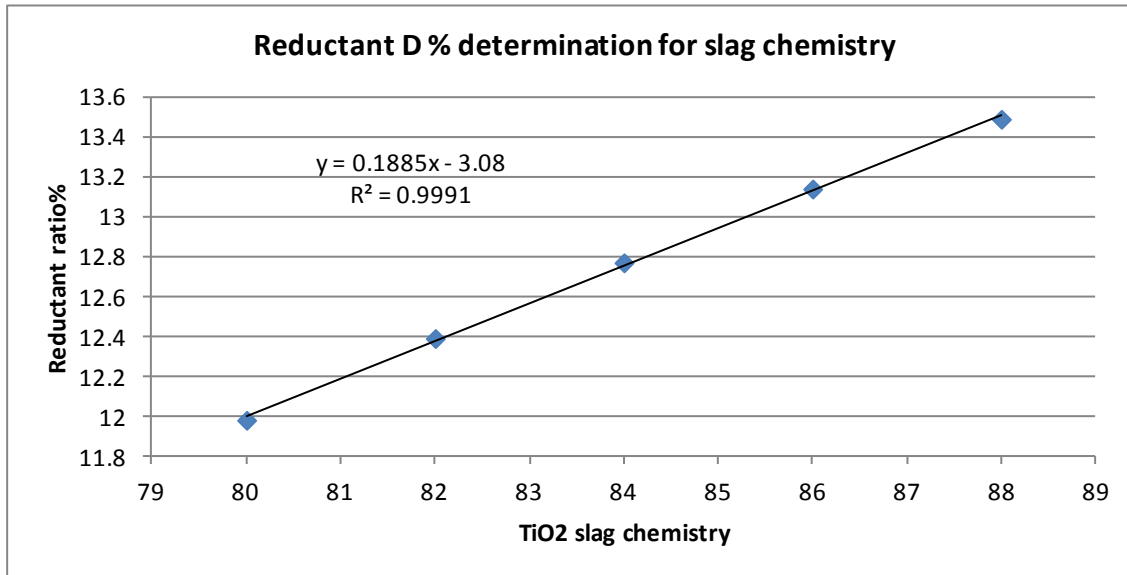


Figure 27: Reductant %D required per ton ilmenite to obtain a desired TiO₂ slag chemistry

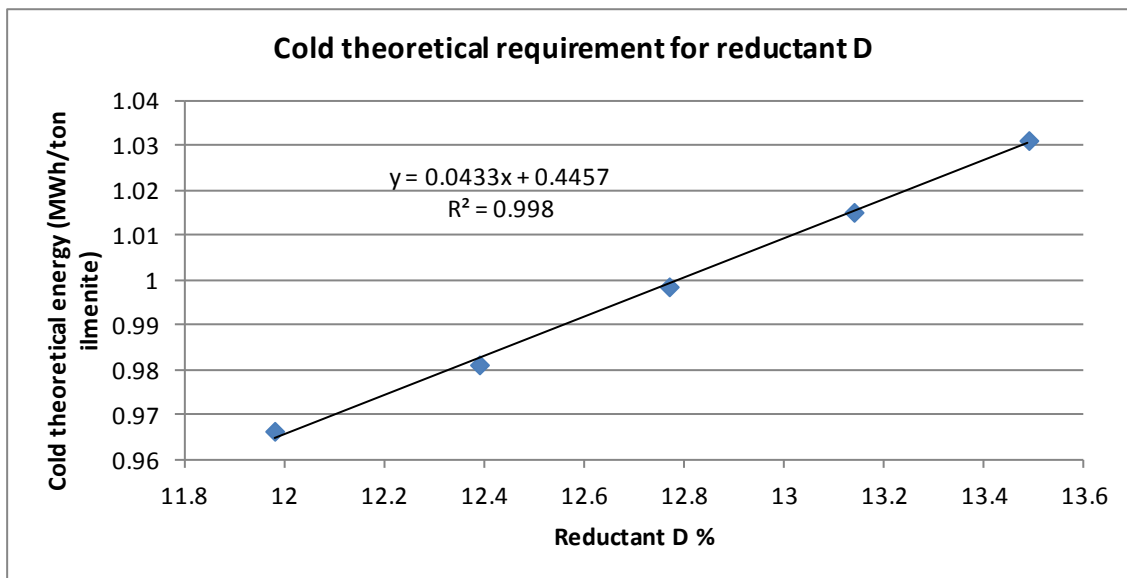


Figure 28: Cold theoretical energy requirement (MWh/Ton ilmenite) for various reductant D feed ratios

6 DISCUSSION - VALUE IN USE MODEL

A Value In Use (VIU) smelter model was created to quantify the value of different anthracites utilized in ilmenite smelting. The battery limits for costing starts at the value received for ilmenite to be smelted and ends at final product sold (Figure 29).

6.1 Treatment cost value calculation

The treatment cost value calculation was determined by adding the total cost of metal treated expressed as R/ton metal. The treatment costs involve the desulphurisation cost, cost of removal to a hazardous waste site, FeSi addition and addition of re-carburizer. The following information was required to calculate the treatment costs:

- 6.1.1 The amount of reductant required to obtain a fixed TiO₂ slag chemistry.
- 6.1.2 The metal and slag yields obtained from the mass and energy balance.
- 6.1.3 The theoretical energy calculated based on corrected carbon efficiencies.
- 6.1.4 Ilmenite and reductant feed rate and metal and slag tons produced.

The treatment cost calculation can be expressed as follows:

$$\text{Reductant}_A \text{ tons required} = [(EE + PF \text{ tons} \times (CTE_A - PFTE_A)] / CTE_A [(TiO_2 \text{ aim} \cdot M_A + C_A)/100] \dots\dots\dots(42)$$

$$\text{Slag yield} = FeO\% \text{ slag} \times M_1 + C_1 \dots\dots\dots(43)$$

$$\text{Metal yield} = FeO\% \text{ slag} \times -M_2 + C_2 \dots\dots\dots(44)$$

$$CTE_A = \text{Reductant}_A \% \times M_A + C_A \dots\dots\dots(45)$$

$$\text{Ilmenite feedrate}_A = [(EE + PF \text{ tons} \times (CTE_A - PFTE_A)] / CTE_A \dots\dots\dots(46)$$

$$\text{Metal tons} = \text{Metal yield} / 100 \times \text{Ilmenite feedrate}_A \dots\dots\dots(47)$$

$$\text{Slag tons} = \text{Slag yield} / 100 \times \text{Ilmenite feedrate}_A \dots\dots\dots(48)$$

$$\text{CTE}_A = \text{Reductant}_A \% \times 0.0352 + 0.4997 \dots\dots\dots(49)$$

$$\text{PFTE}_A = \text{Reductant}_A \% \times M_3 + C_3 \dots\dots\dots(50)$$

$$\text{EE} = \text{Power} \times M_4 + C_4 \dots\dots\dots(51)$$

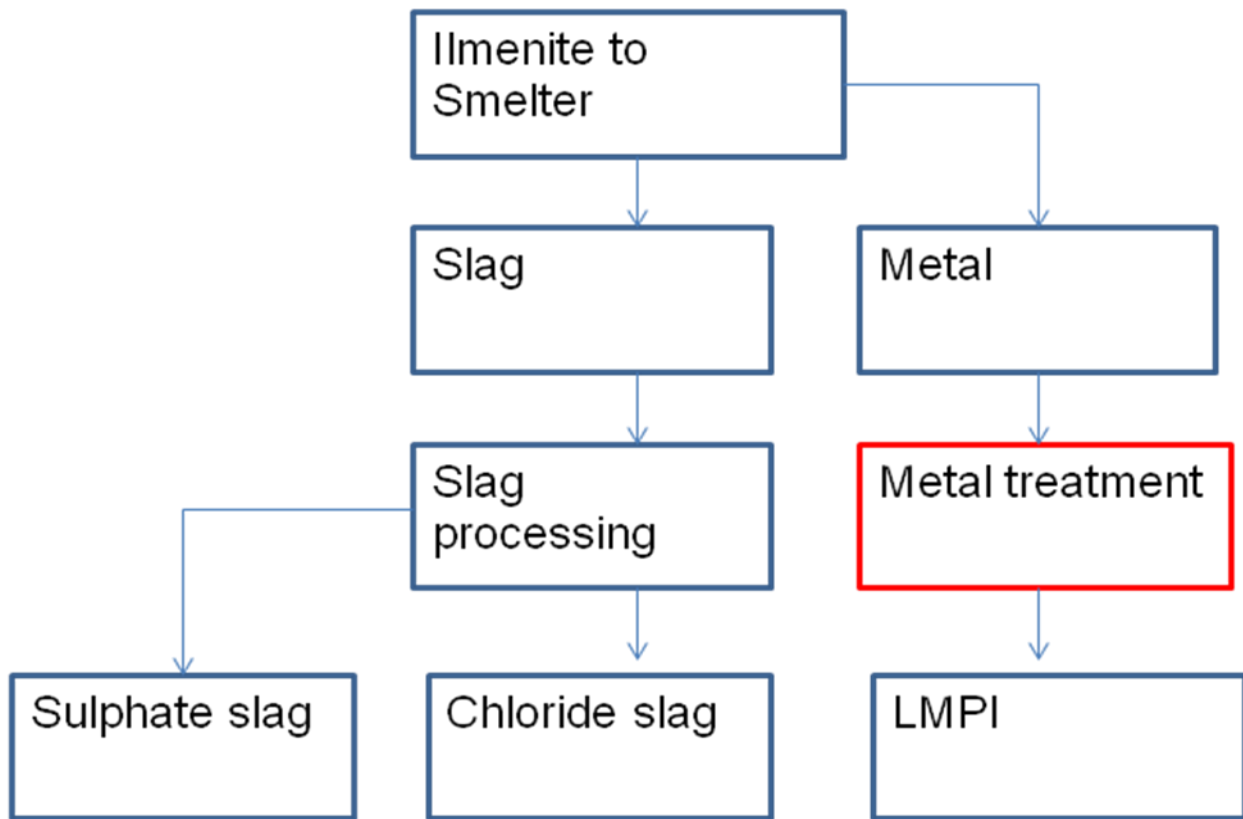


Figure 29: Illustrates the value chain flow and metal treatment costs in relation.

$$\begin{aligned} \text{Treatment costs} = & (\text{CaC}_2 \text{ addition tons} \times \text{CaC}_2 \text{ R/ton}) + (\text{FeSi addition tons} \times \text{FeSi R/ton}) \\ & + (\text{CaS tons} \times \text{R/ton removal}) + (\text{C tons} \times \text{C R/ton}) \dots\dots\dots(52) \end{aligned}$$

$$\text{CaC}_2 \text{ addition tons} = [\text{LN} (\text{Si in metal} / 0.01)] / 0.24 \times \text{metal tons} \dots\dots\dots(53)$$

$$\text{CaS tons generated} = \text{CaC}_2 \text{ tons} / (\text{CaC}_2 \text{ molar mass}) \times (\text{CaS molar mass}) \dots\dots\dots(54)$$

$$\text{FeSi addition tons} = (\text{Aim Si} - \text{Si in metal}) / 100 \times \text{metal tons} / \text{Si\% in FeSi} / \text{FeSi efficiency} \dots\dots\dots(55)$$

$$\text{C tons} = (\text{Aim C} - \text{C in metal}) / 100 \times \text{metal tons} / \text{C\% in recarb} / \text{C efficiency} \dots\dots\dots(56)$$

The treatment costs are expressed as Rand per ton iron produced.

6.2 Reductant cost evaluation

The reductant cost is the physical cost of the reductant and is inclusive of transport cost.

The reductant cost was calculated as follows:

$$\text{Reductant cost} = \text{Reductant}_A \text{ tons required} \times \text{R/ton delivered} \dots\dots\dots(57)$$

6.3 Net smelter profit calculation

The net profit calculation involves the total fixed cost, variable cost, treatment cost and revenue from product sales. The net profit can thus be expressed as revenue from product sales less the expenditure to produce the product.

6.3.1 Variable cost is comprised of the following elements:

- Electricity cost.
- Hollow electrode consumption.
- Treatment costs.
- Reductant costs.
- Ilmenite costs.

6.3.2 Final product revenue is divided into the ratio between chloride and sulphate slag and the associated revenue generated from sales. One product revenue price is assigned to LMPI. Net smelter profit may therefore be calculated as follows:

$$\text{Net smelter profit} = \text{Final product sales revenue} - (\text{fixed cost} + \text{variable cost} + \text{treatment costs} + \text{reductant costs}) \dots\dots\dots(58)$$

6.4 Value in Use results

The reductant percentage requirement for constant slag TiO₂ chemistry was expressed in the Value In Use (VIU) model and related to the treatment cost component. The VIU calculation was performed by using a constant reductant cost from the equation in order to obtain the treatment cost.

6.4.1 Treatment cost NOP evaluation

The treatment cost was expressed as a percentage Net Operating Profit (NOP) contribution to the VIU. It is evident that the treatment costs will increase with an increasing reductant ratio requirement to obtain constant slag TiO₂ chemistry as is indicated in Figure 30. A higher reductant ratio will lead to increased sulphur in the metal and increased disposal costs. The treatment cost percentage to the total NOP varied from 6.5% to 7.3 % between the reductants tested.

An increase in reductant ratio will have a linear cost increase of up to 7 percent on the bottom line treatment costs. The treatment costs amounts to 7 percent of the total NOP.

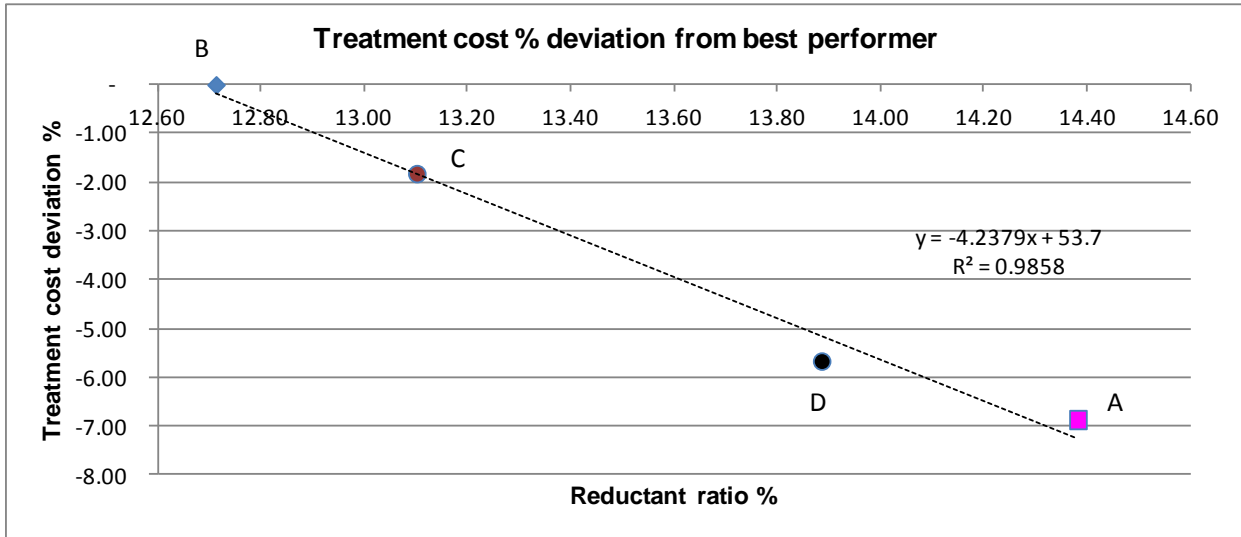


Figure 30: Treatment cost percentage deviation expressed against the best performer for various reductant ratios

6.4.2 Reductant efficiency contribution to NOP.

The reductant efficiency was plotted against the NOP percentage deviation relative to the best performer. A fair correlation exists between the reductant efficiencies and the NOP percentage deviation relative to the best performer as shown in Figure 31. However, the NOP is dependent on the amount of reductant used as a function of fixed carbon and carbon efficiency. The reductant efficiencies relative contribution to the bottom line can be up to 5%.

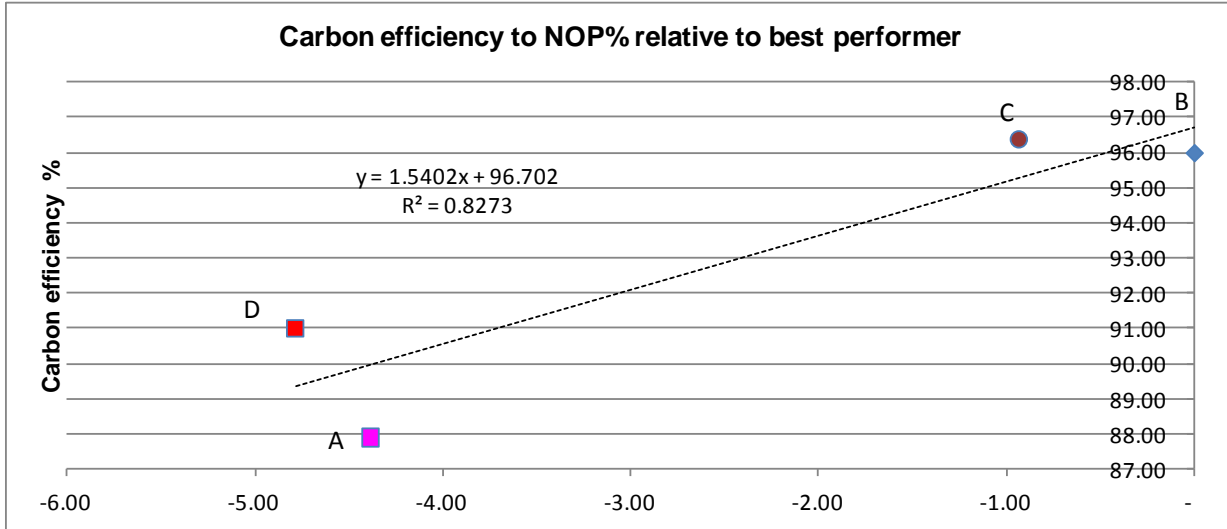


Figure 31: Carbon efficiency against Net Operating Profit percentage deviation from best performer

6.4.3 Reductant consumption correlated to NOP.

The NOP percentage deviation was also expressed in relation to reductant ratio in Figure 32. An increase in reductant ratio occurs due to a decrease in fixed carbon units and reductant efficiency. Increased amounts of reductant lead to increased variable cost since the reductant prices are not necessarily aligned. Increase variable cost decreases the NOP. A decrease in carbon units, leads to an increase in ash content which increases the sulphur content in the tapped metal. Treatment costs (Figure 33) become more expensive due to increased consumption of desulphuriser and increase in sulphur waste product costs, decreasing the NOP. An increase in reductant ratio will require more furnace energy, leading to reduced ilmenite feed tons and to less final product output, decreasing the NOP. Figure 34 illustrates the NOP deviation from best performer and encapsulates all the all the associated costs impacting on NOP.

The reductant ratio deviation can affect the bottom line by up to 5%

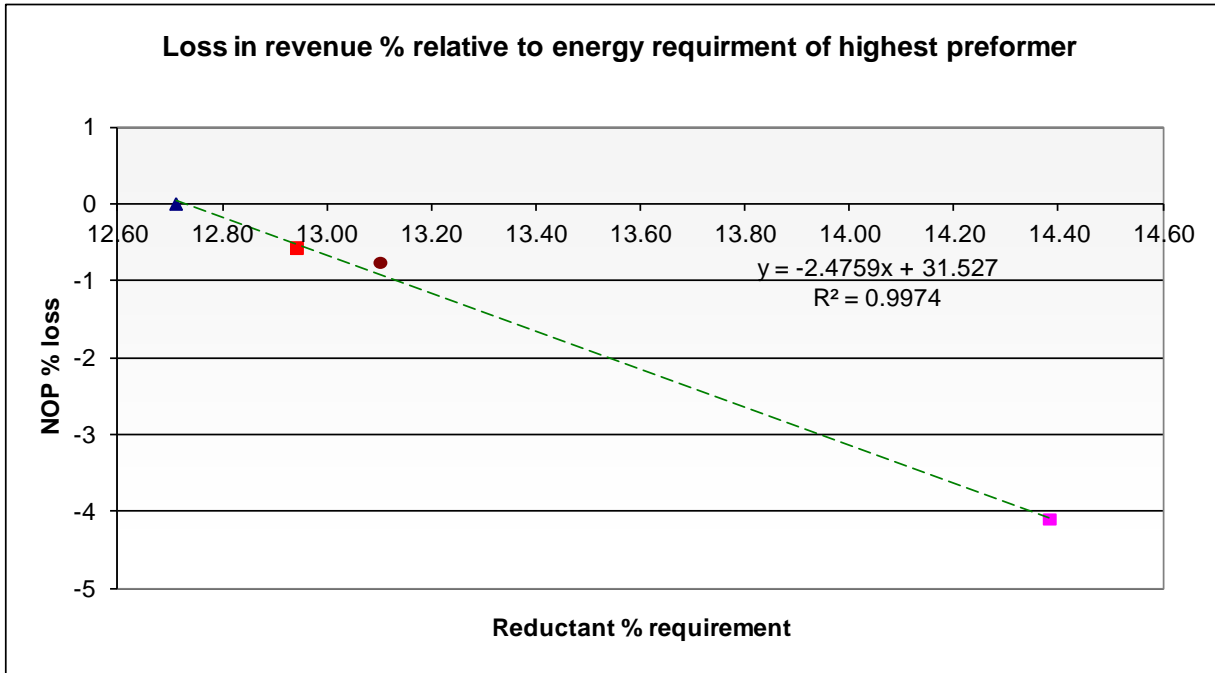


Figure 32: Net operating profit deviation percentage from the best performer as a function of reductant ratio

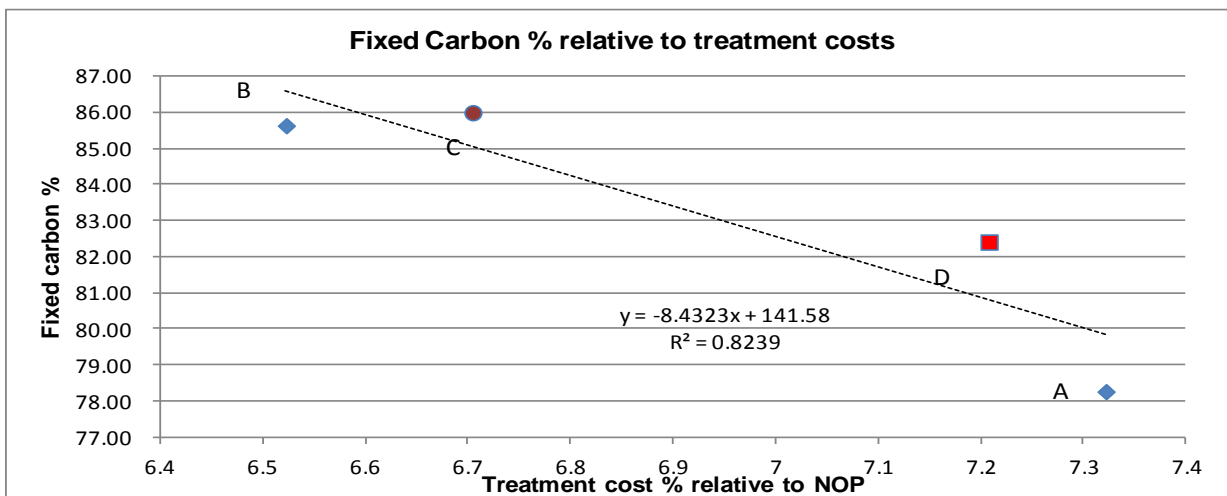


Figure 33: Fixed carbon percentage relative to the treatment costs

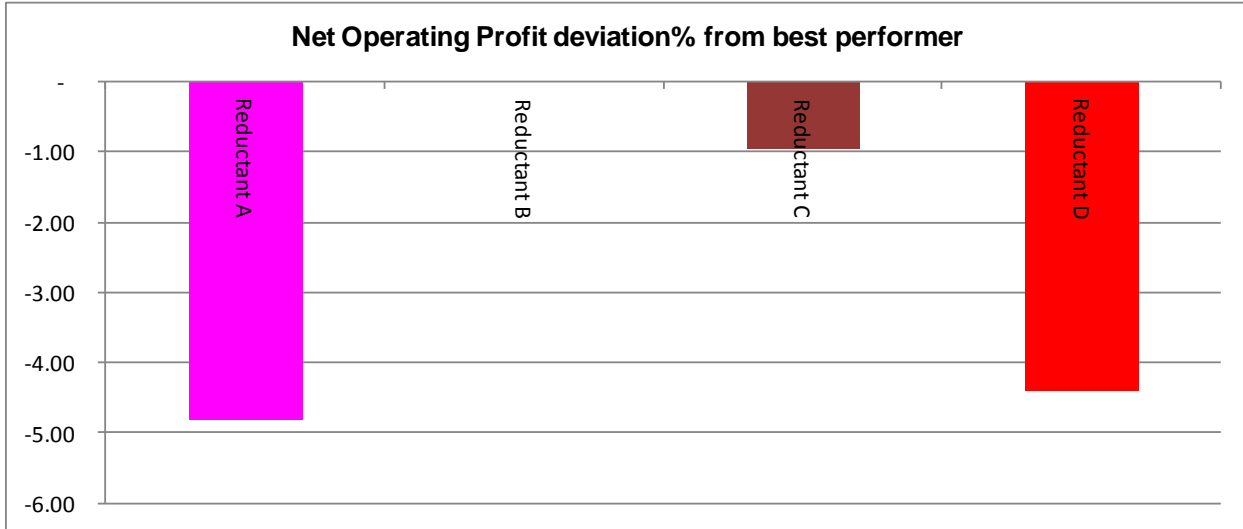


Figure 34: Net operating profit deviation percentage from the best performer.

6.4.4 Summary of VIU results

An increase in reductant ratio due to a decrease in fixed carbon, efficiency variation and increased treatment costs, can decrease the bottom line profit by up to 5% for the reductants tested. The fixed carbon is by far the leading indicator for variable cost variation and output of tons. From a VIU perspective, Reductant B is the preferable choice for smelting ilmenite.

7. CONCLUSIONS

This chapter summarises the conclusions drawn from the results obtained from the assessment of the carbon efficiencies of four carbon reductants and the comparison of these results to the petrographic characteristics of the reductants and to the general furnace conditions in which they were tested. The results of the smelter VIU model is then presented. The conclusions are presented as follows:

- A good correlation exists between reductant efficiencies to anthracite vitrinite content with a regression coefficient of 89%, suggesting that for an increase vitrinite content at a constant size reductant, the carbon efficiencies decrease. The mechanism of reductant loss, expressed as carbon efficiency, seems to be related to shattering of anthracite when exposed to furnace freeboard conditions at approximately 1600°C in the presence of inherent and surface moisture associated with the reductant. No significant correlation was found that relates side feed to reductant loss.
- The d50 particle sizes between the reductants was found to be very similar due to a deliberate size processing step prior to the reductant utilization. No significant correlation could be found between d50 and reductant loss.
- Finer size fraction (-1mm) is fairly well correlated to reductant efficiency as an increase in finer particles would lead to the tendency of increased losses.
- The carbon efficiency is closely correlated to the carbon to metal distribution and slag chemistry, indicating that the higher carbon efficiencies are associated with decreasing reductant losses, providing sufficient carbon for reduction and excess carbon to metal. The correlations for carbon efficiency and metal carbon percentage and carbon efficiency and slag chemistry are 92% and 87% respectively. Calculated carbon equilibrium was found to be approximately one order lower than the actual carbon percentages in the metal. Calculated and actual carbon percentages are well correlated with metal temperatures. Carbon percentages in metal can be correlated to titanium percentages in the metal and

used as an indication of carbon percentage in metal. It must be stated, however, that the mechanism of carbon distribution to metal is not yet clearly understood.

- Lower carbon efficiencies are well correlated with higher metal temperatures indicating that excess energy was applied due to an energy algorithm deviation. The deviation is certain to occur if the fixed carbon units to the system decreases due to losses or reductant feed variation since the energy algorithm is set up for a constant feed chemistry.
- The decrease in carbon in the metal for a decrease in TiO_2 percentage in the slag due to insufficient carbon units is most likely due to a combination of carbon losses occurring due to decrepitation and reporting to dust losses (-1mm fraction) or insufficient carbon units added initially.
- A strong linear dependence exists between reductant ratio percentage and TiO_2 percentages in the slag for the different campaigns. A strong linear dependence exists between theoretical energy requirement for varying reductant percentages. The reductant requirement is strongly dependent on reductant fixed carbon and reductant efficiency.
- Increased reductant ratios due to lower fixed carbons will have a linear cost increase of up to 7 percent on the bottom line treatment costs. The treatment costs are well correlated with fixed carbon percentage in the reductant and reductant efficiencies. An increased fixed carbon percentage in the reductant feed will necessitate lower reductant ratios to ilmenite, leading to lower level of impurities to the metal and less associated treatment costs.
- The reductant efficiencies relative contribution to the bottom line can be up to 5 percent for the selected reductants.
- The fixed carbon percentage is by far the leading indicator for variable cost variation and output of tons. From a VIU perspective, Reductant B is the preferable choice for smelting ilmenite.
- The Value In Use model indicates that higher fixed carbons and higher carbon efficiencies will lead to an overall increase in NOP due to less energy consumed per ton of ilmenite, increasing the ilmenite feed rate and ultimately increasing the throughput.

8. RECOMMENDATIONS

This chapter is focused on the recommendations for continued research on the topic under investigation

- The anthracites tested are classed as anthracites according to ISO11760 and SANS ISO 11760 with a vitrinite content ranging from 48% to 62%. Anthracites of higher and lower vitrinite contents and varying ranks should be tested using the same testing methodology as in this investigation for comparative purposes. Namakwa Sands anthracites should be incorporated in the test methodology.
- Char and Pet Coke should also be performance tested.
- Mechanisms of accretion formation with the use of various reductants in ilmenite smelting should be studied in more detail.
- Larger d50 reductant sizes should be tested to establish the correlation between size and carbon distribution between metal and slag reactions.
- The test methodology should be incorporated in the evaluation of future reductants in ilmenite smelting to obtain higher confidence levels with increased usage of various reductants.
- A gas evolution model should be constructed to anticipate variations in reductant and ilmenite feed chemistry.
- Carbon partition to the metal phase should be studied in more detail coupled with metal temperature behaviour.

9. LIST OF REFERENCES

- Burger H, Bessinger D, and Moodley S (2009). *Technical considerations and viability of higher titania slag feedstock for the chloride process. The 7th International Heavy Minerals Conference 'What next'*, The Southern African Institute of Mining and Metallurgy, 2009. 187-194.
- Falcon, L.M., R Falcon (1987) *Petrographic composition of Southern African coals in relation to friability, hardness and abrasive indices*. J. S. Afr. Inst. Min. Metall. vol. 87, no. 10. Oct 1987. pp. 323-336.
- Falcon R (2005). Exxaro Internal report on assessment of five anthracites samples supplied by Namakwa Sands and a comparison of five foreign anthracites and two previously analysed Vietnamese anthracites.
- Jordan.P. (2009). *Reductant Evaluation for Ilmenite smelting 2008*. Exxaro R&D Internal Report.
- Kotze H, Bessinger D, Beukes J (2006). *Ilmenite smelting at Ticor SA*. Journal of the South African Institute of Mining and Metallurgy. 106. 165-170
Pistorius P.C (2008). *Ilmenite smelting: the basics*. Journal of South African Institute of Mining and Metallurgy. 108. 35-43.
- Mason Walsh, Jr. and Russell Dutcher (1959). *Properties and reactions exhibited by anthracite lithotypes under thermal stress*. Presented before the division of gas and fuels chemistry, American Chemical Society, Boston, Massachusetts, Meeting, April 5-10, 1959.
- Moodley, S. (2011). *Exxaro Sands Reductant Project*. Report submitted to Exxaro Sands on test work of reductants at Namakwa Sands.
- Pistorius P.C (2008). *Ilmenite smelting: the basics*. Journal of South African Institute of Mining and Metallurgy. 108. 35-43
- Pistorius P.C, de Villiers JPR, Gräser P, Venter A (2011). *Partial slag solidification within and ilmenite smelter*
- Sahajwalla V, Dubikova M, Khanna R (2004). *Reductant characterization and selection: implications for ferroalloys processing*. Proceedings 10th International Ferroalloys Congress (INFACON X). 351-362.
- Zietsman J.H, Pistorius P.C (2004). *Process mechanisms in ilmenite smelting*. Journal of the South African Institute of Mining and Metallurgy. 653-660.

10. APPENDICES

10.1 Reductant A size analyses

RPP_BCBN (Sample taken before coarse bin)									
Date Time	(Duplicate Analysis)		Coal Screening 19mm to 1mm						
	Variance Check	% Moisture	% 19 mm Fraction	% 16 mm Fraction	% 10 mm Fraction	% 6.3 mm Fraction	% 1 mm Fraction	% - 1 mm Fraction	% Total screen
2010/09/26 02:00	0.06	1.21	0	0	2.26	21.84	73.05	3.3	100.45
2010/09/26 06:00	0.06	1.92	0	0	1.56	17.94	80.58	0.51	100.59
2010/09/26 22:00	0.04	1.64	0	0	0.69	22.75	67.42	8.68	99.54
2010/09/27 02:00	0.02	1.46	0	0	4.78	21.75	66.03	7.39	99.95
2010/09/28 14:00	0.11	2.13	0	0	1.87	30.04	66.31	1.68	99.9
2010/09/28 18:00			0	0	3.3	25.19	68.68	2.69	99.86
2010/09/30 06:00	0.05	1.58	0	0	0.12	11.45	85.34	3.19	100.1
2010/09/30 10:00	0.03	1.85	0	0	1.02	11.79	84.38	3	100.19
2010/09/30 22:00	0.06	1.65	0	0	0.81	14.76	80.03	4.28	99.88
2010/10/01 02:00	0.13	1.29	0	0	0.61	15.97	78.04	5.26	99.88
2010/10/01 06:00	0.05	1.69	0	0	0.71	14.74	81.78	2.67	99.9
2010/10/02 02:00	0.02	1.57	0	0	1.71	20.79	72.93	4.44	99.87
2010/10/02 22:00	0.04	1.73	0	0	1.65	23.52	73.03	1.75	99.95
2010/10/03 02:00	0.09	1.57	0	0	1.29	17.15	78.64	2.94	100.02
2010/10/03 06:00	0.05	1.58	0	0	0.88	13.7	82.84	2.89	100.31
2010/10/03 22:00	0.01	1.57	0	0	2.34	18.69	76.78	2.34	100.15
2010/10/04 02:00	0.04	1.16	<0	0.19	0.8	22.12	76.03	1.24	100.38
2010/10/04 06:00	0.02	1.33	0	0.03	0.37	17.29	79.63	2.71	100.03
2010/10/04 22:00	0.03	1.67	0	0	0.64	15.99	78.05	5.29	99.97
2010/10/05 02:00			0	0	1.54	19.96	75.14	3.37	100.01
2010/10/06 06:00	0.15	1.55	0	0	1.81	25.12	70.49	2.42	99.84
2010/10/06 10:00	0.01	0.02	0	0	1.75	28.19	68.25	1.62	99.81
2010/10/06 22:00	0.01	1.5	<0	0	0.57	17.83	79.2	2.38	99.98
2010/10/07 02:00	0.06	1.23	0	0	0.63	14.19	81.96	3.2	99.98
2010/10/07 22:00	0.04	1.61	0	0	0.21	9.23	84.41	6.15	100
2010/10/08 02:00	0.06	1.54	0	0	0.25	9.91	84.63	5.22	100.01
2010/10/09 02:00	0.11	1.86	0	0	0.32	13.78	81.33	4.31	99.74
2010/10/10 02:00	0.02	1.34	0	0	0.71	14.75	81.78	2.67	99.91
2010/10/11 02:00	0.07	1.37	0	0	0.41	15.2	82.47	1.99	100.07
2010/10/12 02:00	0.08	1.25	0	0	0.13	18.07	79.41	2.53	100.14
2010/10/12 22:00	0.02	1.17	0	0	0.57	17.83	79.2	2.38	99.98
2010/10/13 02:00	0	1.25	0	0	0.21	9.25	84.4	6.15	100.01
2010/10/14 02:00	0.02	1.46	0	0	1.54	19.96	75.14	3.37	100.01
2010/10/15 02:00	0.04	1.18	0	0	0.16	14.86	82.15	3	100.17
2010/10/15 22:00	0.02	1.15	0	0	0.26	14.33	82.23	3.06	99.88
2010/10/17 02:00	0.01	1.23	0	<0	0.85	27.34	70.79	0.9	99.88
2010/10/17 22:00	0.02	1.12	0	0	0.59	23.78	73.6	1.86	99.83
2010/10/18 02:00	0.01	1.17	0	0	0.57	22.68	74	2.6	99.85
2010/10/18 22:00	0.09	5.04	0	0	1.02	23.09	73.72	2.3	100.13
2010/10/19 02:00	0.12	1.02	0	0	0.15	16.65	79.76	3.81	100.37
2010/10/20 02:00	0.07	1.27	0	0	1.01	25.65	70.86	2.61	100.13
2010/10/20 06:00	0.02	1.1	0	0.01	0.95	19.94	76.47	2.74	100.11
2010/10/20 10:00	0.02	1.07	0	0	0.23	14.12	82.77	2.97	100.09
2010/10/20 22:00	0.02	1.14	0	0	0.16	13.39	82.15	3	98.7
2010/10/21 02:00	0.12	1.35	0	0	0.13	18.07	79.41	2.53	100.14
2010/10/21 22:00	0.06	1.21	0	0	0.21	9.15	84.37	6.14	99.87
2010/10/23 02:00	0	0.91	0	0	0.28	15.66	82.02	2.06	100.02
2010/10/23 06:00	0.01	0.91	0	0	1.07	16.61	79.36	2.78	99.82
2010/10/23 10:00	0.06	1.27	0	0	0.73	15.53	81.42	2.18	99.86
2010/10/23 22:00	0	0.64	0	0	0.62	22.45	75.84	1.13	100.04
2010/10/24 02:00	0.02	1.14	0	0	0.69	19.05	77.97	2.34	100.05
2010/10/24 22:00	0.04	1.17	0	0	0.66	25.85	69.43	3.84	99.78
2010/10/25 02:00	0.02	1.22	<0	<0	0.5	24.84	70.54	4.11	99.99
2010/10/25 22:00	0.07	1.21	0	0	6.94	28.11	61.06	3.8	99.91
2010/10/26 02:00	0.08	1.21	0	0	3.21	33.51	59.59	3.58	99.89

10.2 Reductant A XRF press powder and Proximate analysis

RPP_BCBND (Daily composite of RPP_BCBN)																										
Date Time	XRF COAL														% Inherent Moisture		% ASH (Air dry basis)	% Volatiles (as analysed)		Proximate				% Volatiles (Dry basis)	% ASH (Dry basis)	
	TiO2	SiO2	Al2O3	MgO	CaO	MnO	V2O5	Cr2O3	P2O5	Na2O	K2O	Fe2O3	Elemental P	Ash	Fe(t)	TOTAL	Variance Check	% Inherent Moisture	% Ash (Air dry)	Variance	% Volatile (as analysed)	% Volatile (Dry Basis)	% Ash (Dry basis)	% Fixed carbon	% Volatile (Dry Basis)	% Ash (Dry basis)
2010/09/26 23:45	1.033	58.052	15.679	1.002	4.399	0.073	0.065	0.008	0.087	1.185	1.575	6.377	0.006	12.8	4.46	89.535	0.05	0.6	12.7	0.2	7.3	6.7	12.8	80.5	6.7	12.8
2010/09/30 23:45	1.091	61.402	15.218	0.972	3.388	0.077	0.033	0	0.087	1.547	1.754	5.721	0.006	12.8	4	91.29	0.04	1.8	14	0.02	10.5	8.9	14.3	76.8	8.9	14.3
2010/10/01 23:45	1.059	60.885	16.35	1.051	4.52	0.063	0.042	0	0.083	1.492	1.673	4.79	0.006	13.2	3.35	92.01	0.07	1.7	13	0.04	8.3	6.7	13.2	80.1	6.7	13.2
2010/10/02 23:45	1.096	61.891	15.537	1.032	3.95	0.053	0.036	0	0.081	1.511	1.726	4.895	0.006	13.6	3.42	91.808	0.02	1.4	13.4	0.27	8.2	6.9	13.6	79.5	6.9	13.6
2010/10/03 23:45	2.621	59.792	15.473	1.069	3.989	0.102	0.055	0.006	0.083	1.422	1.681	5.131	0.006	13.3	3.59	91.434	0.07	1.7	13.1	0.06	8.5	6.9	13.3	79.8	6.9	13.3
2010/10/04 23:45	1.073	62.258	16.175	1.039	3.958	0.065	0.076	0	0.085	0.759	1.727	5.139	0.006	13.2	3.59	92.354	0.02	1.8	13	0.1	8.3	6.6	13.2	80.2	6.6	13.2
2010/10/06 23:45	1.154	62.291	15.516	1.02	3.558	0.075	0.039	0.016	0.091	1.444	1.637	5.632	0.007	14.7	3.94	92.473	0.1	2.4	14.3	0.16	7.4	5.1	14.7	80.2	5.1	14.7
2010/10/07 23:45	1.234	63.234	14.886	0.892	3.168	0.072	0.053	0.01	0.093	1.13	1.655	5.975	0.007	14.3	4.18	92.402	0.15	1.7	14.1	0.06	8.7	7.1	14.3	78.6	7.1	14.3
2010/10/08 23:45	1.024	62.381	15.027	0.669	3.144	0.077	0.07	0.008	0.09	1.437	1.622	6.157	0.007	15.9	4.31	91.706	0.03	1.9	15.6	0	7.1	5.3	15.9	78.8	5.3	15.9
2010/10/09 23:45	0.956	60.73	14.626	0.794	3.59	0.092	0.038	0.008	0.098	1.188	1.514	6.763	0.008	16.2	4.73	90.387	0.03	1.7	15.9	0.03	8.1	6.5	16.2	77.3	6.5	16.2
2010/10/10 23:45	1.034	61.401	15.049	0.948	3.468	0.079	0.053	0.01	0.1	1.453	1.645	6.17	0.008	15.5	4.32	91.41	0.04	1.3	15.3	0.11	8.4	7.2	15.5	77.3	7.2	15.5
2010/10/11 23:45	1.017	61.486	14.568	0.788	4.009	0.087	0.063	0.014	0.102	1.516	1.505	6.09	0.008	15.5	4.26	91.245	0.06	1.3	15.3	0.13	7.8	6.6	15.5	77.9	6.6	15.5
2010/10/12 23:45	1.575	61.858	14.784	0.764	3.371	0.086	0.065	0.009	0.095	1.538	1.593	6.035	0.008	15.7	4.22	91.773	0	1.4	15.5	0.22	8.3	7	15.7	77.3	7	15.7
2010/10/13 23:45	1.28	63.863	15.052	0.445	3.84	0.084	0.043	0.008	0.092	1.238	1.685	6.346	0.008	14.5	4.44	93.976	0.04	1.2	14.3	0.02	7.9	6.8	14.5	78.7	6.8	14.5
2010/10/14 23:45	1.354	59.873	15.092	0.723	4.042	0.085	0.058	0.009	0.09	1.375	1.624	6.369	0.004	16.3	4.45	90.694	0.04	1.8	16	0.3	9.7	8	16.3	75.7	8	16.3
2010/10/15 23:45	1.091	58.819	15.163	1.097	3.795	0.098	0.094	0.023	0.093	1.384	1.547	6.846	0.007	15.6	4.79	90.05	0.14	1.9	15.3	0.09	7.9	6.1	15.6	78.3	6.1	15.6
2010/10/16 23:45	1.092	59.453	15.421	1.111	3.688	0.1	0.106	0.024	0.101	1.463	1.519	6.713	0.008	16	4.7	90.791	0.02	1.3	15.8	0	8.3	7.1	16	76.9	7.1	16
2010/10/17 23:45	0.901	56.85	15.049	1.002	3.86	0.094	0.096	0.02	0.095	1.316	1.463	7.865	0.008	16.6	5.5	88.611	0.07	1.5	16.3	0.02	7.1	5.7	16.6	77.7	5.7	16.6
2010/10/18 23:45	0.983	59.825	14.922	0.867	3.897	0.086	0.061	0.013	0.101	1.286	1.57	6.382	0.008	16	4.46	89.993	0.2	1.5	15.8	0.02	8.2	6.8	16	77.2	6.8	16
2010/10/19 23:45	1.027	58.884	14.442	0.712	3.948	0.081	0.055	0.016	0.095	1.421	1.667	6.606	0.008	15.7	4.62	88.954	0.14	0.8	15.6	0	7.5	6.8	15.7	77.5	6.8	15.7
2010/10/20 23:45	0.924	60.287	14.413	0.782	3.793	0.082	0.049	0.002	0.098	1.518	1.616	6.555	0.008	16.3	4.58	90.119	0.02	1.1	16.1	0.14	8.6	7.6	16.3	76.1	7.6	16.3
2010/10/21 23:45	1.01	61.516	15.013	0.722	4.2	0.077	0.035	0.009	0.102	1.335	1.609	5.903	0.008	15.3	4.13	91.721	0.04	2.2	15	0.3	9.3	7.3	15.3	77.4	7.3	15.3
2010/10/22 23:45	0.944	59.823	15.989	0.777	3.928	0.072	0.026	0.008	0.105	1.398	1.63	5.439	0.008	15.5	3.8	90.139	0.02	1.4	15.3	0.04	6.8	5.5	15.5	79	5.5	15.5
2010/10/23 23:46	1.086	62.376	14.637	0.607	4.051	0.068	0.045	0.013	0.1	1.487	1.511	5.623	0.008	14.9	3.93	91.604	0.01	1.1	14.7	0.08	7.5	6.5	14.9	78.6	6.5	14.9
2010/10/24 23:45	0.967	61.097	14.884	0.691	4.128	0.069	0.026	0.002	0.098	1.179	1.539	5.056	0.008	15.7	3.54	89.736	0.1	0.9	15.6	0.06	6.5	5.7	15.7	78.6	5.7	15.7
2010/10/25 23:45	0.97	59.864	14.873	0.622	4.724	0.073	0.049	0.01	0.105	1.61	1.491	5.108	0.009	15.7	3.57	89.499	0.14	1.2	15.7	0.04	6.3	5.2	15.9	78.9	5.2	15.9

10.3 Reductant A Petrographics

TABLE 3 : SUMMARY OF MAJOR PETROGRAPHIC CHARACTERISTICS

PSA 2011	1 Reductant A DUFF 517
RANK (degree of maturity) ISO 11760-2005 Classification of Coals	Anthracite High Rank B
Mean random reflectance %	3.85
Vitrinite e-class distribution Standard deviation σ	V 28 to V 54 0.517
PETROGRAPHIC COMPOSITION (vol. %) Maceral analysis, mineral matter basis Vitrinite content % Total inertinite % Heat altered / graphitized % Visible minerals % Other %	56 35 3 6 0
Maceral analysis - Total: 100%	100

10.6 Reductant A associated furnace data (daily)

Date	Total Ilmenite Ton	Cold Ilmenite Ton	Hot Ilmenite Ton	Suppl Ilmenite Ton	Total Reductant Ton	Total RR %	Center Reductant Ton	Center RR %	Suppl Reductant Ton	Suppl RR %	Power Consumption MWh	Power Ratio MWh/t	Resistance mohm	Slag Ton	Temp °C	Iron Ton	Temp °C
2010/09/28 06:00	660.46	623.92	0	50.63	85.41	12.93	79.83	13.06	6.6	2.7	863.125	1307	2.5	280.902	1689	287.21	1518
2010/09/29 06:00	239.65	34184	0	0	38.37	16.01	44.17	18.43	0	2.7	470.03125	1961	2.5	219.237	1670	68.8	1502
2010/09/30 06:00	522.25	544.42	0	28.41	76.93	14.73	74.89	15.05	3.71	13.7	754.71875	1437	2.5	281.595	1675	217.55	1546
2010/10/01 06:00	365.93	37186	0	2.99	48.71	13.31	51.5	14.7	0.4	13.6	510.375	1393	2.5	212.67	1674	127.8	1544
2010/10/02 06:00	577.53	545.62	0	48.23	79	13.68	74.62	14.05	6.32	13.6	759.46875	1313	2.6	329.197	1688	200.09	1553
2010/10/03 06:00	592.93	554.4	0	45.98	8153	13.75	76.34	13.94	6.05	13.65	757.375	1277	2.6	285.407	1684	232.62	1580
2010/10/07 06:00	469.47	432.28	0	45.88	7176	15.28	65.64	15.47	6.7	15.2	685.625	146	2.5	279.691	1654	211.02	1548
2010/10/08 06:00	498.9	442.03	0	61.4	77.21	15.48	67.96	15.51	9.31	15.5	715.84375	1435	2.5	314.4	1694	130.7	1480
2010/10/09 06:00	497.34	420.55	0	76.78	77.67	15.62	65.58	15.59	2.09	15.4	706.09375	142	2.5	286.737	1703	209.41	1510
2010/10/20 06:00	316.32	310.8	0	8.61	49.74	15.72	48.57	15.78	1.35	15.4	484.16625	1531	2.5	163.6	1702	139.88	1525
2010/10/21 06:00	499.32	512.06	0	0	78.31	15.68	78.31	15.68	0	15.1	738.96875	148	2.5	271.065	1718	128.68	1527
2010/10/22 06:00	513.35	456.54	0	56.81	74.44	14.5	66.22	14.5	8.22	13.4	700.125	1364	2.2	317.36	1720	259.91	1539
2010/10/23 06:00	303.83	278.13	0	29.95	40.04	13.18	36.11	13.11	3.98	13.7	392.25	1289	2.4	347.22	1701	194.64	1542
2010/10/24 06:00	561.7	532.92	0	52.42	78.1	13.9	70.87	13.86	7.22	13.3	742.16625	1311	2.6	330.3	1683	180.31	1642
2010/10/25 06:00	485.69	589.56	0	6.79	65.29	13.44	78.89	13.49	0.93	13.3	747.1875	1264	2.6	338.47	1667	178.86	1598
Sum	7104.67	6956.93	0	514.62	1022.51	14.392083	979.5	14.0794862	72.44	14.0764059	10027.5	1.4113956	12.42	4257.351	1688.13333	184.485333	1543.6

10.8 Reductant B XRF press powder and Proximate analyses

RPP_BCBND (Daily composite of RPP_BCBN)																													
Date Time	XRF COAL																				% Inherent Moisture	% ASH (Air dry basis)	% Volatiles (as analysed)		Proximate			% Volatiles (Dry basis)	% ASH (Dry basis)
	TiO2	SiO2	Al2O3	MgO	CaO	MnO	V2O5	Cr2O3	P2O5	Na2O	K2O	Fe2O3	Elemental P	Ash	Fe(t)	TOTAL	Variances	Inherent Moisture	% Ash (Air dry)	Variance			% Volatile (as analysed)	% Volatile (Dry Basis)	% Ash (Dry basis)	Fixed carbon	% Volatile (Dry Basis)		
2011/08/01 23:45	2.203	45.338	24.911	0.959	1.532	0.104	0.083	0.027	0.101	0.61	3.303	10.574	0.004	9.2	7.4	89.7	0.02	1.4	9.1	0.01	6.1	4.8	9.2	86	4.8	9.2			
2011/08/02 23:45	1.579	46.586	23.757	1.26	2.766	0.034	0.073	0.03	0.081	0.604	2.719	5.588	0.004	10.1	3.91	85.1	0.04	1.4	10	0.03	6.4	5.1	10.1	84.8	5.1	10.1			
2011/08/03 23:45	1.505	46.94	24.333	1.246	2.433	0.022	0.041	0.038	0.073	0.641	3.112	4.445	0.004	11.7	3.11	84.8	0.13	0.9	11.6	0.06	5.8	4.9	11.7	83.4	4.9	11.7			
2011/08/04 23:45	1.582	46.611	24.075	1.679	2.746	0.038	0.073	0.019	0.077	0.6	2.46	5.127	0.004	10.2	3.59	85.1	0.2	2	10	0.03	6	4.1	10.2	85.7	4.1	10.2			
2011/08/05 23:45	1.714	45.674	24.73	0.665	1.195	0.085	0.066	0.019	0.088	0.579	3.52	10.471	0.004	9	7.32	88.8	0	2.5	8.8	0.04	6.8	4.4	9	86.6	4.4	9			
2011/08/07 23:45	1.985	46.441	23.98	1.462	2.308	0.039	0.052	0.018	0.074	0.592	2.709	4.853	0.004	10.9	3.39	84.5	0.1	1.6	10.7	0.01	5.7	4.2	10.9	84.9	4.2	10.9			
2011/08/08 23:45	1.491	46.927	24.006	1.492	2.474	0.014	0.045	0.016	0.073	0.586	2.359	4.52	0.004	10.3	3.16	84	0.1	0.9	10.2	0.09	5	4.1	10.3	85.6	4.1	10.3			
2011/08/09 23:45	1.395	46.417	24.173	1.804	2.606	0.05	0.077	0.161	0.075	0.593	2.394	4.827	0.003	10.5	3.38	84.6	0	2.7	10.2	0	5.7	3.1	10.5	86.4	3.1	10.5			
2011/08/10 23:45	1.572	46.709	23.885	1.803	3.115	0.042	0.073	0.027	0.095	0.6	2.655	4.903	0.004	9.7	3.43	85.5	0.15	2.4	9.5	0.23	6.4	4.1	9.7	86.2	4.1	9.7			
2011/08/11 23:45	1.537	46.88	23.853	1.39	2.435	0.012	0.065	0.026	0.073	0.605	2.691	4.497	0.004	11	3.15	84.1	0.04	1.4	10.8	0.06	6.1	4.8	11	84.2	4.8	11			
2011/08/12 23:45	2.491	46.283	23.916	1.405	2.319	0.059	0.068	0.02	0.075	0.605	2.844	5.731	0.003	9.3	4.01	85.8	0.01	3.1	9	0.03	4.1	1	9.3	89.7	1	9.3			
2011/08/13 23:45	1.583	46.718	23.878	1.493	2.611	0.019	0.066	0.022	0.073	0.601	2.562	4.773	0.004	10.1	3.34	84.4	0.01	1.7	9.9	0.01	6.2	4.6	10.1	85.3	4.6	10.1			
2011/08/14 23:45	1.647	46.685	23.808	1.473	2.746	0.046	0.059	0.112	0.077	0.6	2.471	4.688	0.004	10.4	3.29	84.4	0.07	1.7	10.2	0.18	2.1	0.4	10.4	89.2	0.4	10.4			
2011/08/16 23:45	1.421	46.925	24.575	1.459	2.518	0.01	0.071	0.019	0.075	0.6	2.699	4.497	0.004	10.2	3.15	84.9	0.01	2	10	0.13	7.1	5.2	10.2	84.6	5.2	10.2			
2011/08/18 23:45	1.714	45.465	24.707	0.832	2.027	0.082	0.062	0.027	0.155	0.593	3.466	10.262	0.007	8.8	7.18	89.4	0.08	2.7	8.6	0.07	7.1	4.5	8.8	86.7	4.5	8.8			
2011/08/19 23:45	1.541	46.525	24.208	1.445	2.995	0.022	0.064	0.036	0.076	0.608	2.594	4.523	0.004	10.2	3.16	84.6	0.1	2.7	9.9	0.14	6.2	3.6	10.2	86.2	3.6	10.2			
2011/08/20 23:45	1.918	44.057	23.389	0.874	1.561	0.127	0.069	0.031	0.14	0.616	3.098	13.087	0.006	9.5	9.15	89	0.06	3	9.2	0.07	8.8	6	9.5	84.5	6	9.5			
2011/08/21 23:45	1.759	45.328	24.819	0.813	1.716	0.114	0.051	0.022	0.152	0.597	3.543	10.128	0.007	8.9	7.08	89	0.02	2.1	8.7	0.03	8.9	6.9	8.9	84.2	6.9	8.9			
2011/08/22 23:45	1.784	45.555	24.931	0.631	1.814	0.088	0.059	0.026	0.168	0.602	3.751	9.499	0.008	8.8	6.64	88.9	0.02	1.5	8.7	0.15	8.5	7.1	8.8	84.1	7.1	8.8			
2011/08/23 23:45	1.818	45.967	24.61	1.371	1.974	0.06	0.077	0.027	0.099	0.597	2.986	7.031	0.004	9.5	4.92	86.6	0.02	0.5	9.4	0	7	6.5	9.5	84	6.5	9.5			
2011/08/24 23:45	1.611	44.621	24.518	0.792	1.647	0.075	0.06	0.031	0.146	0.593	3.256	9.015	0.006	9	6.31	86.4	0.02	2.1	8.8	0.04	6.7	4.7	9	86.3	4.7	9			
2011/08/25 23:45	1.757	45.132	24.328	0.688	1.79	0.146	0.051	0.019	0.157	0.591	3.381	11.545	0.007	9.7	8.07	89.6	0.09	0.8	9.6	0.12	6.7	5.9	9.7	84.4	5.9	9.7			
2011/08/26 23:45	1.934	45.753	24.679	0.711	1.369	0.115	0.054	0.025	0.119	0.589	3.607	10.121	0.005	8.6	7.08	89.1	0.15	0.5	8.6	0.12	6.4	5.9	8.6	85.5	5.9	8.6			
2011/08/27 23:45	1.764	45.327	24.666	0.57	1.59	0.106	0.058	0.028	0.15	0.587	3.43	9.83	0.006	8.6	6.88	88.1	0.05	2.4	8.4	0.01	8.7	6.5	8.6	84.9	6.5	8.6			
2011/08/28 23:45	2.099	45.01	24.556	0.704	1.922	0.143	0.075	0.025	0.166	0.588	3.411	11.008	0.007	9	7.77	89.7	0.08	2.7	8.5	0.1	7.1	4.5	8.7	86.8	4.5	8.7			
2011/08/29 23:45	2.085	44.714	24.038	0.916	1.89	0.15	0.072	0.022	0.142	0.59	3.38	11.384	0.006	8.6	7.96	89.4	0.03	2.6	8.4	0.02	7.7	5.2	8.6	86.2	5.2	8.6			

10.9 Reductant B Petrographics

SOUTH AFRICAN BUREAU OF STANDARDS COAL AND ORGANIC PETROLOGY												
PETROLOGY CONTRACT NO.: P 083-2007						DATE : 26-11-2007						
COMPANY NAME : VRYHEID COAL LABORATORIES CC, PO BOX 689 VRYHEID						ATTN. : MR. JIMMY RONALD						
ORDER NUMBER: J RONALD 002/07						SAMPLES RECEIVED : 30-10-2007						
SABS NO.	COMPANY NO.		PETRO- GRAPHIC NO. 2007/C	MACERAL ANALYSIS (PERCENT BY VOLUME, MINERAL MATTER BASIS)							RANK	
				VIT	F/SF/SEC	MA/INT/MI	TOTAL I	HEAT ALTERED	GRAPHITIZED VITRINITE	MINERAL MATTER	REFLECTANCE	
				%	%	%	%	%	%	%	Rr %	σ
1	BREEZE	STOCKPILE	334	54	22	15	37	3	0	6	3.22	0.366
2	MIDLINGS	PEAS	335	51	23	15	38	3	0	8	3.29	0.401
3	DUFF	STOCKPILE	336	70	14	11	25	2	0	3	2.86	0.254

MACERAL ANALYSIS (REF: ISO 7404 - 3, 1994) VIT: VITRINITE F/SF/SEC: FUSINITE / SEMIFUSINITE / SECRETINITE MA/INT/MI: MACRINITE / INERTODETRINITE / MICRINITE TOTAL I: TOTAL INERTINITE MM: VISIBLE MINERALS	RANK (REF: ISO 7404 - 5, 1994) Rr: RANDOM REFLECTANCE, OIL IMMERSION σ STANDARD DEVIATION
---	--

10.12 Reductant B associated furnace data

Date	Total Ilmenite Ton	Cold Ilmenite Ton	Hot Ilmenite Ton	Suppl Ilmenite Ton	Total Reductant Ton	Total RR %	Center Reductant Ton	Center RR %	Suppl Reductant Ton	Suppl RR %	Power Consumption M Wh	Power Ratio M Wh/t	Resistance mohm	Slag Ton	Temp °C	Iron Ton
2011/08/02 06:00	604.71	477.36	0	127.35	76.25	12.61	60.1	12.59	16.15	8.98	762.6875	1261	12.6	335.1	1683	229.7
2011/08/03 06:00	228.22	228.37	0	6.25	29.13	12.77	28.73	12.95	0.79	0	334.025	1464	12.6	166.9	1658	60.6
2011/08/04 06:00	565.73	578.59	0	0	69.99	12.37	72.58	12.79	0	0	7715625	1361	12.3	286.3	1672	181
2011/08/05 06:00	576.82	425.07	0	151.75	74.68	12.95	53.71	13.21	23.24	12.723	7510625	1299	12.3	343.9	1684	248.3
2011/08/06 06:00	606.18	443.12	0	176.88	77.39	12.77	56.24	12.96	22.46	12.728	768.8125	1268	12.3	339.5	1671	124.2
2011/08/07 06:00	593.38	44182	0	169.5	76.37	12.87	56.32	13.12	2159	12.744	764.6875	1287	12.3	337.5	1638	187.1
2011/08/08 06:00	594.75	427.36	0	161.55	77.79	13.08	54.9	13.24	23.29	12.827	761.125	128	12.3	336.7	1682	193.3
2011/08/09 06:00	594.91	438.13	0	176.03	77.75	13.07	56.34	13.34	22.61	12.826	768.4375	1291	12.3	345.8	1684	248.7
2011/08/10 06:00	588.48	430.75	0	170.2	76.65	13.02	55.5	13.18	219	12.889	7515625	1277	12.3	286.5	1683	178.7
2011/08/11 06:00	589.76	417.62	0	187.96	76.59	12.99	53.77	13.26	24.14	12.853	7515625	1274	12.3	344.4	1695	250.1
2011/08/12 06:00	579.52	412.8	0	188.07	76.13	13.14	53.21	13.32	24.16	12.84	740.9375	1278	12.3	289.8	1692	176.5
2011/08/13 06:00	599.16	417.41	0	204.13	78.35	13.08	53.81	13.32	26.19	12.846	767.9375	1281	12.3	348.8	1693	249.7
2011/08/14 06:00	607.62	409.65	0	215.58	78.97	13	52.48	13.3	27.51	12.723	7619375	1253	12.3	340.2	1690	189.3
2011/08/15 06:00	609.05	409.47	0	219.98	78.16	12.83	52.37	13.26	27.97	12.725	766.25	1258	12.3	346.5	1689	243.5
2011/08/16 06:00	596.61	407.43	0	211.54	76.86	12.88	51.89	13.38	26.75	12.612	755	1265	12.3	380.6	1689	222.5
2011/08/17 06:00	286.54	277.09	0	15.43	36	12.56	35.01	12.85	194	0	409.6875	1424	12.3	171.3	1666	65.1
2011/08/18 06:00	503.96	435.04	0	80.92	64.33	12.77	55.18	13.01	10.19	12.579	677.625	1342	12.3	277.8	1681	191.7
2011/08/19 06:00	596.97	417.94	0	187.07	76.71	12.85	52.85	13.08	24.83	12.618	760.875	1275	12.3	336.2	1688	185.9
2011/08/20 06:00	599.22	395.1	0	217.43	75.76	12.64	50.13	12.95	27.35	12.6	754	1258	12.2	333.4	1688	235.8
2011/08/21 06:00	606.51	406.41	0	220.81	77.72	12.81	51.55	13.18	27.87	12.603	7714375	1267	12.2	331.9	1687	201
2011/08/22 06:00	590.3	387.46	0	215.42	75.71	12.83	49.5	13.04	27.48	12.675	743.875	126	12.2	334.2	1678	241.6
2011/08/23 06:00	575.13	386.32	0	205.16	74.05	12.88	49.15	13.15	26.4	12.9	735.4375	1279	12.2	335.8	1670	184.3
2011/08/24 06:00	571.56	382.59	0	206.65	74.05	12.96	48.69	13.24	26.62	12.779	742.5	1299	12.2	278.4	1682	241.5
2011/08/25 06:00	577	389.17	0	203.9	74.05	12.83	49.34	13.1	26.1	12.807	736.0625	1276	12.2	326.3	0	183.5
2011/08/26 06:00	547.32	394.23	0	177.29	69.62	12.72	49.25	12.95	22.47	2.105	706.9375	1288	12.2	334.6	0	174.4
2011/08/27 06:00	578.42	400.55	0	214.31	74.51	12.88	50.16	13.4	27.07	5.83	750.4375	1297	12.2	331.1	1684	248.2
2011/08/28 06:00	602.69	406.96	0	222.95	75.77	12.57	51.02	12.98	28.2	12.675	769.625	1275	12.2	340.6	1681	197.6
2011/08/29 06:00	547.92	366.02	0	187.85	68.92	12.58	45.75	12.91	25.08	4.725	690.025	126	12.4	341.4	1686	186.8
2011/08/30 06:00	531.1	449.77	0	94.08	67.07	12.63	56.19	12.85	1192	0	698.625	1315	12.5	291	1685	243.5
2011/08/31 06:00	156.26	166.02	0	0	20.54	13.15	20.95	13.4	0	0	254.4375	1628	12.79	45.6	1648	0
2011/09/01 06:00	488.08	504	0	0	62.1	12.72	63.46	13	0	0	708.625	1452	12.3	317.9	1667	164.3

10.13 Reductant C size analyses

RPP_BCBN (Sample taken before coarse bin)									
Date Time	% MOISTURE (Duplicate)		Coal Screening 19mm to 1mm						
	Variance Check	% Moisture	% 19 mm Fraction	% 16 mm Fraction	% 10 mm Fraction	% 6.3 mm Fraction	% 1 mm Fraction	% - 1 mm Fraction	% Total screen
2011/04/20 22:00	0.01	1.88	0	0	1.69	21.18	74.5	0.77	98.14
2011/04/21 02:00	0.02	1.95	0	0	1.88	12.9	81.53	1.92	98.23
2011/04/21 22:00	0.05	1.2	0	0	2.55	29.29	66.84	1.21	99.89
2011/04/22 02:00	0	1.88	<0	0	2.34	23.37	73.08	0.33	99.12
2011/04/22 22:00	0.04	1.76	0	0	0.31	14.77	82.29	2.6	99.97
2011/04/23 02:00	0	1.95	0	0	0.5	19.54	77.39	2.48	99.91
2011/04/24 02:00	0.01	1.86	0	0	0.69	14.63	80.94	3.6	99.86
2011/04/24 22:00	0.05	1.67	0	0	0.65	19.57	77.09	2.66	99.97
2011/04/25 22:00	0.04	1.83	0	0.46	0.95	20.15	77.05	1.37	99.98
2011/04/26 22:00	0.07	1.74	0	0	2.16	42.69	52.05	3.06	99.96
2011/04/27 02:00	0.03	1.56	0	0	8.47	37.08	52.46	2.04	100.05
2011/04/27 22:00	0	1.91	0	0	7.82	39.94	51.41	0.86	100.03
2011/04/28 02:00	0.08	2.24	0	0	6.18	30.29	60.4	3.14	100.01
2011/04/28 22:00	0.07	2.09	0	0	4.16	28.73	65.61	1.32	99.82
2011/04/29 02:00	0.11	1.93	0	0	4.6	21.66	71.55	2.19	100
2011/04/30 02:00	0.02	2.13	0	0	5.7	28.36	65.33	0.49	99.88
2011/04/30 06:00	0.07	2.01	0	0	3.15	24.5	71.81	0.41	99.87
2011/04/30 22:00	0.01	1.63	0	0	6.23	27.67	62.75	3.21	99.86
2011/05/01 02:00	0.11	1.83	0	0.33	3.95	30.36	61.28	4.04	99.96
2011/05/01 22:00	0.13	2.36	0	0	1.89	25.01	68.55	4.52	99.97
2011/05/02 22:00	0.01	1.77	0	0.01	1.94	20.56	75.12	2.32	99.95
2011/05/03 02:00	0.07	1.7	0	0	0.99	19.4	76.67	2.93	99.99
2011/05/03 22:00	0.06	1.76	0	0	2.18	22.59	73.19	1.97	99.93
2011/05/04 22:00	0.01	1.77	0	0	1.7	30.02	64.65	3.65	100.02
2011/05/05 16:30	0.06	1.87	0.01	0.39	1.41	18.32	76.27	3.44	99.84
2011/05/06 02:00	0.07	1.84	0	0	3.27	31.02	61.62	4.1	100.01
2011/05/06 22:00	0.02	1.93	0	0.31	0.72	18.44	76.61	3.99	100.07
2011/05/07 02:00	0.13	2.25	0	<0	0.57	17.88	78.67	2.92	100.04
2011/05/07 14:00			0	0	3.3	35.37	59.36	1.94	99.97
2011/05/08 02:00	0.11	1.24	0	0	0.47	15.94	81.09	2.34	99.84
2011/05/08 22:00	0.01	1.36	0	0	0.03	12.24	84.81	2.66	99.74
2011/05/09 02:00	0.06	2.39	0	0	1.07	29.56	66.36	2.92	99.91
2011/05/09 22:00	0.05	1.97	0	0	2.47	26.78	65.91	4.75	99.91
2011/05/10 22:00	0.02	1.7	0	0	1.16	26.61	70.65	1.48	99.9
2011/05/11 22:00	0.05	1.79	0	0	1.02	21.26	71.06	6.58	99.92
2011/05/12 22:00	0.04	1.8	0	0	1.82	39.41	56.9	1.88	100.01
2011/05/13 22:00	0.03	1.69	0	0	5.63	39.15	53.69	1.49	99.96
2011/05/14 02:00	0.02	1.74	0	0	3.29	23.26	67.39	6.06	100
2011/05/14 22:00	0.1	2.09	0.36	<0	2.97	20.8	73.26	2.17	99.56
2011/05/15 02:00	0.07	1.98	0	0	1.15	22.67	73.1	2.56	99.48
2011/05/15 22:00	0.04	1.85	0	0	1.4	18.2	78.07	2.18	99.85
2011/05/16 02:00	0.03	1.78	0	0	0.36	13.43	83.45	2.62	99.86
2011/05/16 22:00	0.04	1.92	0	1.26	1.07	22.52	71.87	3.12	99.84
2011/05/17 02:00	0.02	2.03	0	0.03	0.15	14.92	81.83	2.77	99.7
2011/05/17 22:00	0.01	1.85	0	0	9.96	46.93	40.42	2.51	99.82
2011/05/18 22:00	0.01	1.83	0	0	1.65	24.33	72.6	1.45	100.03
2011/05/19 02:00	0.03	1.93	0	0	2.56	22.56	73.39	1.5	100.01
2011/05/19 22:00	0.02	1.97	0.01	0.01	2.16	19.19	75.54	3.11	100.02
2011/05/20 02:00	0.02	1.76	0	0	3.56	31.78	63.54	1.08	99.96

10.14 Reductant C XRF press powder and Proximate analyses

RPP_BCBND (Daily composite of RPP_BCBN)																										
Date Time	XRF COAL												% Inherent Moisture	% Ash (Air dry basis)	% Volatiles (as analysed)	Proximate			% Volatiles (Dry basis)	% Ash (Dry basis)						
	TiO2	SiO2	Al2O3	MgO	CaO	MnO	V2O5	Cr2O3	P2O5	Na2O	K2O	Fe2O3				Elemental P	Ash	Fe(t)			TOT AL	Varia nce Check	Inherent Moist ure	% Ash (Air dry)	Variance	% Volatile (as analysed)
2011/04/20 23:45	1.965	45.042	23.385	0.908	1.534	0.101	0.074	0.022	0.114	0.589	3.204	10.13	0.005	9.4	7.08	87.1	0.12	1.5	9.3	0.09	6.1	4.7	9.4	85.9	4.7	9.4
2011/04/22 23:45	1.736	45.526	24.033	0.887	1.38	0.06	0.024	0.022	0.107	0.585	3.377	9.734	0.005	9.4	6.81	87.5	0.06	2.7	9.1	0.05	3.5	0.8	9.4	89.8	0.8	9.4
2011/04/23 23:45	1.441	44.492	20.848	0.916	1.605	0.132	0	0.014	0.127	0.603	2.708	12.404	0.006	9.4	8.68	85.3	0.09	2.5	9.2	0.04	9.9	7.6	9.4	83	7.6	9.4
2011/04/25 23:45	1.835	45.804	23.225	0.898	1.498	0.098	0.021	0.019	0.135	0.588	3.142	11.218	0.006	8.9	7.85	88.5	0.05	2.4	8.7	0.3	7.3	5	8.9	86.1	5	8.9
2011/04/26 23:45	1.727	46.048	24	0.906	1.346	0.091	0.006	0.016	0.13	0.601	3.279	9.079	0.006	9.1	6.35	87.2	0.01	1.2	9	0.04	6.8	5.7	9.1	85.2	5.7	9.1
2011/04/27 23:45	1.458	45.083	24.132	0.955	1.578	0.103	0.035	0.025	0.098	0.587	2.794	12.79	0.005	10.4	8.95	89.6	0.07	0.8	10.3	0.07	6.6	5.8	10.4	83.8	5.8	10.4
2011/04/28 23:45	1.565	45.853	22.758	0.919	1.609	0.091	0.042	0.019	0.112	0.602	2.999	11.612	0.005	10.1	8.12	88.2	0.02	1.8	9.9	0.03	7.9	6.2	10.1	83.7	6.2	10.1
2011/04/29 23:45	1.437	44.553	20.054	0.907	1.612	0.089	0.06	0.033	0.111	0.598	2.679	10.728	0.005	9.9	7.5	82.9	0.06	2.1	9.7	0.06	9.8	7.9	9.9	82.2	7.9	9.9
2011/04/30 23:45	1.662	45.184	23.382	0.901	1.406	0.084	0	0.016	0.141	0.593	3.13	10.872	0.006	9	7.6	87.4	0.03	3.2	8.7	0.03	6.2	3.1	9	87.9	3.1	9
2011/05/01 23:45	1.726	47.709	18.546	0.899	1.751	0.097	0.023	0.014	0.087	0.594	2.474	9.498	0.005	11.1	6.64	83.4	0.08	2.8	10.8	0.04	4.2	1.4	11.1	87.5	1.4	11.1
2011/05/02 23:45	1.686	45.498	23.814	0.93	1.505	0.084	0.045	0.031	0.137	0.598	3.474	10.011	0.008	11.1	7	87.8	0.03	2.8	10.8	0.09	3.5	0.7	11.1	88.2	0.7	11.1
2011/05/03 23:45	1.922	45.723	23.873	0.898	1.338	0.077	0.006	0.015	0.121	0.606	3.254	9.83	0.005	8.9	6.88	87.7	0.14	2.7	8.7	0.28	7.5	4.9	8.9	86.2	4.9	8.9
2011/05/04 23:45	1.615	44.493	24.718	0.929	1.427	0.069	0.061	0.018	0.114	0.606	2.994	9.948	0.005	8.9	6.96	87	0.01	1.6	8.8	0	6.5	5	8.9	86.1	5	8.9
2011/05/05 23:45	1.621	45.023	25.099	0.936	1.477	0.122	0.034	0.028	0.124	0.605	3.245	10.517	0.005	8.5	7.36	88.8	0.03	1.5	8.4	0	5.7	4.3	8.5	87.2	4.3	8.5
2011/05/06 23:45	1.781	45.766	23.899	0.892	1.375	0.066	0.07	0.032	0.125	0.602	3.246	10.244	0.005	9.1	7.16	88.1	0.14	2.6	8.9	0.08	7.5	5	9.1	85.9	5	9.1
2011/05/07 23:45	1.946	46.164	23.946	0.883	1.1	0.883	0.038	0.02	0.106	0.592	3.571	8.975	0.005	10.3	6.28	88.2	0.07	1.6	10.1	0.05	7.7	6.2	10.3	83.5	6.2	10.3
2011/05/08 23:45	1.637	45.254	24.22	0.902	1.214	0.078	0.016	0.02	0.105	0.56	3.561	8.599	0.005	10	6.01	86.2	0	2.9	9.7	0.11	7.6	4.8	10	85.2	4.8	10
2011/05/09 23:45	1.704	45.728	24.262	0.887	1.33	0.066	0.085	0.034	0.126	0.594	3.44	9.83	0.005	8.8	6.88	88.1	0.03	0.8	8.7	0.12	8.2	7.5	8.8	83.7	7.5	8.8
2011/05/10 23:45	2.044	45.038	22.883	0.889	1.29	0.084	0.069	0.032	0.111	0.559	3.26	13.872	0.004	8.3	9.7	90.1	0.02	1	8.2	0.04	6.2	5.3	8.3	86.4	5.3	8.3
2011/05/11 23:45	1.793	45.249	23.089	0.886	1.328	0.077	0.022	0.02	0.154	0.589	3.312	11.174	0.007	8.8	7.82	87.7	0.01	1.1	8.7	0.01	8.3	7.3	8.8	83.9	7.3	8.8
2011/05/12 23:45	1.731	45.831	23.765	0.887	1.509	0.053	0	0.016	0.13	0.594	3.458	9.835	0.006	9.7	6.88	87.8	0.01	0.8	9.6	0.03	8.9	8.2	9.7	82.1	8.2	9.7
2011/05/13 23:45	1.83	46.015	24.2	0.887	1.399	0.064	0.007	0.018	0.129	0.584	3.39	9.498	0.005	8.5	6.64	88	0.13	1	8.4	0.04	5.5	4.5	8.5	87	4.5	8.5
2011/05/14 23:45	1.649	45.892	23.981	0.887	1.242	0.064	0	0.018	0.11	0.596	3.405	9.789	0.004	8.8	6.85	87.6	0	2.3	8.6	0.02	7.3	5.1	8.8	86.1	5.1	8.8
2011/05/15 23:45	1.743	45.535	22.865	0.882	1.394	0.071	0.075	0.042	0.12	0.592	3.225	13.523	0.005	8.4	9.46	90	0.04	2.3	8.2	0.04	2	-0.3	8.4	91.9	-0.3	8.4
2011/05/16 23:45	1.682	45.853	23.303	0.876	1.526	0.023	0.031	0.026	0.14	0.581	3.194	9.82	0.006	8.8	6.87	87.1	0.14	1.9	8.6	0.02	3.1	1.2	8.8	90	1.2	8.8
2011/05/17 23:45	2.71	45.56	24.957	0.747	1.041	0.119	0.057	0.021	0.112	0.596	3.625	9.186	0.004	8	6.42	88.7	0.03	0.5	8	0.07	5.5	5	8	87	5	8
2011/05/18 23:45	1.798	45.895	24.926	0.82	1.346	0.072	0.047	0.024	0.12	0.592	3.755	9.461	0.005	9.4	6.62	88.9	0.19	2.4	9.2	0.15	7	4.7	9.4	85.9	4.7	9.4
2011/05/19 23:45	1.871	45.378	25.091	0.838	1.351	0.101	0.056	0.024	0.125	0.582	3.393	9.376	0.005	8.6	6.56	88.2	0	2	8.4	0.04	7.4	5.5	8.6	85.9	5.5	8.6

10.15 Reductant C Petrographics

	Vitrinite (%)	Inertinite (%)	Mineral Matter (%) (Visible)	Reflectance R_r %
Reductant C	48	45	4	3.35

10.18 Reductant C associated furnace data

Date	Total Ilmenite Ton	Cold Ilmenite Ton	Hot Ilmenite Ton	Suppl Ilmenite Ton	Total Reductant Ton	Total RR %	Center Reductant Ton	Center RR %	Suppl Reductant Ton	Suppl RR %	Power Consumption MWh	Power Ratio MWh/t	Resistance mohm	Slag Ton	Temp °C	Iron Ton	Temp °C
2011/04/15 06:00	511.72	511.72	0	0	63.93	12.49	63.93	12.49	0	0	699.625	1367	12.2	342.3	1684	231.1	1475
2011/04/16 06:00	583.69	583.69	0	0	72.92	12.49	72.92	12.49	0	0	746	1278	12.5	334.8	1667	180.9	1497
2011/04/17 06:00	548.82	548.82	0	0	68.57	12.49	68.57	12.49	0	0	723.75	1319	12.2	336.8	1666	182.4	1470
2011/04/18 06:00	464.08	436.58	0	27.5	59.56	12.83	55.98	12.82	3.58	2.796	644.75	1389	12.2	277.5	1665	168	1482
2011/04/19 06:00	552.02	484.17	0	67.85	71.76	13	62.9	12.99	8.86	12.972	734.875	133	12.7	291.6	1680	214.7	1589
2011/04/20 06:00	536.92	442.16	0	94.76	69.39	12.92	57.09	12.91	12.3	12.905	701.125	1306	12.7	287.6	1683	180.7	1551
2011/04/21 06:00	506.49	420.25	0	86.24	65.37	12.91	54.18	12.89	11.19	12.957	648.5	128	12.7	280.8	1677	187.1	1532
2011/04/22 06:00	521.36	454.6	0	66.76	67.24	12.9	58.59	12.89	8.64	12.967	676.875	1298	12.7	337.4	1676	200.3	1534
2011/04/23 06:00	515.72	420.7	0	95.03	66.55	12.9	54.22	12.89	12.33	4.804	664.875	1289	12.7	273.5	1683	182.5	1528
2011/04/24 06:00	517.08	424.45	0	92.63	66.01	12.77	54.07	12.74	11.94	12.78	656.625	127	12.7	246.6	1690	182.4	1518
2011/04/25 06:00	587.66	481.97	0	105.69	74.84	12.73	61.31	12.72	13.53	12.867	743.5	1265	12.5	342.6	1688	186.9	1517
2011/04/26 06:00	566.1	474.41	0	91.68	70.57	12.47	58.77	12.39	11.8	12.873	712.375	1258	12.5	286.1	1673	248.3	1523
2011/04/27 06:00	596.13	485.09	0	111.04	76.32	12.8	62.06	12.79	14.26	12.793	751.175	1261	12.5	332.1	1681	207.8	1529
2011/04/28 06:00	294.25	282.93	0	11.32	37.07	12.6	35.65	12.6	142	0	407.875	1384	12.5	163.4	1668	64.3	1498
2011/04/29 06:00	569.53	542.29	0	27.2	73.59	12.92	66.32	12.94	7.47	13.082	741.625	1302	12.5	324.7	1672	195.2	1522
2011/04/30 06:00	569.04	505.21	0	64.62	74.01	13.01	65.68	13.02	8.43	13.104	739.825	13	12.8	274.7	1681	205.6	1533
2011/05/01 06:00	548.04	479.13	0	68.91	71.46	13.04	62.4	13.02	9.05	14.76	708.0625	1292	12.8	282.2	1690	210.8	1535
2011/05/02 06:00	561.09	489.8	0	71.29	71.47	12.74	62.26	12.71	9.2	12.792	710.5625	1266	12.8	342	1680	201.1	1519
2011/05/03 06:00	602.29	476.47	0	125.82	77.59	12.88	61.35	12.88	16.23	3.276	753.125	125	12.5	276.1	1686	216.3	1502
2011/05/04 06:00	457.56	457.56	0	0	59.05	12.9	59.05	12.9	0	0	623.825	1363	12.5	287.8	1689	157.5	1501
2011/05/05 06:00	548.16	447.49	0	100.67	70.73	12.9	57.71	12.9	13.02	12.991	695.825	1269	12.5	328.2	1682	186.1	1502
2011/05/06 06:00	556.36	460.7	0	95.66	72.35	13	59.84	12.99	12.51	13.035	715.9375	1287	12.5	329.4	1681	193.5	1514
2011/05/07 06:00	559.33	479.63	0	79.71	72.68	12.99	62.32	12.99	10.36	13.014	716.375	1281	12.5	278.5	1683	197.7	1531
2011/05/08 06:00	557.21	469.93	0	87.28	72.42	13	61.06	12.99	11.36	13.007	713.6875	1281	12.5	341.6	1655	183.8	1529
2011/05/09 06:00	555.94	437.26	0	118.68	72.19	12.99	56.78	12.99	15.41	13.01	699.875	1258	12.6	284.3	1687	180.8	1536
2011/05/10 06:00	538.03	526.97	0	11.06	69.67	12.99	68.43	12.99	144	0	703.5	1308	12.6	278.7	1681	201.5	1531
2011/05/11 06:00	292.67	292.67	0	0	37	12.64	37	12.64	0	0	400.75	1369	12.4	163	1666	140.4	1468
2011/05/12 06:00	535.42	535.42	0	0	69.47	12.98	69.47	12.98	0	0	733.0625	1369	11.8	323.8	1676	189.8	1402
2011/05/13 06:00	566.59	505.9	0	60.83	73.61	12.99	65.71	12.99	7.9	4.82	733.0625	1294	12.61	310.1	1688	190	1483
2011/05/14 06:00	536.51	474.46	0	63.41	68.43	12.75	60.28	12.74	8.19	12.55	692.5	1291	12.3	308.8	1691	189.8	1511

10.19 Reductant D size analyses

RPP_BCBN (Sample taken before coarse bin)									
Date Time	% MOISTURE (Duplicate)		Coal Screening 19mm to 1mm						
	Variance Check	% Moisture	% 19 mm Fraction	% 16 mm Fraction	% 10 mm Fraction	% 6.3 mm Fraction	% 1 mm Fraction	% - 1 mm Fraction	% Total screen
2012/07/21 06:00	0.01	1.91	0	0	4.98	23.09	66.31	5.51	99.89
2012/07/21 18:00	0.01	1.02	0	0.47	4.96	23.93	65.68	4.69	99.73
2012/07/21 22:00	0.05	0.99	0	0	4.64	23.08	69.02	2.9	99.64
2012/07/22 02:00	0.09	1.14	0	0	6.39	24.73	65.39	3.26	99.77
2012/07/22 06:00	0.08	1.19	0	0	1.89	20.99	71.47	5.6	99.95
2012/07/22 10:00	0.01	1.38	0	0	6.3	33.49	55.99	4.32	100.1
2012/07/22 14:00	0.02	1.28	0	0	4.49	28.02	63.41	5.19	101.11
2012/07/22 18:00	0.05	0.7	0	0	6.59	29.02	59.94	4.23	99.78
2012/07/22 22:00	0.04	0.7	0	0	8.49	29.28	57.03	4.93	99.73
2012/07/23 02:00	0.02	0.37	0	0	5.94	29.24	60.1	4.52	99.8
2012/07/23 06:00	0.04	1.44	0	0	6.98	23.1	61.34	8.01	99.43
2012/07/23 10:00	0.08	1.49	0	0	8.95	31.55	56.11	2.61	99.22
2012/07/23 14:00	0.11	2.52	0	0	9.17	29.8	58.31	2.26	99.54
2012/07/24 06:00	0.15	1.97	0	0	5.71	26.75	64	2.96	99.42
2012/07/24 10:00	0.09	1.67	0	0	1.97	27.53	67.5	2.5	99.5
2012/07/24 22:00	0.12	1.69	0	0	4.25	23.76	67.76	5.24	101.01
2012/07/25 06:00	0.05	1.84	0	0	5.31	30.75	60.66	2.53	99.25
2012/07/25 22:00	0.09	2.25	0	0	7.02	35.73	49.86	5.97	98.58
2012/07/26 02:00	0.13	1.91	0	0	4.33	26.84	59.58	8.61	99.36
2012/07/26 18:00	0.14	1.75	1.42	0	5	23.09	66.31	5.51	101.33
2012/07/27 06:00	0.13	0.83	0	4.68	48.23	29.92	15.83	0.89	99.55
2012/07/27 10:00	0.1	1.73	0.8	4.81	46.11	30.79	16.99	0.24	99.74
2012/07/27 14:00	0.04	1.68	0	3.65	51.02	29.91	13.63	1.69	99.9
2012/07/28 02:00	0.15	2.57							
2012/07/28 10:00	0.09	2.51	0	1.79	28.99	25.7	33.13	9.39	99

10.20 Reductant D XRF press powder and Proximate analysis

RPP_BCBND (Daily composite of RPP_BCBN)																												
Date Time	XRF COAL																		% Inherent Moisture	% ASH (Air dry basis)	Volatiles (as analysed)			Proximate			% Volatiles (Dry basis)	% ASH (Dry basis)
	TiO2	SiO2	Al2O3	MgO	CaO	MnO	V2O5	Cr2O3	P2O5	Na2O	K2O	Fe2O3	Elemental P	Ash	Fe(t)	TOTAL	Check	Inherent Moisture			% Ash (Air dry)	Variance	% Volatile (as analysed)	% Volatile (Dry Basis)	% Ash (Dry basis)	% Fixed carbon		
2012/07/21 23:45	1.66	42.848	24.21	0.946	5.248	0.152	0.114	0.023	0.011	0.591	1.325	6.883	0.011	12.3	4.81	84	0.03	2.7	12	0.06	8.5	6	12.3	81.7	6	12.3		
2012/07/22 23:45	2.45	41.899	23.78	0.944	5.767	0.151	0.089	0.021	0.15	0.595	1.285	6.281	0.01	13.7	4.39	83.4	0.05	2	13.4	0.12	7.3	5.4	13.7	80.9	5.4	13.7		
2012/07/23 23:45	1.689	42.092	24.911	0.941	4.041	0.138	0.115	0.034	0.172	0.605	1.217	5.879	0.01	11.8	4.11	81.8	0.07	2.9	11.5	0.09	7.3	4.5	11.8	83.7	4.5	11.8		
2012/07/24 23:45	1.831	42.849	25.191	0.966	3.7	0.145	0.095	0.043	0.01	0.603	1.164	6.240	0.01	12.5	4.37	82.8	0.02	0.8	12.4	0.23	5.2	4.4	12.5	83.1	4.4	12.5		
2012/07/25 23:45	2.373	42.638	24.098	0.939	4.681	0.146	0.095	0.034	0.152	0.601	1.365	6.141	0.009	12.1	4.3	83.3	0.03	1.4	11.9	0.06	6.7	5.4	12.1	82.5	5.4	12.1		
2012/07/26 23:45	1.748	42.621	24.36	0.937	3.958	0.136	0.063	0.024	0.157	0.593	3.958	5.729	0.008	10	4.01	84.3	0.09	2.1	9.8	0.04	7.6	5.6	10	84.4	5.6	10		
2012/07/27 23:45	1.247	30.717	20.815	0.918	1.595	0.124	0.023	0.011	0.101	0.602	1.973	8.228	0.005	9.8	5.75	66.4	0.05	1.2	9.7	0.24	7.2	6.1	9.8	84.1	6.1	9.8		

10.21 Reductant D Petrographics

TABLE 1 SUMMARY OF COAL AND ORGANIC PETROGRAPHY

Sample Identification	Vitrinite %	Liptinite %	Inertinite %	Mineral Matter	RANK	
					Reflectance $R_{rand}\%$	σ
KZN Anthracite	62.2	0	36.9	1.0	3.23	0.89

10.22 Reductant D associated metal analyses

FC1_LIM2M (Taphole 2 metal tap samples middle of tap)														
Date Time	OES FECAIR													
	C	Si	S	Mn	Cr	V	Ti	Al	Co	P	Cu	Ni	Mo	Nb
2012/07/21 08:50	2.131	0.036	0.2	0.035	0.066	0.037	0.051	0.313	0.022	0.033	0	0.02	0.005	0.007
2012/07/21 18:39	2.047	0.034	0.197	0.034	0.061	0.032	0.049	0.244	0.022	0.032	0	0.02	0.004	0.006
2012/07/22 02:15	1.967	0.033	0.21	0.034	0.064	0.032	0.042	0.454	0.022	0.033	0	0.02	0.006	0.006
2012/07/22 09:25	1.978	0.034	0.202	0.033	0.064	0.029	0.043	0.107	0.022	0.033	0	0.021	0.003	0.005
2012/07/22 14:22	1.902	0.037	0.21	0.035	0.068	0.031	0.045	0.385	0.022	0.034	0	0.02	0.005	0.006
2012/07/22 23:45	2.345	0.096	0.206	0.043	0.071	0.036	0.061	0.679	0.021	0.024	0	0.02	0.007	0.008
2012/07/23 18:35	1.823	0.049	0.209	0.043	0.073	0.031	0.053	0.359	0.022	0.034	0	0.02	0.005	0.008
2012/07/23 23:10	1.834	0.053	0.213	0.044	0.074	0.032	0.053	0.21	0.022	0.035	0	0.02	0.004	0.009
2012/07/24 21:15	1.789	0.058	0.214	0.047	0.078	0.032	0.058	0.362	0.021	0.036	0	0.02	0.005	0.01
2012/07/25 04:46	1.854	0.059	0.214	0.048	0.078	0.032	0.056	0.49	0.022	0.037	0	0.021	0.006	0.01
2012/07/25 13:35	2.028	0.061	0.212	0.051	0.084	0.038	0.07	0.348	0.021	0.036	0	0.02	0.005	0.012
2012/07/25 21:30	1.997	0.059	0.21	0.057	0.082	0.046	0.082	2.664	0.021	0.034	0	0.02	0.016	0.013
2012/07/26 02:00	2.203	0.055	0.208	0.048	0.082	0.048	0.074	0.439	0.021	0.031	0	0.02	0.006	0.012
2012/07/26 05:17	2.175	0.054	0.215	0.048	0.08	0.048	0.072	0.128	0.022	0.031	0	0.02	0.004	0.012
2012/07/26 23:05	1.979	0.044	0.218	0.04	0.068	0.037	0.042	0.209	0.022	0.036	0	0.021	0.004	0.008
2012/07/27 06:58	1.987	0.054	0.211	0.043	0.073	0.042	0.045	0.29	0.022	0.034	0	0.02	0.005	0.009
2012/07/27 18:50	1.951	0.073	0.214	0.049	0.079	0.05	0.047	0.349	0.022	0.034	0	0.021	0.005	0.013
2012/07/28 02:30	1.891	0.072	0.212	0.048	0.078	0.047	0.048	0.279	0.022	0.033	0	0.02	0.005	0.012

10.23 Reductant D associated slag analyses

FC1_LTS1M (Taphole 1 slag tap samples middle of tap)																	
Date Time	XRF SLAG																
	Al2O3	CaO	Cr2O3	FeO	K2O	MgO	MnO	Na2O	P2O5	SiO2	TiO2	V2O5	Nb2O5	ZrO2	Fe (Total)	Ti (Total)	
2012/07/21 06:50	1.42	0.2	0.26	10.4	0.02	1.03	1.81	0	0.001	2.47	83.8	0.43	0.11	0.2	11.6	8.084	50.238
2012/07/21 11:17	1.42	0.2	0.26	10.2	0.02	1.06	1.81	0	0.001	2.37	84.1	0.43	0.11	0.19	11.3	7.928	50.418
2012/07/21 16:50	1.4	0.19	0.26	12.1	0.02	1.01	1.81	0	0.001	2.26	82.7	0.43	0.11	0.19	13.5	9.405	49.579
2012/07/22 00:15	1.45	0.19	0.3	10.8	0.02	1.06	1.83	0	0.001	2.38	83.7	0.43	0.11	0.18	12	8.395	50.178
2012/07/22 04:09	1.459	0.199	0.309	12.27	0.02	1.032	1.867	0	0.001	2.395	82.4	0.417	0.104	0.18	13.631	9.534	49.401
2012/07/22 08:25	1.51	0.21	0.31	10.8	0.02	1.02	1.9	0	0.001	2.5	83.2	0.43	0.11	0.19	12	8.395	49.878
2012/07/22 12:25	1.5	0.2	0.3	10.1	0.02	1.04	1.88	0	0.001	2.44	84	0.43	0.11	0.19	11.2	7.851	50.358
2012/07/22 20:21	1.45	0.2	0.3	14.1	0.02	0.95	1.89	0	0.001	2.4	80.5	0.41	0.1	0.18	15.7	10.96	48.26
2012/07/23 01:10	1.41	0.21	0.3	17.3	0.02	0.86	1.87	0	0.001	2.36	78.2	0.39	0.1	0.17	19.2	13.45	46.881
2012/07/23 07:57	1.45	0.2	0.28	10.6	0.02	0.95	1.89	0	0.001	2.38	83.4	0.42	0.11	0.19	11.7	8.239	49.998
2012/07/23 10:25	1.52	0.22	0.29	9.4	0.02	1.07	1.95	0	0.001	2.47	84.7	0.42	0.12	0.21	10.5	7.307	50.778
2012/07/23 21:15	1.51	0.23	0.28	9	0.02	1.03	1.97	0	0.001	2.53	85.4	0.42	0.12	0.21	10	6.996	51.197
2012/07/24 02:37	1.5	0.22	0.27	8.4	0.02	1	1.93	0	0.001	2.47	85.2	0.43	0.12	0.21	9.3	6.529	51.077
2012/07/24 22:10	1.68	0.24	0.3	15.5	0.02	1	2.01	0	0.001	2.53	75	0.39	0.11	0.2	17.2	12.05	44.963
2012/07/25 02:12	1.51	0.24	0.28	9.1	0.02	1	2.03	0	0.001	2.56	82.9	0.41	0.13	0.23	10.1	7.073	49.699
2012/07/25 06:45	1.506	0.225	0.273	8.736	0	1.039	1.945	0	0.001	2.394	85.04	0.423	0.126	0.222	9.708	6.79	50.981
2012/07/25 10:00	1.528	0.219	0.267	8.298	0.015	1.154	1.869	0	0.001	2.316	86.8	0.435	0.119	0.216	9.222	6.45	52.038
2012/07/25 16:00	1.47	0.21	0.27	9.3	0.01	1	1.8	0	0.001	2.25	84.6	0.43	0.11	0.21	10.3	7.229	50.718
2012/07/25 19:40	1.5	0.21	0.25	8.9	0.02	1.08	1.74	0	0.001	2.22	86.3	0.44	0.1	0.2	9.9	6.918	51.737
2012/07/26 00:05	1.44	0.2	0.25	11.6	0.01	0.98	1.77	0	0.001	2.2	82.5	0.42	0.1	0.19	12.9	9.017	49.459
2012/07/26 06:50	1.472	0.182	0.247	15.03	0.014	1.057	1.67	0	0.001	2.176	81.39	0.415	0.084	0.172	16.707	11.69	48.791
2012/07/26 09:40	1.48	0.199	0.246	9.685	0.017	1.012	1.782	0	0.001	2.291	83.39	0.427	0.105	0.2	10.764	7.528	49.989
2012/07/26 21:10	1.45	0.19	0.27	12.2	0.01	1.01	1.73	0	0.001	2.23	83.3	0.43	0.1	0.18	13.5	9.483	49.938
2012/07/27 01:10	1.48	0.21	0.26	9.4	0.02	0.99	1.86	0	0.001	2.38	84.3	0.42	0.12	0.21	10.5	7.307	50.538
2012/07/27 04:47	1.546	0.214	0.25	8.173	0.016	1.139	1.799	0	0.001	2.379	86.23	0.439	0.111	0.208	9.083	6.353	51.696
2012/07/27 10:45	1.53	0.22	0.25	9.3	0.02	1.07	1.87	0	0.001	2.47	84.7	0.42	0.11	0.21	10.3	7.229	50.778
2012/07/27 14:50	1.55	0.23	0.24	8.4	0.02	1.13	1.87	0	0.001	2.5	85.8	0.43	0.11	0.21	9.3	6.529	51.437
2012/07/27 20:10	1.515	0.216	0.256	16.56	0.016	0.961	1.835	0	0.001	2.429	77.76	0.379	0.094	0.231	18.402	12.87	46.618
2012/07/28 05:00	1.57	0.23	0.25	8.6	0.02	1.25	1.88	0	0.001	2.49	85.9	0.42	0.12	0.23	9.5	6.685	51.497
2012/07/21 20:20	1.44	0.19	0.28	11	0.02	1.09	1.8	0	0.001	2.33	84	0.43	0.1	0.18	12.2	8.55	50.358
2012/07/28 09:45	1.54	0.22	0.24	8.6	0.02	1.23	1.86	0	0.001	2.43	85.6	0.43	0.11	0.22	9.6	6.685	51.317

10.24 Reductant D associated furnace data

Date	Total Ilmenite Ton	Cold Ilmenite Ton	Hot Ilmenite Ton	Suppl Ilmenite Ton	Total Reductant Ton	Total RR %	Center Reductant Ton	Center RR %	Suppl Reductant Ton	Suppl RR %	Power Consumption MWh	Power Ratio MWh/t	Constant Deviation MW	Resistance mohm	Slag Ton	Temp °C	Iron Ton	Temp °C
2012/07/21 06:00	575.42	386.67	0	188.74	77.6	13.49	52.39	13.55	25.21	13.31	708.13281	1231	145	13	338.6	1690	179.8	1578
2012/07/22 06:00	460.01	299.66	0	160.35	63.67	13.84	41.62	13.89	22.06	0	577.5625	1256	4.9	13.2	238.7	1682	192.2	1602
2012/07/23 06:00	437.7	294.3	0	143.41	62.03	14.17	41.59	14.13	20.44	0	562.125	1284	15	15	233	1688	117.1	1533
2012/07/24 06:00	246.31	206.21	0	40.09	34.7	14.09	29.13	14.12	5.58	13.897	339.05469	1377	15.15	13.18	120	1682	125.9	1539
2012/07/25 06:00	599.62	446.61	0	153.01	81.52	13.6	60.82	13.62	20.7	13.286	757.04688	1263	1397	13.2	293.5	1699	229.5	1568
2012/07/26 06:00	431.48	324.67	0	106.81	59.33	13.75	44.76	13.79	14.57	13.683	558.69531	1295	16	13.2	293.6	1687	63.6	1569
2012/07/27 06:00	512.79	363.42	0	149.37	71.47	13.94	50.31	13.84	21.6	5.617	657.03125	1281	1.97	13.19	242.7	1694	196.5	1620
	3263.33	2321.54	0	941.79	450.33	13.84	320.61	13.85	129.72	11.959	4159.6484	1.239	1.937	13.42	1760.2	1689	1104.6	1573
	Sum	Sum	Sum	Sum	Sum	ZAvg	Sum	ZAvg	Sum	ZAvg	Sum	CatTot	ZAvg	ZAvg	Sum	ZAvg	Sum	ZAvg

10.25 Factsage metal results

gram LIQL #2			
(1450 C, 1 εtm,	a=1.0000)	
(96.823 wt.%	Fe	
+	0.3252 wt.%	C	
+	0.11083 wt.%	Cr	
+	4.93E-06 wt.%	Al	
+	4.83E-02 wt.%	Mn	
+	3.82E-03 wt.%	N	
+	0.50539 wt.%	P	
+	2.07E-03 wt.%	S	
+	2.55E-02 wt.%	Si	
+	3.97E-04 wt.%	Ti	
+	0.67718 wt.%	V	
+	8.01E-09 wt.%	Mg	
+	3.88E-03 wt.%	O	

32.774 gram LIQLD#1			
(32.774 g ram, 0.5927 mol)		
(1500 C, 1 εtm,	a=1.0000)	
(98.712 wt.%	Fe	
+	0.26356 wt.%	C	
+	3.97E-02 wt.%	Cr	
+	6.85E-06 wt.%	Al	
+	3.99E-02 wt.%	Mn	
+	4.04E-03 wt.%	N	
+	1.33E-02 wt.%	P	
+	7.21E-04 wt.%	S	
+	4.15E-02 wt.%	Si	
+	7.22E-04 wt.%	Ti	
+	0.42861 wt.%	V	
+	9.78E-09 wt.%	Mg	
+	5.65E-03 wt.%	O	

32.551 gram LIQLD#1			
(32.551 g ram, 0.5882 mol)		
(1550 C, 1 εtm,	a=1.0000)	
(98.715 wt.%	Fe	
+	0.25782 wt.%	C	
+	4.11E-02 wt.%	Cr	
+	1.38E-05 wt.%	Al	
+	5.16E-02 wt.%	Mn	
+	4.10E-03 wt.%	N	
+	1.34E-02 wt.%	P	
+	6.75E-04 wt.%	S	
+	9.86E-02 wt.%	Si	
+	1.79E-03 wt.%	Ti	
+	0.43186 wt.%	V	
+	1.90E-08 wt.%	Mg	
+	5.95E-03 wt.%	O	

32.275 gram LIQLD#1			
(32.275 g ram, 0.5849 mol)		
(1600 C, 1 εtm,	a=1.0000)	
(98.672 wt.%	Fe	
+	0.24759 wt.%	C	
+	4.14E-02 wt.%	Cr	
+	2.57E-05 wt.%	Al	
+	6.49E-02 wt.%	Mn	
+	4.15E-03 wt.%	N	
+	1.35E-02 wt.%	P	
+	6.08E-04 wt.%	S	
+	0.20345 wt.%	Si	
+	4.06E-03 wt.%	Ti	
+	0.43577 wt.%	V	
+	3.40E-08 wt.%	Mg	
+	6.34E-03 wt.%	O	

10.26 Typical Value in Use model inputs and Outputs

Ilmenite selection	%
Ilmenite A	100
Ilmenite B	0
Ilmenite C	0
Ilmenite D	0
Reductant selection	
Reductant A	1
Reductant B	0
Aim TiO2	85
Supp feed	0
CD	1.3
MWh	34
Centre feed	12.65
Side feed	11.65
Standing time inclusive of additioning	1
Slowtime	0
Total	1
EBITDA	XXXX

Ilmenite feed		Reductant feed	
TiO2	47.80%	Inherent moist	1.99% TiO2 1.45%
FeO	33.80%	Surface moist	1.00% FeO 0.00%
Fe2O3	15.00%	Ash	3.00% Fe2O3 12.79%
SiO2	1.20%		SiO2 45.08%
Al2O3	0.42%		Al2O3 24.13%
MgO	0.51%		MgO 0.95%
CaO	0.06%		CaO 1.57%
MnO	1.12%	C	86.00% MnO 0.10%
V2O5	0.24%	H	2.40% V2O5 0.04%
Cr2O3	0.19%	O	0.99% Cr2O3 0.03%
ZrO2	0.10%	N	1.79% ZrO2 0.00%
P2O5	0.02%	S	0.88% P2O5 0.10%
K2O	0.00%		K2O 2.79%
Na2O	0.00%		Na2O 0.59%
SO3	0.00%		SO3 0.00%

Slag		Metal	
TiO2 equivalent	85.00%	Ti	0.049%
FeO	9.00%	Si	0.013%
SiO2	2.19%	Al	0.004%
Al2O3	0.89%	Ca	0.000%
CaO	0.11%	Mg	0.000%
MgO	0.92%	Mn	0.033%
MnO	1.95%	Cr	0.064%
Cr2O3	0.28%	V	0.021%
V2O5	0.39%	P	0.023%
P2O5	0.00%	Zr	0.000%
ZrO2	0.17%	K	0.000%
K2O	0.01%	Na	0.000%
Na2O	0.00%	S	0.115%
S	0.00%		